LAKE SENSITIVITY TO LATE-HOLOCENE CLIMATE CHANGE IN THE WESTERN GREAT LAKES REGION BASED ON DIATOM-DEPTH RECONSTRUCTION

A THESIS

SUBMITTED TO THE FACULTY OF THE GRADUATE SCHOOL OF THE UNIVERSITY OF MINNESOTA

BY

PHILLIP SCOTT WOODS

IN PARTIAL FULFILLMENT OF THE REQUIREMENTS

FOR THE DEGREE OF

MASTER OF SCIENCE

JULY 2018

Acknowledgements

All work reported here was completed by the author except for the following: loss on ignition and ground penetrating radar was analyzed by Chris Nevala-Plageman, lake inundation models were created by Jason Ulrich, and most R code created by Adam Heathcote."

The research support and partial funding provided by the National Science Foundation grant, DEB-0816762 is greatly appreciated. Additional funding was provided by the Conservation Sciences Graduate Program, University of Minnesota and Iowa Lakeside Laboratory, Iowa State University/University of Iowa.

Thanks to my co-advisor, Randy Calcote, for the introduction to paleoecology and paleolimnology. He introduced me to the adventures of lake sediment coring in the freezing cold. Thank you.

Thanks to my co-advisor, Mark Edlund, for introducing me to the wonderful world of diatoms, bringing ample amounts of enthusiasm to the project, and for believing in me. Thank you.

Thanks to Rob Blair, you inspired me to be a better steward of the earth.

Thanks to Amy Myrbo for help in dating analysis and also helping me discover the joy of science and teaching others. Thank you.

Thanks to the St. Croix Watershed Research Station for providing me with research facilities, scientific support and lab equipment.

Thanks to my fellow Conservation Sciences graduate students.

Thanks to my family, Katie, Kassidy, Mackenzie, and Violet, for their undying support and belief in me. Without their support I never would have had the courage to finish. Thanks to my parents for their support and guidance, thanks Mom and Dad.

`

ABSTRACT

Lake sediments provide an unparalleled source of proxy records of Holocene climate change and landscape response. Existing studies show overall synchrony in the upper Midwest (USA) to major climate periods (e.g., Holocene Thermal Maximum, and cooler/wetter late-Holocene), but less synchrony in response to shorter climate anomalies such as the Medieval Climate Anomaly (MCA) and the Little Ice Age (LIA). We examined a sediment core from Cheney Lake (northwest Wisconsin, USA), a lake positioned high in the landscape to reconstruct regional hydrologic climate response using diatom records to predict lake depth for the last 3500 years.

To reconstruct historical changes in lake depth, a single lake diatom-based model was constructed based on species-depth relationships from 18 modern surface samples collected at depths of 0.5 to 5 m from Cheney Lake. Based on redundancy analysis (RDA), lake depth explained ~27% of the variance in diatom community abundance. A transfer function for reconstructing lake depth was developed using weighted averaging (WA) regression with inverse deshrinking. The transfer function was applied to downcore diatom communities in a 93-cm long ^{14}C-dated core collected from a littoral zone site, to estimate lake level changes over the last 3500 years.

Results suggest that Cheney Lake was almost 6 m deeper beginning ~3500 cal. yr BP, nearly twice as deep as the modern lake, a condition that persisted for several thousand years. An abrupt decrease in water depth occurred around 1500 cal. yr BP, reaching minimal depths around 700 cal. yr BP during the Medieval Climate Anomaly.

Lake levels then rebounded and remained ~4 m above modern lake level until ~0 cal. yr BP (1950 CE). An abrupt decrease in moisture availability is evident in the last ~60 years, when lake levels fell to current low levels.

`

Table of Contents

`

`

List of Figures

`

List of Tables

`

LAKE SENSITIVITY TO LATE-HOLOCENE CLIMATE CHANGE IN THE WESTERN GREAT LAKES REGION BASED ON DIATOM-DEPTH RECONSTRUCTION

Phillip Woods[1]; Mark B. Edlund[2]; Randy Calcote[1,3]; Adam J. Heathcote[2]; Jason Ulrich[2]

[1]Conservation Sciences, University of Minnesota, 135B Skok Hall, St. Paul, MN 55108

[2]St. Croix Water Research Station, Science Museum of Minnesota, 16910 152nd St. N., Marine on St. Croix MN 55047

[3]Department of Earth Sciences, University of Minnesota, 116 Church Street SE, Minneapolis, MN 55455

INTRODUCTION

Lakes are sentinels of climate change (Adrian et al., 2009) and their depositional environments record and distill climate effects, as well as landscape and watershed perturbations (Williamson et al., 2009). Using a variety of paleolimnological approaches, including analysis of organic content of sediment, pollen and/or diatom analysis, we can understand how lakes and landscapes changed over time (Adrian et al., 2009). Lakes and streams are also important sentinels of sustainable water use and ecosystem health, and the connections between changing climate and land use practices must be examined more closely to better understand and forecast future freshwater availability (Schindler, 2009, Williamson et al., 2009). Lake level is one important indicator that integrates climate

impacts, landscape perturbations, and importantly the availability of fresh water (Williamson et al., 2009).

Understanding how different lake types respond to relatively small fluctuations in climate is essential to understanding how future climate change will affect freshwater availability. Studies in North America have linked lake level fluctuations to long-term climate impacts such as the extent of ice sheet formation and thawing on a global scale over the Holocene (Adrian et al., 2009). Other studies have measured climate effects on lakes using sediment features and the locations and elevations of paleoshorelines to determine the extent and magnitude of drought in North America (Williamson et al., 2009). However, there are relatively few long-term (>40 yrs) monitoring studies (Laird, Kingsbury and Cumming, 2010) that examine lake level fluctuations in North America and only a few active long-term monitoring programs exist (Laird *et al.*, 2011). Moreover, short-term (decadal) studies rarely represent the full range of natural climate variability over thousands of years.

Using sediment records from drainage or seepage lakes (as opposed to closed basin lakes; Hobbs, Fritz, *et al.*, 2011) in mid-latitude regions to infer lake level fluctuations and drought conditions is often complex (Laird *et al.*, 2011) and requires specialized methods (e.g., sampling protocols, counting procedures, statistical methods). Studies in central Canada used within lake calibration sets to link lake depth with diatom assemblages in surface sediment samples along a depth transect to develop models that are applied to historical diatom assemblages in sediment cores to infer past fluctuations in lake level (Moos, Laird and Cumming, 2005; Laird and Cumming, 2008, 2009; Laird, Kingsbury and Cumming, 2010; Laird *et al.*, 2011; Ma *et al.*, 2013). Using within-lake

relationships between diatom species assemblages and depth has significantly advanced lake depth reconstructions (Yang and Duthie, 1995; Nguetsop, Servant-Vildary and Servant, 2004). Canadian studies on boreal lakes have used this method and determined that diatoms are a good indicator of lake depth (Moos, Laird and Cumming, 2005, 2009; Laird and Cumming, 2009; Laird *et al.*, 2011; Ma *et al.*, 2013; Gushulak *et al.*, 2017). Up to ~20% of variation in diatom species assemblages is often independently explained by depth (Gushalak et al., 2017). Lake depth optima are estimated for each diatom species using weighted averaging regression based on the calibration set of surface samples (Laird et al., 2011). To reconstruct historical lake levels, the diatom-depth calibration set is applied to sediment cores collected at the transition zone between the littoral and profundal zone of lakes; the sediment record in this transition is thought to be most apt to preserve signals of lake-level change in the diatom record (Laird et al., 2010). Weighted averaging regression and calibration is robust and based on sound science when used with appropriate caution (Juggins, 2013; Juggins *et al.*, 2013), and for lake depth reconstruction relies heavily on known habitat preferences of diatoms between littoral and profundal habitats (Gushalak et al., 2017). The method, when applied within a single lake, also minimizes issues associated with space for time sampling that are typical of multi-lake calibration sets commonly used for pH, salinity, and TP inference models (Ramstack *et al.*, 2003; Hobbs, Vinebrooke, *et al.*, 2011).

The western Great Lakes region extends from western Michigan, Wisconsin and Minnesota (USA) and is characterized by long-term positive hydrologic balance with greater precipitation than evapotranspiration. Its western border with the Great Plains is defined by a shift to greater evapotranspiration, and this border has fluctuated by over 50

km during the Holocene (McAndrews, 1967). Within the western Great Lakes region, the Wisconsin Sand Plain is positioned near the floristic boundary separating northern forests and prairie, and within the sand plain Cheney Lake is located at the transition between the central jack pine barrens and northern mixed pine forest (Lynch et al., 2006; Fig. 1). The western Great Lakes region and specifically the Wisconsin Sand Plain's transitional position have made them focal research areas for paleoclimate reconstructions. There are several time periods during the late-Holocene where climate impacts in this region are of interest, namely the mid-Holocene Thermal Maximum (HTM; 8-4 cal. yr BP), the Medieval Climate Anomaly (MCA, ~1500-1100 cal. yr BP), the Little Ice Age (LIA, ~700-150 cal. yr BP), and the post-European settlement period (~150 cal. yr BP-Present). Many regional studies have linked vegetation change, especially changes in upland woody taxa, with climate variation over the last several thousand years. Few studies have considered paleohydrology based on past lake response (but see Brugam, Grimm and Eyster-Smith, 1988; Brugam et al. 1998, Shuman et al. 2009, Calcote *et al.,* in prep) and few studies have made quantitative lake level reconstructions (Brugam, McKeever and Kolesa, 1998; Brugam, Owen and Kolesa, 2004).

During the HTM (8k-4k cal. yr BP), the western Great Lakes region was warm and dry (Grimm, 1983; Brugam, Grimm and Eyster-Smith, 1988; Brugam, McKeever and Kolesa, 1998; Davis *et al.*, 2000; Umbanhowar, 2004; Nelson and Hu, 2008; Calcote 2003). Following the HTM, the climate in the western Great Lakes region was probably cooler and wetter, although there is still some discord among studies based on proxy type and study site (Brugam, Grimm and Eyster-Smith, 1988; Umbanhowar, 2004; Dasgupta *et al.*, 2010). The onset of the MCA (~1500-1100 cal. yr BP) brought warmer and/or

drier conditions to the western Great Lakes region (Gajewski et al. 1985, Calcote *et al.*, in prep). Pollen-based studies infer that the MCA was drier based on increases in jack pine (*Pinus banksiana*)/red pine (*Pinus resinosa*) and other xeric (low moisture) tree taxa (Lynch, Calcote and Hotchkiss, 2006; Tweiten *et al.*, 2009; Lynch *et al.*, 2014). Other studies infer warmer and drier conditions using sediment characteristics and loss on ignition (LOI) (Shuman *et al.*, 2009; Calcote *et al.*, 2018 in prep), but there remains controversy among studies and sites on the timing, magnitude, and duration of MCA climate conditions.

The timing and expansion of mesic taxa (moderate moisture) correspond with the onset of the LIA. Pollen-based studies indicate that mesic taxa increased at the prairie-forest border and on the NW Wisconsin Sand Plain ~700 years ago (Lynch, Calcote and Hotchkiss, 2006; Hotchkiss, Calcote and Lynch, 2007; Tweiten *et al.*, 2009; Lynch *et al.*, 2014). Conversely, a recent study inferred, based on low sediment organic matter at two lakes, that lake levels remained low well after 750 BP. Suggesting an alternative hypothesis of warmer and drier LIA conditions as the Big Woods expanded (Shuman et al. 2009). During the last ~150 years the region has changed significantly with the expansion of human activities including logging, and agriculture, and urban development—the Anthropocene (Crutzen and Stoermer, 2000)—coupled with global warming. Euro-American land use changes in the last 100-150 years are clear from a decrease in white pine (*Pinus strobus)* pollen due to logging and an increase in *Ambrosia* pollen, with the increase in agriculture (Swain, 1978; Grimm, 1983; Gajewski, Winkler and Swain, 1985; Lynch, Calcote and Hotchkiss, 2006; Hotchkiss, Calcote and Lynch, 2007; Lynch *et al.*, 2014). There are also shifts in algal communities in the last 100 years

that may represent a rapid response to global warming, although this signal is strongly confounded by local land use changes and other global processes (Saros *et al.*, 2012; Rühland, Paterson and Smol, 2015; Saros and Anderson, 2015),

There are few Late-Holocene climate records that are independent of vegetation and pollen in the western Great Lakes region, and inconsistencies among studies and research sites remain problematic. A more direct measure of the interplay between temperature and moisture is needed. Many lakes respond to changes in precipitation and evapotranspiration (P/E) through changes in lake level, and additional regional paleohydrological studies based on lake response may resolve inconsistencies among studies and sites by providing a more direct and quantitative measure of P/E, namely lake level (Laird et al., 2011).

Landscape position of the study site within a watershed is critical in reconstructing climate signals that can often be very small or abrupt. Lakes high in a watershed receive a higher fraction of their freshwater inputs from precipitation, thus making them more susceptible to small fluctuations in climate and moisture balance (Almendinger, 1990; Webster *et al.*, 1996). Lakes lower on the landscape receive a higher fraction of their freshwater inputs from groundwater flow or drainage from higher elevations (Almendinger, 1990; Webster *et al.*, 1996), making them less responsive to small fluctuations in climate. Whereas, most surface sediment diatom-depth models have been constructed for and applied to larger and more complex lake systems (Moos, Laird and Cumming, 2005; Laird and Cumming, 2008, 2009; Laird *et al.*, 2011; Ma *et al.*, 2013), our study targets a closed basin lake, high in the watershed in order to take advantage of its sensitivity to moisture balance.

This study focuses on the paleohydrology of a single lake in the northwestern Wisconsin Sand Plain. Cheney Lake is a relatively small (<10 ha) seepage lake on the Wisconsin Sand Plain with a single deep basin (6.4 m; WDNR, 2011), simple bathymetry, is surrounded by an undeveloped watershed dominated by jack pine plantations, and has a high landscape position. We develop a diatom-based lake level reconstruction that provides high temporal resolution of climatic variation and hydrology over the last ~3500 yr. We analyzed lake sediments from a transect of shallow water cores from Cheney Lake to determine lithological and biological signals of depth change in response to climate-driven variation in evapotranspiration and precipitation during the last ~3500 yr. An intralake diatom-based transfer function was developed for estimating historical lake depth.

This study further broadens the applicability of the within-lake diatom-depth calibration method. By using a small, shallow basin with simple bathymetry we are able to use fewer surface sediment samples (n=18), but achieve similarly robust model performance compared to other studies that use significantly more surface sediment samples and on much deeper lakes whose diatom assemblages are dominated by planktonic taxa.

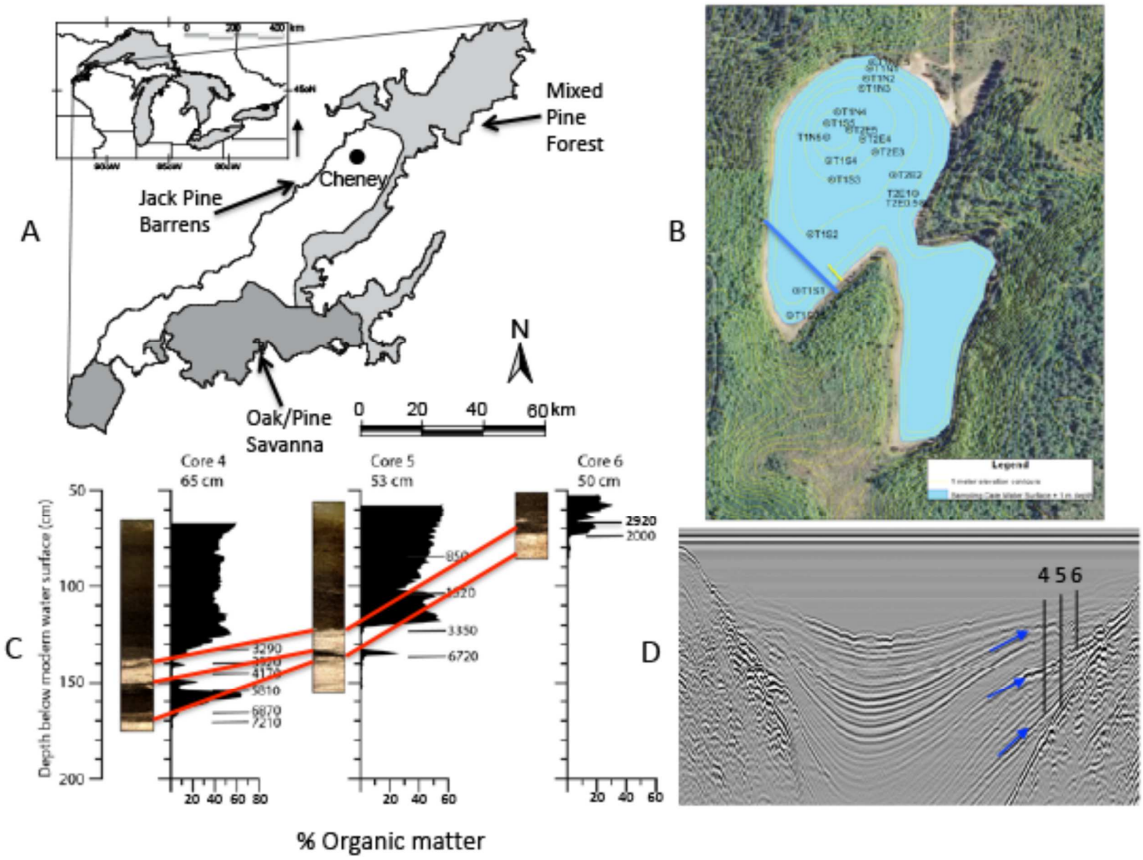

Figure 1. A. Location of the NW Wisconsin Sand Plain and Cheney Lake. Light colored central region is coarse sand dominated by jack pine. Northern region (light grey) was mixed pine. Southern region (dark grey) was oak-pine savannas in the PLS data (Radeloff *et al.*, 1999) B. Cheney Lake surface sample locations, ground penetrating radar (GPR) transect (blue line), and near shore sediment core transect (yellow line). Yellow bands are 1 m bathymetry. C. Cheney Lake near shore sediment cores 4-6. Images of split cores with LOI (loss on ignition, % organic matter) profiles and AMS radiocarbon dates (Modified from Nevala-Plageman 2012). D. GPR image of transect marked on (B) showing sampling locations of cores 4-6 (black vertical lines). Darkest bands transecting black core vertical lines indicate paleoshorelines or unconformities (blue arrows) that correspond to sand lenses shown in core images (C).

STUDY SITE

Cheney Lake (46.38°N, -91.70°W) is located in the northwestern Wisconsin Sand Plain at the top of the Bois Brule watershed (~340 m elevation), Douglas County, Wisconsin (Fig. 1). The surrounding area has sandy, well-drained soils dominated by jackpine *(Pinus banksiana)* plantations, and lacks residential development. Cheney Lake

is a relatively small (surface area ~7.9 ha) mesotrophic (Secchi depth 1.6 m), closed basin, seepage lake with a surface water drainage area of ~362 ha (U.S. Geological Survey, 2017) and a maximum modern depth of 6.4 m (Fig. 1; WDNR, 2016). The water is not considered impaired for nutrients or chlorophyll (WDNR, 2016). Shallow littoral areas and the shoreline are dominated by macrophytes, and dead tree stumps, suggesting that the lake was both shallower, and deeper for extended periods in the past. USGS topographical maps also indicate a more extensive basin system to the north and south, suggesting the lake could have been much deeper in the past (U.S. Geological Survey, 2017). There is currently no development in the basin, but there was, at some point, a small scout camp at the northern end of the lake where remains of a concrete floor are still visible.

METHODS

Sediment Coring and Basin Characterization

Ground Penetrating Radar (GPR; Shuman *et al.*, 2005) was used to visualize the stratigraphy and structure of the lake sediment using density variations caused by sand or peat deposited during periods of low lake levels. Unlike singular events of erosion or sediment slumping, continuous sediment features surrounding the entire basin indicate historical basin wide lake level change (Digerfeldt 1986, Shuman et al. 2009). The GPR transect had several sediment discontinuities extending throughout the basin (Fig. 1, also see Calcote *et al.,* in prep).

In order to develop a calibration dataset of diatom surface samples of different depths, 18 short gravity cores were taken throughout the lake (Fig. 1). Cores were

collected in April 2012 using an HTH corer (Renberg and Hansson 2008). Several transects of cores were collected that spanned modern water depths of 0.5 to 5 m, and the upper 0-1 cm section was removed by vertical extrusion and prepared for diatom analysis as described below.

Lake level reconstructions were done using sediment cores collected in 2010 along a shallow water transect tane across discontinuities identified in the GPR profile (Fig. 1). Each core was taken in a single drive with a 6.5 cm diameter polycarbonate tube fitted with a piston. Three cores along the transect (cores 4-6) were collected in shallow water ranging from ~50 to 65 cm water depth along the gradual slope in the southeast corner of the lake (Fig. 1). Core sediment-water interfaces were stabilized with Zorbitrol (Tomkins *et al.*, 2008); cores were sealed and transported back to the laboratory for processing.

Core Imaging and Geochemistry

Piston cores were split lengthwise, the fresh sediment surface was described at a macroscopic scale, and smear slides of whole sediment were analyzed to confirm microscopic sediment composition. Split core sections were imaged with a Geotek Geoscan-III (Noren, 2008), analyzed for magnetic susceptibility on a Geotek multi-sensor core logger (Geotek MSCL manual, http://www.geotek.co.uk/sites/-default/files/manual.pdf).), and core 5 subsampled for diatom slide preparation (0.5-cm increments for the length of the core). Cores are archived at the National Lacustrine Core Repository, University of Minnesota-Twin Cities (LacCore, National Lacustrine Core Repository, http://lrc.geo.umn.edu/laccore).

Subsamples (~1-5 cm^3) were taken at 0.5-cm intervals for the entire core length in cores 4-6 and analyzed by loss on ignition (LOI) following Dean (1974) and LacCore LOI standard operating procedure (Myrbo *et al.*, 2013). Loss on ignition (LOI) data from Nevala-Plageman (2012) were used to identify changes in organic matter (OM) content.

Cheney Lake (sediment core number)	**Sample Code and Depth**	**Material type**	**Process**	**Accession #**	**Age cal. yr BP**	**Age Err years**
Core 4	CHEN10 4A-1P-1 (83.5-85.5 cm)	Sediment Organic carbon	(OC) Organic Carbon	OS-85777	3070	35
Core 4	CHEN10 4A-1P-1 (89-91 cm)	Sediment Organic carbon	(OC) Organic Carbon	OS-85778	3850	30
Core 4	CHEN10 4A-1P-1 (89-91 cm)	Plant/Wood	(OC) Organic Carbon	OS-84413	3610	40
Core 4	CHEN10 4A-1P-1 (96-97 cm)	Plant/Wood	(OC) Organic Carbon	OS-84414	3790	25
Core 4	CHEN10 4A-1P-1 (105-105.5 cm)	Plant/Wood	(OC) Organic Carbon	OS-84415	5050	30
Core 4	CHEN10 4A-1P-1 (118-120 cm)	Sediment Organic carbon	(OC) Organic Carbon	OS-85779	6030	30
Core 4	CHEN10 4A-1P-1 (121.5-123.5 cm)	Sediment Organic carbon	(OC) Organic Carbon	OS-85780	6260	30
Core 5	Chen10-5A-1P-1 (0 cm)	Surface Sediment	Sample collected AD 2010		-60	2
Core 5	Chen10-5A-1P-1 (21.5 cm)	*Ambrosia* increase	Increased *Ambrosia* pollen		70	2
Core 5	Chen10-5A-1P-1 (35 cm)	Plant/Wood	(OC) Organic Carbon	OS-112793	915	20
Core 5	CHEN10 5A-1P-1 (57.5 cm)	Plant/Wood	(OC) Organic Carbon	OS-84416	1640	25
Core 5	CHEN10 5A-1P-1 (75 cm)	Plant/Wood	(OC) Organic Carbon	OS-84417	3120	40
Core 5	Chen10-5A-1P-1 87-89	Sediment Organic carbon	(OC) Organic Carbon	OS-112791	5890	30
Core 6	Chen10-6A-1P-1 18	Plant/Wood	(OC) Organic Carbon	OS-112794	2920	20
Core 6	Chen-10-6A-1P-1 23-25	Sediment Organic carbon	(OC) Organic Carbon	OS-112792	2040	20

Table 1. Sample depths and dating for cores 4-6 including AMS radiocarbon dates, surface sediment dates, and *Ambrosia* pollen increase for core 5. Dated levels of cores 4-6 are labelled with sample number, sample depth (cm), and dated material type. All but one date above 70 cm in core 5 were used to develop an age-depth models in R using the rbacon package (Blaauw and Christeny, 2011). The date at 35 cm was discarded as an outlier.

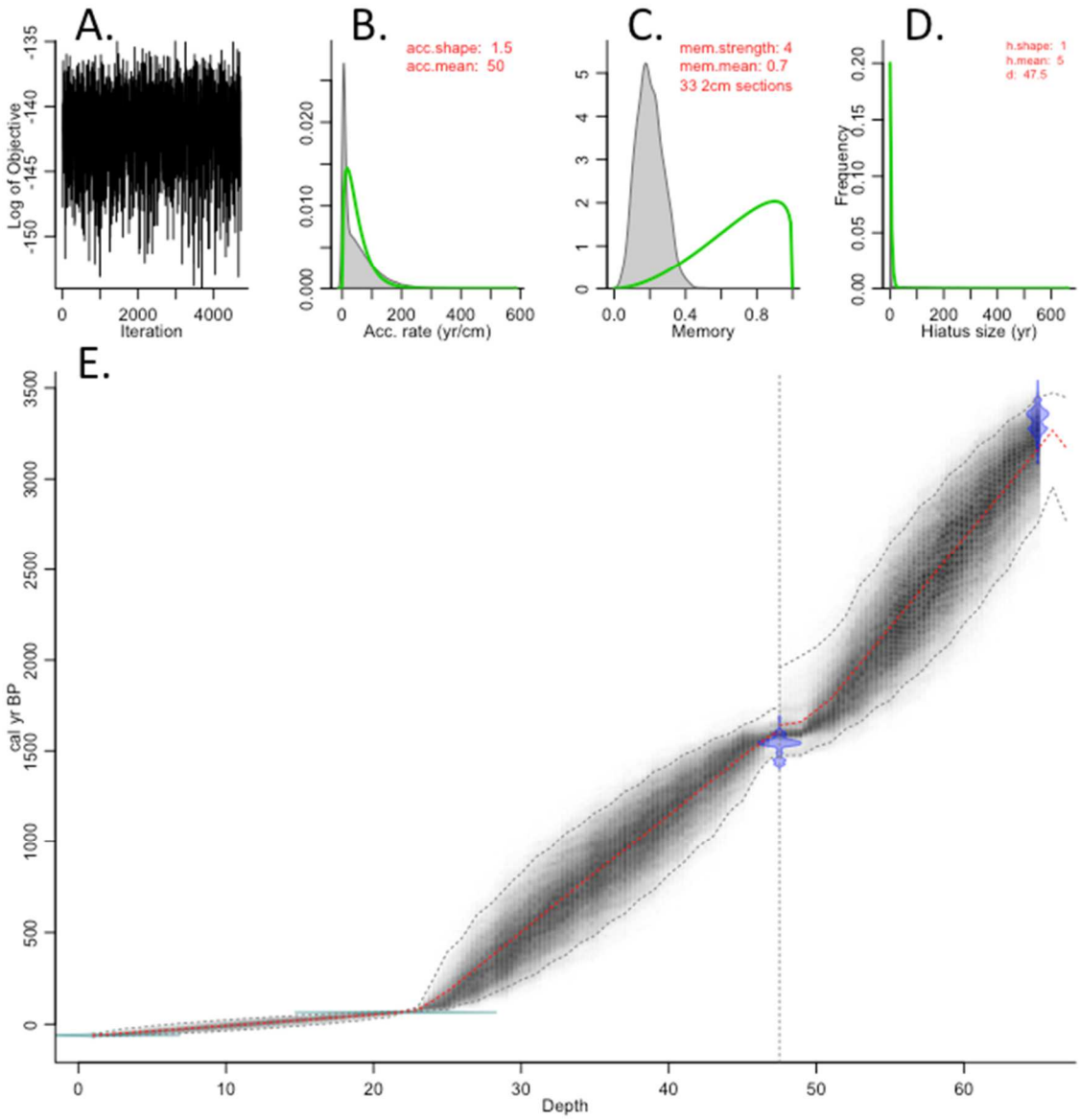

Figure 2. E. Age-depth model for Cheney Lake core 5 using AMS radiocarbon dates, *Ambrosia* rise, and surface sediment date (Table 1.). One date (915 +/- 20 cal. yr BP, TABLE 1) fell outside probable date-sample location parameters and was omitted for continuity of the model. Flat grey and blue bubbles indicate sediment depth of ^{14}C date and error estimate, vertical line indicates hiatus. A. Markov Chain Monte Carlo iterations, sectioned estimate of the mean accumulation rate (yr/cm). B. Mean accumulation rate (yr/cm) using prior information and autocorrelation between samples. C. Memory strength (yr/cm), influence of previous samples ages. D. Hiatus mean size in years and depth (cm) in sediment.

Core Chronology

The Core chronology was developed using a combination of surface sediment dates, *Ambrosia* pollen increases (described in Lynch et al, Calcote and Hotchkiss, 2006; Hotchkiss et al. 2007), and accelerator mass spectrometry (AMS) radiocarbon dates (Table 1). Some of the AMS samples were small pieces of wood (Table 1), they were cleaned with distilled water and sent for analysis to Woods Hole Oceanographic Institute (WHOI, whoi.edu). The remainder of AMS dates were also obtained through WHOI using pollen concentrated from 3 to 6 mL of wet sediment. Samples were treated with KOH, HF, and bleach to remove silica and organics other than pollen (Lynch *et al.*, 2014). Chronologies for cores 4 and 6 are not presented here. The chronology for core 5 is based on four AMS radiocarbon dates, the *Ambrosia* pollen increase (70 cal. yr BP) and a modern surface sediment age (2010 AD) (Table 1). Age-depth models for core 5 were developed using rbacon v2.2, IntCal13 in *R* (**R** Core Team, 2013). Dates are reported in cal. yr BP, where 'present' is AD 1950.

Diatom Analysis

Diatom microslides were prepared from ~ 1 cm^3 subsamples of the 18 surface sediment samples and core 5 subsamples using fuming 30% H_2O_2 (3 hr, 85°C). Processed material was alternately centrifuged and rinsed with ddH_2O to remove oxidation byproducts. The remaining material was settled onto coverslips and mounted onto microslides with Zrax® (MicrAP, Pennsylvania).

A minimum of 300 diatom valves per slide were counted along random transects on an Olympus BX51 microscope outfitted with differential interference contrast (DIC) optics (NA 1.40) under oil immersion at 1000X magnification. Diatom microfossils representing over 50% of a whole valve were counted to their lowest identifiable taxonomic level. Chrysophyte cysts were counted as a single group and used in relation to diatom counts as an indicator of lake habitat and productivity (Laird et al. 2010). Primary taxonomic references were: Patrick and Reimer, 1975, 1966; Krammer and Lange-Bertalot, 1986, 1988, 1991a and b; Camburn and Charles, 2000; Fallu, Allaire and Pienitz, 2000; Krammer, 2003; Antoniades *et al.*, 2008; Lavoie, I. *et al*., 2008. All diatom data were converted to percent abundance by taxon relative to total diatom counts. Downcore diatom data were also converted to a planktonic:benthic ratio and a chrysophyte cyst:diatom ratio (Laird and Cumming, 2008).

Diatom-Depth Model and Diatom-inferred Depth Reconstruction

Diatoms present at >1% abundance in more than two samples were used in numerical analysis of the surface sediment and core 5 samples. Abundance data were square-root transformed to downweight the most abundant taxa (Juggins and Birks, 2012).

Surface sediment assemblages were used to develop a diatom-depth predictive model. Principal components analysis (PCA) was used to ordinate the diatom assemblages. Redundancy analysis (RDA) was then used to partition variation in diatom assemblages explained by water depth. Depth was a significant and independent predictor of diatom abundance, so a quantitative diatom-depth model was developed using

weighted-averaging (WA) regression (Laird *et al.*, 2011). Because the same data are used to generate and test the WA model (Fritz *et al.*, 1999), model validation and error estimation can be estimated by cross-validation using *crossval* (Juggins, 2017) which implements leave-one out, leave-group-out, or bootstrapping with error estimated as the root mean square error of prediction (RMSEP; Ter Braak and Barendregt, 1986).

Dominant taxa and ecologically significant groups in core 5 were plotted stratigraphically. Constrained hierarchical cluster analysis (CONISS) using the broken stick method was performed to identify and test the significance of major stratigraphic zones (Bennett, 1996).

The diatom-depth WA model was applied to downcore diatom assemblages from core 5 using weighted averaging and inverse deshrinking (Gushulak *et al.*, 2017) to estimate historical water depths in Cheney Lake from ~3500 cal. yr BP to present. All analyses were implemented using R software v3.3.4 (R Core Team 2013; *Rioja* package*;* Juggins, 2012).

Lake Inundation Models

Diatom-inferred lake depths over time were projected onto modern topography in order to determine if the lake would reach a spillway at projected high lake levels. Maps of Cheney Lake surface area at four water surface elevations were created by merging the digital elevation model (DEM; 9 m cell resolution) from USGS (2017) with digitized 5 foot depth contours from a 1940 bathymetry map of the lake (Wisconsin Conservation Dept., 1940). ESRI's ArcGIS 10.3 (https://www.esri.com/en-us/arcgis/products/index) was used for all GIS operations. The bathymetric map was first georectified to match

aerial photos from 2008, a year where the water surface depth/area coincided with that depicted on the bathymetric map. The DEM was interpolated to 1-foot contours using ArcGIS Spatial Analyst and any lines that intersected the extent of the digitized bathymetry contours were removed. The two contour layers were merged and converted to a 3 m DEM using ArcGIS 3D Analyst. A lake surface raster was created for the water surface elevation observed on the sampling date (2010) by taking the merged DEM elevation (i.e., the lake bottom) at the core location and adding 53 cm (the observed depth of water at the core location on the sampling date). Three additional lake surface rasters were created using ArcGIS Spatial Analyst by adding 2, 4 and 6 meters of water depth above (corresponding to historical diatom-inferred lake levels) the 2010 water surface raster.

Modern lake levels analyzed using Google Earth images and the fixed location of a concrete slab located on the northern shoreline yielded fluctuations over 2 meters in just the last 25 years. These fluctuations correlate to changes in precipitation over the same time period as reported by the local weather service (Duluth Weather Forecast Office, National Weather Service, http://w2.weather.gov/climate/index.php?wfo=dlh).

Results

Depositional Environment

GPR profiles from Cheney Lake showed three distinct facies (Fig. 1D), which are also visible in GPR transects throughout the basin (Calcote *et al.*, in prep). The facies correspond to sand lenses found in the three nearshore sediment cores (see

Lithology; Fig. 1C)-and suggest that past lake levels were lower than current conditions

Core Lithology and Geochemistry

The three sediment cores 4-6 share features including organic-rich sediments interbedded with sand lenses (Fig. 1C). The sand lenses are consistent with the GPR facies and have been interpreted to indicate multiple periods of lower lake level in the history of Cheney Lake (Nevala-Plageman, 2012; Calcote *et al*., in prep). Loss on ignition (LOI) profiles for all three cores (Fig. 1C) are similar in that they all have sand lenses with low organic content in the bottom half of the core. Organic matter content ranges from > 60% in the dark, organic-rich fine sediment to < 10% in the sand layers. The deepest core, Core 4 (Fig. 1) has a sand lens at the base, indicating that before 7000 cal BP the lake level was >1.5m lower than the modern lake level. Low organic contene (<10%) indicates that the lake level was also low between about 5000 and 4000 cal yr BP. (< 10%). Percent organic matter in core 5 (Fig. 1C) is similar, but orgaic sediment deposition begins later, and it includes a later zone of low lake level (~100 cm below the modern water surface, Fig. 1.C), where organics decline to ~25%. Core 6 is short and includes two sand lenses where organic-rich sediments decline to < 30% around 65 cm. Sand-rich sediments ending around 73 cm are consistent with the two other cores and past lake level fluctuations.

Dating Model

Radiocarbon dates were obtained for all three cores (Table 1) and demonstrate the relationship between stratigraphic markers in different cores. The date at 3290 cal. yr BP (146 cm from water surface) in core 4 marks the beginning of a sharp increase in organic content (Fig. 1.c) and matches well with a similar rise in organic content in core 5 (128 cm), which dated to 3350 cal. yr BP. The date at 6870 cal. yr BP in core 4 also marks the beginning of a steep rise in organic content, and matches well with the deepest date (6720 cal. yr BP) in core 5, where a short, but sharp increase in organics occurs. Core 6 has two radiocarbon dates at 2000 cal. yr BP (73 cm) and 2920 cal. yr BP (68 cm) above the bottom sand lens.

A Bayesian age-depth model for the last 3500 years of core 5 was constructed (Fig. 2). The youngest AMS ^{14}C date (915 +/- 20 cal. yr BP; Table 1) was excluded from the age-depth model; we determined from the age and location in the sediment core that the dated material was likely transported from the lake margin and re-deposited in younger sediments. The calibrated ages, ranges, and full date model (Fig. 2) shows that average accumulation rate for this core was approximately 45 yr cm^{-1}. Sedimentation rates vary throughout core 5. From 1 to 20 cm (-61 to 51 cal. yr BP), sedimentation rates average 5.6 yr cm^{-1} from 20 to 22 cm (51 to 68 cal. yr BP), average sedimentation is 10 yr cm^{-1}, from 23 to 43 cm (78 to 1348 cal. yr BP) sedimentation rate averages 63 yr cm^{-1}. There is a small 1 cm sand lens at 47.5 cm (1633 cal. yr BP), but the surrounding samples (44-51 cm) average sedimentation rate is 30 cm yr^{-1} (1348 to 1720 cal. yr BP). Sedimentation rates increase to approximately 100 yr cm^{-1} from 51 to 66 cm (1780 to 3265 cal. yr BP).

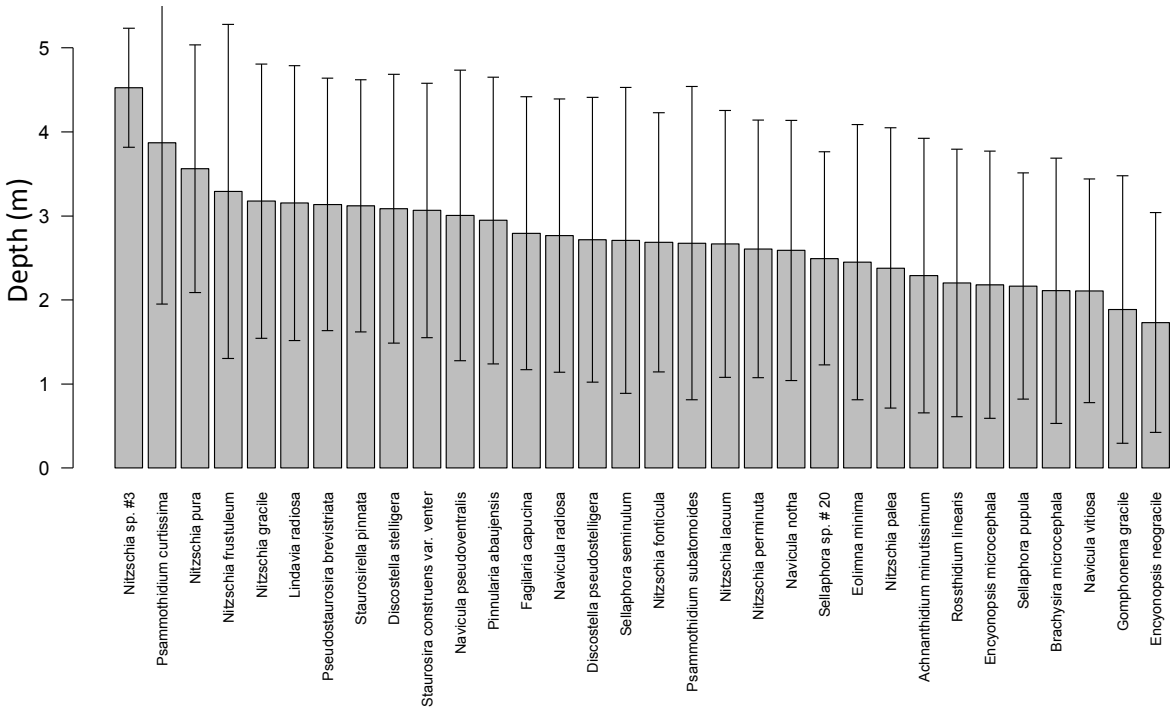

Figure 3. Diatom depth optima (bars), and tolerance (error bars) for select species used in the surface sample training set. Taxa that were above 1% relative abundance in at least two samples are included in the analysis. Diatoms with the deepest optima are on the left, diatoms with the lowest depth optima on the right. Some species like *Psammothidium curtissima* have broad depth tolerances and others like *Nitzschia* sp. #3 have narrower depth tolerances.

Diatom-Depth Model

A total of 141 diatom taxa (38 taxa were found in more than two samples at >1% abundance) were identified from the 18 surface-sediment samples. Depth optima estimated using weighted averaging (Fig. 3) ranged from 1.7 m *(Encyonema neogracile)* to 4.5 m *(Nitzschia* sp*. #3).* Diatom taxa were highly constrained by depth; an RDA with lake depth constrained to axis 1 showed that lake depth explained ~27% of the independent variation among diatom

Performance of the WA model was tested using bootstrap comparison of observed vs. predicted lake depth with an r^2_{boot} of 0.89 and an RMSEP of 0.65 m (Fig. 4). The MAT (modern analog technique; Legendre and Gallagher, 2001) was also tested, but it underperformed in all metrics (see Appendix A) compared to WA with an r^2_{boot} 0.503 and RMSEP of 1.29 m.

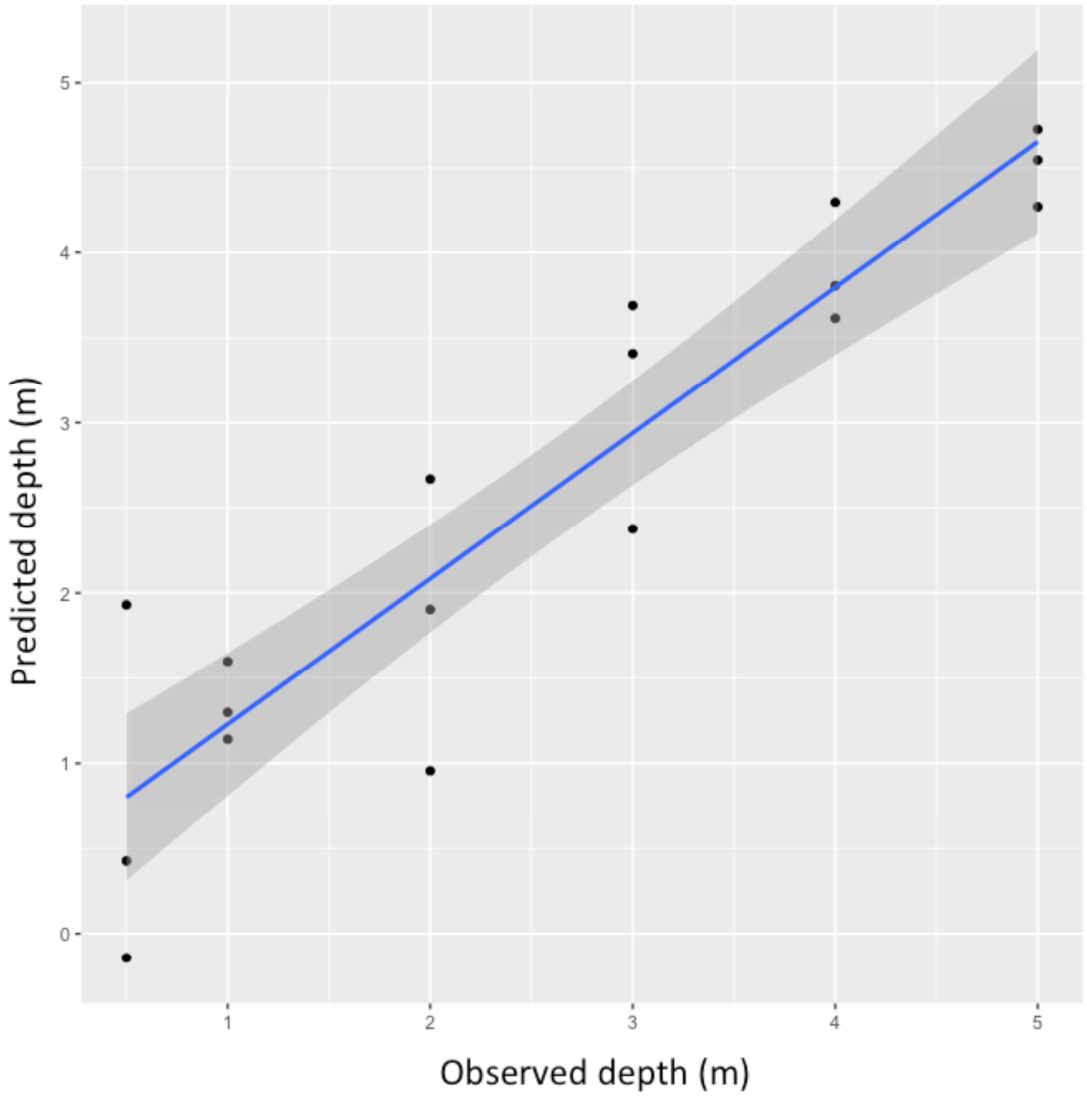

1. **Figure 4**. Observed water depth at diatom surface sample locations vs predicted depth from the Cheney Lake diatom-depth model. Predicted depths (m), $r^2 = 0.89$ and RMSEP 0.6 m. Solid blue line indicates best fit error prediction plus one standard deviation (shaded area).

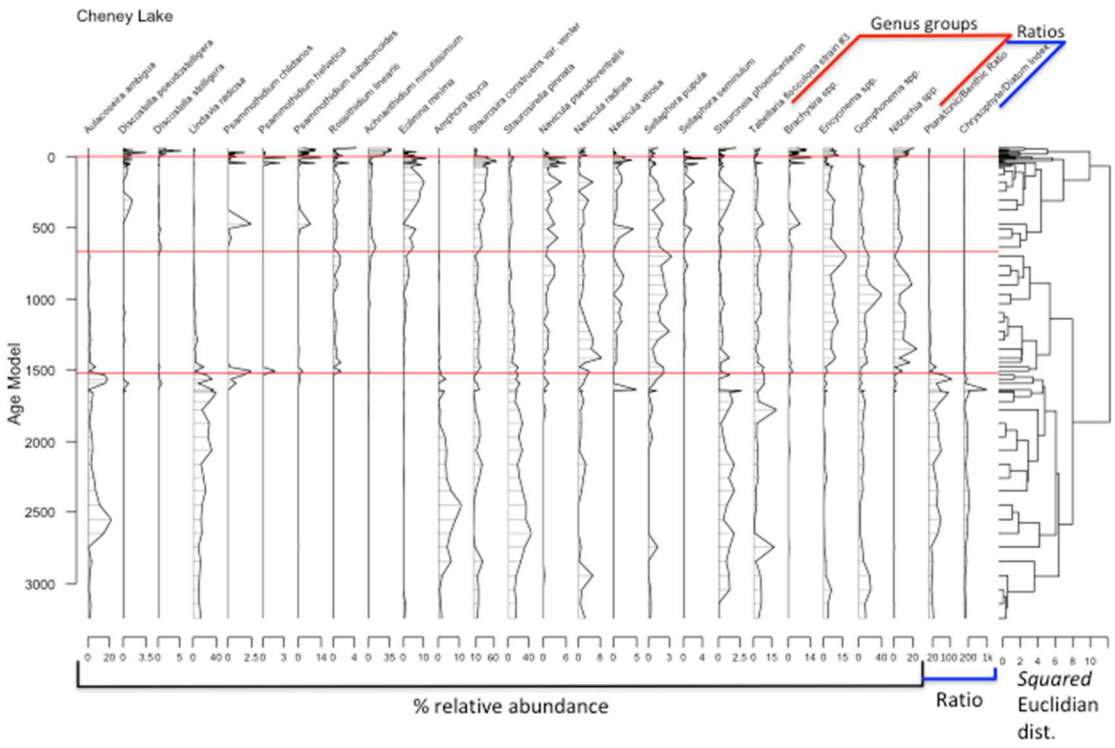

Figure 5. Stratigraphic diagram showing relative abundance of diatom taxa over time (cal. yr. BP). Genus-level grouped species shown to the right along with planktonic/benthic and chrysophyte/diatom ratios. Constrained cluster analysis based on squared Euclidean distance shown in right panel with four significant diatom zones separated by red horizontal lines.

Downcore Diatom Communities

A total of 91 diatom species were found in core 5 with 36 taxa in more than two samples at >1% abundance. A constrained cluster analysis of core 5 diatom assemblages identified four significant stratigraphic zones (Fig. 5).

Zone 1 (-61 to 0 cal. yr BP) is dominated by benthic motile and attached taxa that live on and among benthic substrates or aquatic macrophytes. Taxa commonly found in this zone are in the genera *Achnanthidium, Eolimna, Brachysira, Encyonopsis, Eunotia, Staurosira*, *Navicula, Nitzschia*, and *Tabellaria. Achnanthidium*

minutissimum, Encyonopsis microcephala, and *Staurosira construens* var*. venter* make up most of the assemblage in this zone. Planktonic species including *Discostella stelligera* and *D*. *pseudostelligera* can also be found in this zone.

Zone 2 (700 to 0 cal. yr BP) comprises mostly benthic taxa from the genera *Eolimna, Brachysira, Encyonopsis, Encyonema, Staurosira, Gomphonema,* and *Navicula*. *Eolimna minima* and *Staurosira construens* var*. venter* dominate this zone. Other taxa like *Staurosirella pinnata* also show up in the community.

Zones 3 (1480 to 700 cal. yr BP) and 4 (3265 to 1480 cal. yr BP) represent the period with the deepest lake level reconstruction; planktonic and tychoplanktonic diatom taxa are in high abundance. In Zone 3 and 4, the diatom community is predominantly *Aulacoseira ambigua, Discostella stelligera/pseudostelligera* and *Lindavia radiosa* with some *Eunotia*, *Gomphonema,* and *Tabellaria flocculosa III*. Zone 4 is similar to Zone 3, but with greater abundance of *Amphora libyca, Staurosirella pinnata* and *Aulacoseira ambigua* in Zone 4*.*

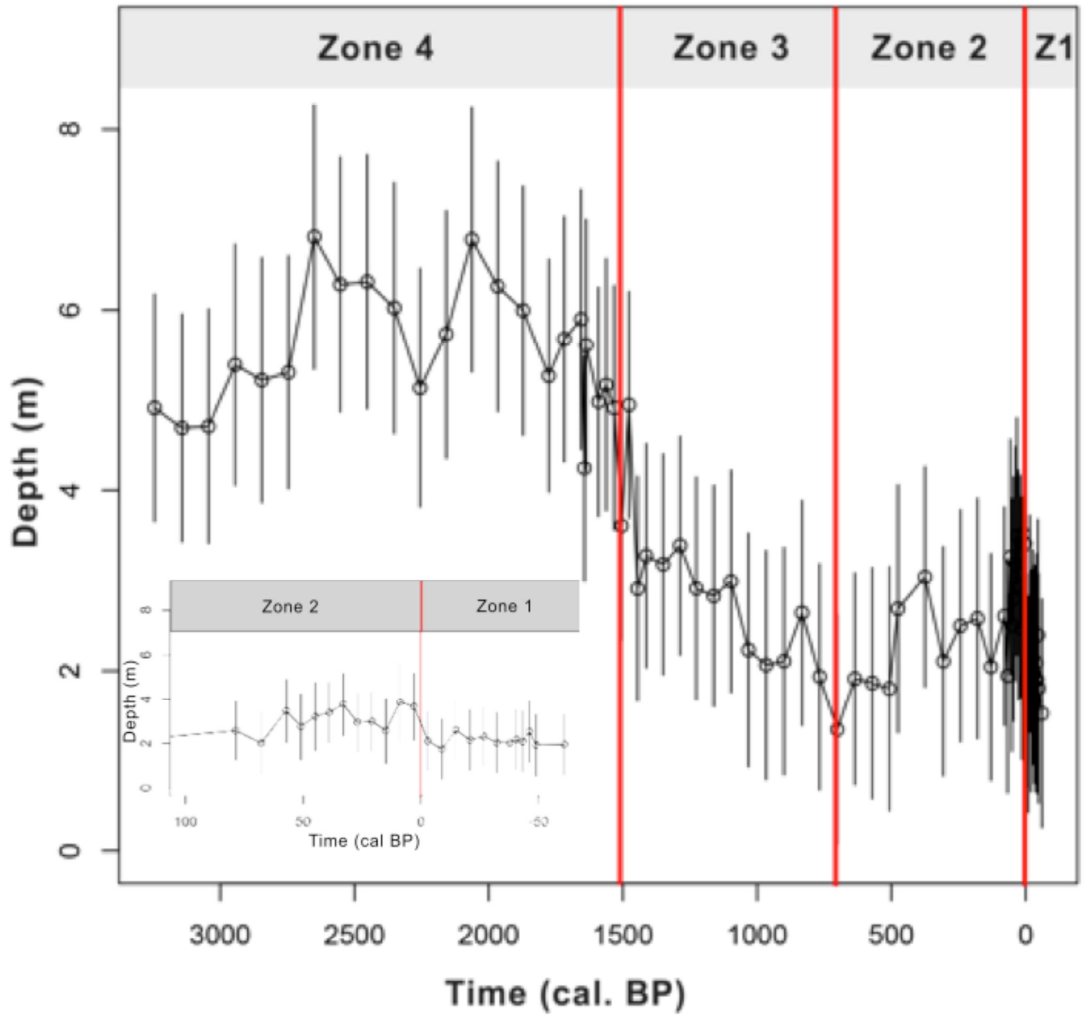

Figure 6. Diatom-based lake level (m above 2010 lake level) reconstruction (~3500 years) using WA with inverse deshrinking. The expanded inset includes the most recent 150 years. Error bars equal RMSEP for each sample based on WA model.

Diatom-Inferred Lake Level

The lake level reconstruction spans almost 3300 years (Fig.6.) Based on the WA model, lake levels were much higher in the transition from the mid- to Late-Holocene. Cheney Lake was approximately 6 meters deeper from 3000 cal. yr BP until about 1500 cal. yr BP when lake level declined sharply. At around 1200 cal. yr BP the lake was at its shallowest in the last 3200 years, with a depth of about 1 m. Lake levels start to rebound in the LIA, after ~700 cal. yr BP, to approximately 3 m depth and climbed to almost 4 m around 500 cal. yr BP. Approximately 60 years ago lake levels dropped sharply and have remained low with respect to the mid-Holocene and LIA high stands and nearly as low as the Medieval Climate Anomaly minima at 700 cal. yr BP.

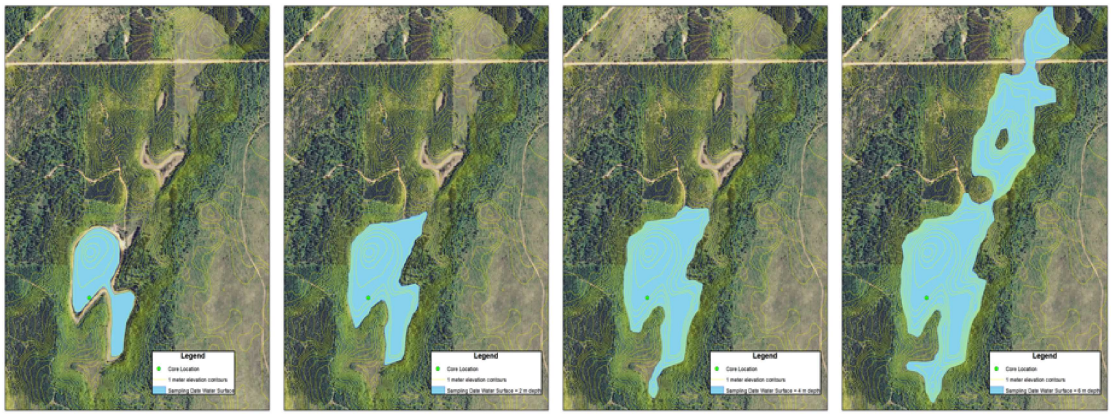

Figure 7. Reconstructed Cheney Lake basin morphometry (~3500 to 0 cal. yr BP) showing that it is possible for the lake to get 6 m deeper (2500 cal. yr BP) without reaching a spill point. Water surface elevations were created by merging the digital elevation model (DEM; 9 meter cell resolution) from USGS (2017) with digitized 5 foot depth contours from a 1940 bathymetry map of the lake (Wisconsin Conservation Dept., 1940).

Lake Inundation Models

Lake inundation models indicate that the lake basin expands north and south when lake levels increase (Fig. 7). At 2500 cal. yr BP a depth increase of 6 m could inundates a large area to the north and south without reaching a spill point, i.e., it is possible for the lake to increase to the levels predicted in the diatom-depth model. Modern lake levels correspond closely to minimum levels reached at 700 cal. yr BP at the end of the MCA (Fig. 7).

Discussion

To explore the connection between Late-Holocene climate and lake-level change, our work focused on Cheney Lake, whose high landscape position in the

Bois Brule watershed of northern Wisconsin (USA) and simple basin morphometry promised high lake level response to climate forcing across the Late-Holocene cool period, the MCA, the LIA, and during the Anthropocene. We developed a diatom-based lake depth model that reconstructed lake depth over time and provided a clearer understanding of Late-Holocene lake response to regional changes in precipitation-evaporation (P/E). We also develop a regional climate synthesis using the Cheney Lake diatom-based lake level reconstruction in conjunction with other sites studied with various paleoproxies in the western Great Lakes ecoregion. We organize our discussion of the Cheney Lake sediment record and modeling results by exploring this first use of diatom-based lake level modeling on small and shallow lakes, the depth-climate signal preserved in Cheney Lake, how temperate lakes respond to climate change, and develop a regional synthesis of the late-Holocene in this important ecotonal region of the upper Midwest

Diatom-depth models for shallow lakes

Our diatom-depth model differs from most diatom-based lake level reconstructions in four important ways. First, we chose Cheney Lake because it is a seepage lake located at the top of the Bois Brule watershed. The lake-landscape position hypothesis (Almendinger, 1990; Webster *et al.*, 1996) suggests these lakes show more responsive lake level changes because their hydrology is most strongly controlled by precipitation. Other diatom-based lake level reconstructions have focused on drainage lakes (Moos, Laird and Cumming, 2005; Laird and Cumming, 2008, 2009; Laird, Kingsbury and Cumming, 2010; Laird *et al.*, 2011; Ma *et al.*, 2013;

Gushulak *et al.*, 2017). Salinity-based reconstructions of drought history in closed basin lakes are more similar to the Cheney Lake scenario, but rather than reconstructing depth, they reconstruct salinity changes that result as rising and falling water levels lower or raise salinity, respectively (Laird *et al.*, 1996; Fritz *et al.*, 2000, 2010; Hobbs, Fritz, *et al.*, 2011).

Second, Cheney Lake has simple bathymetry. Most diatom-depth models have been done on lakes with complex bathymetry where loss of littoral habitat in shallow embayments are isolated from the benthic-planktonic boundary of the larger lake and may not be generalizable to the whole lake (Laird et al., 2010). In Cheney Lake, a simple bowl-like bathymetry in a small lake ensures a broad depositional basin that extends into shallow waters and is preserved even during low stands. Sediment lithology confirms that depth changes were commonplace in the late-Holocene in Cheney Lake.

Third, we used many fewer surface sediment samples (18) compared to previous diatom-based lake level reconstruction work (Moos, Laird and Cumming, 2005; Laird and Cumming, 2008, 2009; Laird, Kingsbury and Cumming, 2010; Laird *et al.*, 2011; Kingsbury, Laird and Cumming, 2012; Ma *et al.*, 2013; Gushulak *et al.*, 2017) where surface sediment calibration sets typically number around 50 samples . Even with the smaller number of samples, the independent variance in diatom communities explained by depth in this study is almost 27%, similar to other depth models based on higher sample size (Ma *et al.*, 2013; Gushulak *et al.*, 2017), and much higher than in other diatom-based nutrient inference models for the region (~9%) (Ramstack et al., 2003a and b). R^2 and RMSEP values are consistent with

model statistics in other diatom-depth studies done outside the region (Laird and Cumming, 2008; Laird, Kingsbury and Cumming, 2010; Laird *et al.*, 2011; Ma *et al.*, 2013; Gushulak *et al.*, 2017).

Fourth, the Cheney Lake depth model relies more heavily on the depth response of benthic and attached taxa compared to most studies. The shallow nature of Cheney Lake precludes it from having a well-structured planktonic diatom flora forcing the model to rely on depth optima and tolerances of benthic taxa. Other diatom-depth models are heavily driven by a planktonic diatom community structure (Moos, Laird and Cumming, 2005; Ma *et al.*, 2013; Gushulak *et al.*, 2017) that is common in lakes that are deeper and with more complex basins. Overall, our data suggest that you can get equally explanatory diatom-depth models and reconstruction results in shallow lakes with simple basins, using fewer surface sediment samples, and with greater reliance on benthic diatom response to depth.

Depth-climate signal in Cheney Lake

GPR transects across Cheney Lake exhibit continuous littoral facies below the modern littoral zone and are consistent with interbedded intervals of organic-rich sediments and sand laminations indicative of deeper and shallower depositional sites, respectively (Johnston 2010). Loss on ignition data confirm strong shifts in organic matter across these intervals in Cheney Lake. However, the LOI signal in lakes can be less responsive than other depth proxies to small shifts in sediment deposition and lake level change (Shuman *et al.*, 2009) and supports that additional depth proxies be used for paleoclimate reconstructions. LOI data suggest that lake

levels were high during the Late-Holocene wet period (~3500-1500 cal. yr BP), dropped during the MCA (1500-700 cal. yr BP), a change recorded only in core 5, and that lake levels steadily rose after 700 cal. yr BP following the MCA thermal maxima. However, LOI does not indicate that lake levels have shifted over the last 100 years, in contrast with details that emerge using a diatom-based reconstruction. Poorly resolved lake depth change recorded in sediments over the last 100 years is consistent with other LOI records (Shuman 2003, Shuman et al. 2009, Shuman et al. 2010, Pribyl and Shuman 2014).

Lake depth reconstruction for Cheney Lake based on diatoms provides greater detail on timing and extent of depth change during the late-Holocene. Lake depths were up to 6 m higher from ~3500 – 1500 cal. yr BP. Lake levels then fell to levels more consistent with modern shallow conditions during the MCA, reaching shallowest depths approximately 700 cal. yr BP. Lake levels rose again to 3-3.5 m during the LIA, before falling over the last ~60 years to modern levels that are similar to MCA lake levels. Diatom-based reconstructions using a within lake calibration dataset from a small simple basin high in its watershed provides a higher resolution climate history that other methods such as loss on ignition (Shuman, 2003) or pollen-based proxies (Lynch, Calcote and Hotchkiss, 2006). Improved climate histories for this region could leverage additional effort directed at mapping and analysis of paleoshorelines to validate inundation model results for Cheney Lake. Our results show a wider range of lake level responses to climate change, including higher lake levels. Our method can reconstruct water depth extremely well, as >20% of diatom community variance within a lake can be explained by

depth (Kingsbury, Laird and Cumming, 2012; Ma *et al.*, 2013; Gushulak *et al.*, 2017; this study).

Lake response to climate change

The lake-landscape position of Cheney Lake makes it extremely susceptible to small fluctuations in precipitation and evapotranspiration (P/E) (Almendinger, 1990; Webster *et al.*, 1996). The main drivers of lake water depth change in Cheney Lake are likely fluctuations in P/E driven by winter precipitation and summer temperatures, because the precipitation evaporation fraction is smaller in the winter versus summer (Shuman *et al.*, 2005). Because Cheney Lake's depth is highly responsive to fluctuations in P/E, it is a good site for high-resolution climate reconstructions.

The focal periods (zones 1-4) that we identify in our ~3500 year record are the late-Holocene wet/cool period (3500-1500 cal. yr BP), the MCA (~1500 to 700 cal. yr BP), the LIA (700-0 cal. yr BP) and the more recent Anthropocene period. It is widely accepted that the late-Holocene was wetter and cooler than the previous warmer/drier periods from 9000 to 4000 cal. yr BP (Grimm *et al*., 2011, Gavin *et al*., 2011). From about 4000 cal. yr BP to the onset of the MCA at ~1500 cal. yr BP, climate in the western hemisphere was probably variable with moderately increasing moisture and temperature regimes (Steig, 1999; Calcote, 2003; Gavin *et al.*, 2011; Grimm, Donovan and Brown, 2011). However, model results at Cheney Lake suggest that from 3500 to 1500 cal. yr BP lake levels were between 4-6 meters higher than they are presently, a large departure from modern lake levels. These

high lake levels during the late-Holocene are consistent with other climate reconstructions including some based on diatom-depth models (Laird and Cumming 2008, 2009; Shuman and Marsicek, 2016) and suggest the lake may have been much larger before the late-Holocene cool period. Our reconstructions of lake size indicate the Cheney basin could support a lake that was up to 6 m deeper. During the MCA, climate in the western hemisphere was most likely warmer/drier than the previous ~4000 years, for example notably drier in the western half of North America (Osborn and Briffa, 2006; Stine 1994). Diatom-based climate reconstructions using both lake levels and salinities also indicate that the MCA climate was drier throughout the Great Plains region, west of the prairie-forest border (Fritz *et al*., 2000; Hobbs *et al*., 2011).

The LIA is a more perplexing variable in its global impact and there are many conflicting narratives in the western Great Lakes region as to when the LIA began and ended (Fritz *et al*., 2000; Mathews and Briffa, 2005; Shuman and Marsicek, 2016; Shuman *et al*. 2009). In Cheney Lake, the LIA was likely cooler and most likely wetter as lake levels rebounded from their MCA low stage.

The Anthropocene is possible to characterize, to larger spatial scales, with the use of surface temperature climate model reconstructions to describe climate patterns over the last ~100 years (St. George and Nielsen, 2002). Based on inferred lower lake levels since 0 cal. yr BP, Cheney Lake data suggest that local climate has become warmer and drier since the mid-twentieth century, consistent with Northern Hemisphere climate reconstructions (Mann et al., 1998).

Regional synthesis

Climate reconstructions based on diatom derived modeling indicate that lake levels have been highly responsive to climate change over the last ~3500 years (Laird *et al.*, 2011). The sediment record from Cheney Lake preserves a high-resolution climate record from the late-Holocene wet period (~3500-1500 cal. yr BP) to present day.

The late-Holocene wet period is characterized by higher water levels and greater abundance of deeper water planktonic diatom species, notably *Lindavia radiosa* and *Aulacoseira ambigua* at Cheney Lake. There are numerous studies that have characterized the mid-Holocene in the western Great Lakes region as drier than the last ~4000 years. Moisture increased throughout the region, however, between 4000-3000 BP (Grimm, 1983; Davis *et al.*, 1998, 2000; Delcourt *et al.*, 2002; Calcote, 2003; Nelson and Hu, 2008) resulting in higher lake levels at multiple sites throughout the western Great Lakes region (Brugam, Grimm and Eyster-Smith, 1988; Brugam, 1993; Brugam, McKeever and Kolesa, 1998; Brugam, Owen and Kolesa, 2004).

A decrease in white pine (*Pinus strobus*) and increased benthic diatom taxa at Crooked Lake occurred at the beginning of the late-Holocene wet period (Brugam et al. 1998). Additionally, an increase in planktonic diatoms (*Stephanodiscus*) occurred around 4000 years ago. Regional expansion of peatlands and an increase in hemlock (*Tsuga)* pollen also occurred. The regional increase in *Tsuga* pollen has been interpreted as an increase in moisture (Davis *et al.*, 1986, 1998; Brugam, McKeever and Kolesa, 1998; Parshall, 2002; Ireland *et al.*, 2013).

Additional support for increased moisture after 4000 cal. yr BP comes from a study in the Big Woods region of Minnesota, where the climate was warm/dry during the mid-Holocene, and increased precipitation led to a rise in oak (*Quercus*) pollen between 4000 and 1100 years ago (Umbanhowar, 2004). Similarly, higher flood indices were recorded in stalagmites of the Spring Valley Caverns, Minnesota, between 3000, 2000, 1750 and 1500 cal. yr BP (Dasgupta *et al.*, 2010).

Previous diatom studies also find increased moisture after 4000 BP. Brugam *et* al. (2004) reported planktonic species like *Aulacoseira ambigua* were more prevalent at Glimmerglass Lake, Michigan, after 5000 cal. yr BP. Additionally, a climate reconstruction from Pagonia Bog Pond, Minnesota, shows that a period of peatland development occurred around 2000 cal. yr BP, indicating cooler/wetter conditions and the expansion of peatlands westward toward the prairie-forest border (Brugam and Swain, 2000). Moreover, higher charcoal accumulation rates near the prairie-forest border (Moon Lake, West Olaf Lake, Deep Lake, Steel Lake) MN from ~3500 to 2000 cal. yr BP indicate that there may have been wetter conditions and more available fuel on the landscape to burn (Nelson and Hu, 2008).

Most of the proxy evidence and climate interpretations concur with the onset of drier conditions beginning around 1500 cal. yr BP, consistent with our findings at Cheney Lake. At Cheney Lake, MCA lake levels decline (1500-700 cal. yr BP), as indicated by greater abundance of benthic diatom species, notably *Staurosira constrens* var. *venter* and multiple *Nitzschia* spp. Pollen records from the Wisconsin Sand Plains indicate large vegetation shifts at some sites ~1500 cal. yr BP, with decreased *Quercus* (oak) and increased xeric taxa (jack/red pine) (Lynch, Calcote

and Hotchkiss, 2006; Tweiten *et al.* 2009; Lynch *et al.*, 2014). Lake levels at Cheney Lake declined rapidly at the onset of the MCA, coincident with this vegetation change. Similar increases in jack/red pine pollen abundances and increased fire were recorded in the Minnesota Big Woods around 1100 BP, suggesting warmer/drier conditions in southern Minnesota, ~ 320 km SW of Cheney Lake (Umbanhowar, 2004).

Other studies also suggest drier conditions during the MCA in this region. Diatom based proxy records from Lily Lake, MN show increased planktonic diatoms like *Melosira perglabra,* increased eutrophication, and higher levels of humic material indicating more arid conditions and declining lake levels during the MCA (Brugam, Grimm and Eyster-Smith, 1988). A recent study at Wolsfeld Lake, Minnesota, shows low lake level events from sand/high inorganic sediment constituents beginning around 950 cal. yr BP, consistent with sand lenses found in core 5 (Fig. 1; Shuman *et al.*, 2009). Ombrotrophic peatlands at both Hole-in-the-Bog, Minnesota, and Minden Bog, Michigan, show declines in peat formation and an increase in the depth to water table from around 1000 to 700 cal. yr. BP (Booth *et al.*, 2006).

Lake levels rebound in Cheney Lake to about 3.5 m during the LIA from around 700 to 0 cal. yr BP. A different assemblage of benthic diatom species, most notably Staurosira constrens var. venter, Eolimna minima and Achnanthidium minutissimum, characterizes the LIA increase in lake levels at Cheney Lake. Other studies on the northwest Wisconsin Sand Plain also suggest increased moisture during the LIA. White pine pollen increases and jack/red pine declines at roughly

the same time, indicating an increase in moisture availability (Lynch, Calcote and Hotchkiss, 2006; Hotchkiss, Calcote and Lynch, 2007; Lynch *et al.*, 2014). Similarly, a testate amoebae and pollen study shows increased moisture balance and increased white pine pollen from around 700 to 100 cal. yr BP (Tweiten *et al.*, 2009).

Cheney Lake diatom communities transition from littoral zone habitats to mid-depth benthic habitats when lake salinities also decline across North Dakota (Fritz *et al.*, 2000; Hobbs, Fritz, *et al.*, 2011). Another pollen-based study exhibits similar timing and extent of white pine pollen increases at Lake of the Clouds, Minnesota, suggesting the climate was both cooler/wetter (Swain, 1978).

One recent study, however, at Wolsfeld Lake and Bufflehead Pond, Minnesota, has hypothesized that the region remained dry well into the LIA with a gradual increase in moisture over the last 600 years (Shuman et al., 2009). Big Woods pollen types such as *Ostrya* and *Acer* increase while lake levels are still low (Shuman *et al.*, 2009). Contrary to most regional paleolimnological studies, the study at Wolsfeld Lake and Bufflehead Pond does present compelling LOI and pollen evidence (Shuman *et al.*, 2009) for lower lake levels occurring well after most studies agree that moisture availability increased.

The last ~60 years of lake level change at Cheney Lake represents significant change in response to the Anthropocene. The decline in lake levels to almost as low as the MCA is characterized by an unusual diatom assemblage, most notably small planktonic diatom taxa, *Discotella stelligera* and *D. pseudostelligera,* as well as an increase in benthic attached taxa like *Achnanthidium minutissimum.* This diatom assemblage maybe caused by other environmental factors not related to changes in

depth. Two lakes in Minnesota (Lake Mina and Elk Lake) show that along with increases in ragweed pollen (*Ambrosia* type) no overall change in varve thickness (except for the 1930s dust bowl) occurred during the last ~60 years (St. Jacques, Cumming and Smol, 2008). Most studies across the western Great Lakes region do in fact have declines in white pine pollen and increased *Ambrosia* pollen that cannot be linked to climate, but rather Anthropogenic logging land disturbance (Swain, 1978; Grimm, 1984; Gajewski, Winkler and Swain, 1985) .

Studies using more paleohydrologically-oriented proxies, however, can help overcome a muddied climate signal in pollen based studies. A testate amoebae-based peatland study at Hole-in-the-Bog, Minnesota, and Minden Bog, Michigan, indicates that from approximately 0 cal. yr BP to present drier conditions persisted with increased depth to water table measurements, suggesting lower overall water availability across the western Great Lakes region (Booth *et al.*, 2006). On the contrary, at Spring Valley Caverns stalagmites record high flood index values for the last several hundred years indicating higher than average water availability in southeastern Minnesota (Dasgupta *et al.*, 2010). Climate-driven increases in flood frequency and magnitude over the last several hundred years are consistent with other flood-based hydrological models for the western Great Lakes region (Knox, 1993; Pinter *et al.*, 2008). Higher frequency flooding due to heavy rain events is thought to be coupled with anthropogenic driven changes in atmospheric composition and increasing global temperatures (Milly *et al.*, 2002). Magnuson *et al.* (1997) indicates that throughout the Laurentian Great Lakes system increased precipitation does not necessarily translate to higher than average lake levels;

multiple hydrological models show declines in lake levels throughout the region in response to higher evapotranspiration due to increases in global surface temperatures, an observation supported by our Cheney Lake reconstruction.

Conversely, relatively high LOI values, where there is little change in the sediment composition with respect to changes in percent organic material, at Cheney Lake indicate the possibility of positive moisture balance for the last 1500 years (Fig. 1; Calcote *et al*., 2018 in prep). Interpreting LOI records can and does prove difficult with respect to fluctuations at the 'sediment limit' when a lake responds to long-term variability in water balance (Shuman, 2003). The sediment limit concept is discussed in detail in Shuman (2003). LOI variation in organic material is not clearly linked to productivity in oligotrophic systems where nutrients do not fluctuate frequently.

Whereas there is variation in the types of proxies and the spatial and temporal resolution of paleolimnological studies in the western Great Lakes region, there is a coherent story to be gleaned. For the most part there is broad agreement across multiple study sites and proxies that the mid-Holocene was warmer and drier than the late Holocene, and that it was followed by a rapid increase in moisture availability after 4000 cal. yr BP. The climate was also warmer and/or drier during the MCA, beginning around 1500 cal. yr BP and ending near 700 cal. yr BP. Moisture availability increased again during the LIA, and the vegetation responded in a manner consistent with wetter conditions.

Lastly, the Anthropocene is somewhat more difficult to characterize based on proxies directly bound to anthropogenic processes, specifically the clearance of land

for agriculture and development. Furthermore, it is clear that anthropogenic land processes have impacted Cheney Lake and others, and indicates that a lower lake level state-change may persist because of these anthropogenic land processes coupled with projected rapid climate change in the near future.

Acknowledgements:

I thank Chris Nevala-Plegeman (Luther College, Decorah, IA) for his help with Cheney Lake LOI and GPR analysis. Suggestions from reviewers improved this paper. The LacCore facility at the University of Minnesota provided equipment, facilities, initial core description, sediment analysis and core archiving. We thank colleagues at the St. Croix Watershed Research Station for the use of their lab and equipment, and also many conversations about statistical analysis. This material is based on work supported by the National Science Foundation under Grant DEB-0816762 to R. Calcote. Additional funding provided by the Conservation Sciences Graduate Program, University of Minnesota and Iowa Lakeside Laboratory, Iowa State University and University of Iowa.

References

Adrian, R. et al. (2009) 'Lakes as sentinels of climate change', Limnology and Oceanography, 54(6part2), pp. 2283–2297. doi: 10.4319/lo.2009.54.6_part_2.2283.

Almendinger, J. (1992) 'The Late Holocene History of Prairie, Brush-Prairie, and Jack Pine (Pinus banksiana) Forest on Outwash Plains, North-Central Minnesota, USA', The Holocene, 2(1), pp. 37–50. doi: 10.1177/095968369200200105.

Almendinger, J. (1990) 'Groundwater control of closed-basin lake levels under steady-state conditions', Journal of Hydrology, 112(3–4), pp. 293–318. doi: x

Almendinger, J. and Leete, J. H. (1998) 'Peat characteristics and groundwater geochemistry of calcareous fens in the Minnesota River Basin, U.S.A', Biogeochemistry (Dordrecht), 43(1), pp. 17–41. doi: 10.1023/A:1005905431071.

Antoniades, D. et al. (2008) Freshwater diatoms of the Canadian High Arctic Islands: Ellef Ringnes, northern Ellesmere and Prince Patrick islands. Iconographia Diatomologica.

Armstrong, W. H., Collins, M. J. and Snyder, N. P. (2014) 'Hydroclimatic flood trends in the northeastern United States and linkages with large-scale atmospheric circulation patterns', Hydrological Sciences Journal, 59(9), pp. 1636–1655. doi: 10.1080/02626667.2013.862339.

Bennett, K. D. (1996) 'Determination of the number of zones in a biostratigraphical sequence', New Phytologist, 132(1), pp. 155–170. doi: 10.1111/j.1469-8137.1996.tb04521.x.

Blaauw, M. and Christeny, J. A. (2011) 'Flexible paleoclimate age-depth models using an autoregressive gamma process', Bayesian Analysis, 6(3), pp. 457–474. doi: 10.1214/11-BA618.

Booth, R. K. (2002) 'Testate amoebae as paleoindicators of surface-moisture changes on Michigan peatlands: Modern ecology and hydrological calibration', Journal of Paleolimnology, 28(3), pp. 329–348. doi: 10.1023/A:1021675225099.

Booth, R. K., Jackson, S. T. and Thompson, T. A. (2002) 'Paleoecology of a Northern Michigan Lake and the relationship among climate, vegetation, and Great Lakes water levels', Quaternary Research, 57(1), pp. 120–130. doi: 10.1006/qres.2001.2288.

Booth, R. K. et al. (2006) 'Widespread drought episodes in the western Great Lakes region during the past 2000 years: Geographic extent and potential mechanisms', Earth and Planetary Science Letters, 242(3–4), pp. 415–427. doi: 10.1016/j.epsl.2005.12.028.

Brugam, R. B. (1993) Surface sample analogues of Elk Lake fossil diatom assemblages, Special Paper of the Geological Society of America. doi: 10.1130/SPE276-p189.

Brugam, R. B., Grimm, E. C. and Eyster-Smith, N. M. (1988) 'Holocene environmental changes in Lily Lake, minnesota inferred from fossil diatom and pollen assemblages', Quaternary Research, 30(1), pp. 53–66. doi: 10.1016/0033-5894(88)90087-7.

Brugam, R. B., McKeever, K. and Kolesa, L. (1998) 'A diatom-inferred water depth reconstruction for an Upper Peninsula, Michigan, lake', Journal of Paleolimnology, 20(3), pp. 267–276. doi: 10.1023/A:1007948616511.

Brugam, R. B., Owen, B. and Kolesa, L. (2004) 'Continental-scale climate forcing factors and environmental change at Glimmerglass Lake in the Upper Peninsula of Michigan', Holocene, 14(6), pp. 807–817. doi: 10.1191/0959683604hl761rp.

Calcote, R. (2003) 'Mid-Holocene climate and the hemlock decline: The range limit of Tsuga canadensis in the western Great Lakes region, USA', Holocene, 13(2), pp. 215–224. doi: 10.1191/0959683603hl608rp.

Camburn, K. and Charles, D. (2000) Diatoms of Low-Alkalinity Lakes in the Northeastern United States (Academy of Natural Sciences of Philadelphia Special Publication). Philadelphia: Academy of Natural Sciences.

Carpenter, S. R., Stanley, E. H. and Vander Zanden, M. J. (2011) 'State of the World's Freshwater Ecosystems: Physical, Chemical, and Biological Changes', Annual Review of Environment and Resources, 36(1), pp. 75–99. doi: 10.1146/annurev-environ-021810-094524.

Case, R. A. and MacDonald, G. M. (2003) 'TREE RING RECONSTRUCTIONS OF STREAMFLOW FOR THREE CANADIAN PRAIRIE RIVERS1', JAWRA Journal of the American Water Resources Association, 39(3), pp. 703–716. doi: 10.1111/j.1752-1688.2003.tb03686.x.

Clark, J. S. et al. (2001) 'Ecological forecasts: An emerging imperative', Science, pp. 657–660. doi: 10.1126/science.293.5530.657.

Clark, J. S. (1993) 'Fire, climate change, and forest processes during the past 2000 years', Geological Society of America Special Papers, 276, pp. 295–308. doi: 10.1130/SPE276-p295.

Clark, J. S. (1990) 'Fire and climate change during the last 750 yr in northwestern Minnesota', Ecological Monographs, 60(2), pp. 135–159. doi: 10.2307/1943042.

Clark, J. S. et al. (2001) 'Effects of Holocene climate change on the C4 grassland/woodland boundary in the Northern Plains, USA', Ecology, 82(3), pp. 620–636. doi: 10.1890/0012-9658(2001)082[0620:EOHCCO]2.0.CO;2.

Cook, B. I., Miller, R. L. and Seager, R. (2009) 'Amplification of the North American "Dust Bowl" drought through human-induced land degradation', Proceedings of the National Academy of Sciences, 106(13), pp. 4997–5001. doi: 10.1073/pnas.0810200106.

Crutzen, P. J. and Stoermer, E. F. (2000) 'The Anthropocene', IGBP [International Geosphere-Biosphere Programme] Newsletter, 41(17), p. No page numbers given.

Dasgupta, S. et al. (2010) 'Three thousand years of extreme rainfall events recorded in stalagmites from Spring Valley Caverns, Minnesota', Earth and Planetary Science Letters, 300(1–2), pp. 46–54. doi: 10.1016/j.epsl.2010.09.032.

Davis, M. B. et al. (1986) 'Dispersal versus climate: Expansion of Fagus and Tsuga into the Upper Great Lakes region', Vegetatio, 67(2), pp. 93–103. doi: 10.1007/BF00037360.

Davis, M. B. et al. (1998) 'Patchy invasion and the origin of a hemlock-hardwoods forest mosaic', Ecology, 79(8), pp. 2641–2659. doi: 10.1890/0012-9658(1998)079[2641:PIATOO]2.0.CO;2.

Davis, M. et al. (2000) 'Holocene climate in the western Great Lakes National Parks and Lakeshores: Implications for future climate change', Conservation Biology, 14(4), pp. 968–983. doi: 10.1046/j.1523-1739.2000.99219.x.

Dean, W. E. et al. (1994). A high-resolution record of climatic change in Elk Lake, Minnesota for the last 1500 years. Denver.

Dean, W. E. (1997) 'Rates, timing, and cyclicity of Holocene eolian activity in north-central United States: Evidence from varved lake sediments', Geology, 25(4), pp. 331–334. doi: 10.1130/0091-7613(1997)025<0331:RTACOH>2.3.CO;2.

Delcourt, P. A. et al. (2002) 'Holocene lake-effect precipitation in northern Michigan', Quaternary Research, 57(2), pp. 225–233. doi: 10.1006/qres.2001.2308.

Digerfeldt, G. (1986) 'Studies on past lake-level fluctuations', in Berglund, B. ((ed.) Handbook of Holocene paleoecology and palaeohydrology. Wiley & Sons, Chichester, pp. 127–143.

Doak, D. F. et al. (2008) 'Understanding and predicting ecological dynamics: Are major surprises inevitable?', Ecology, pp. 952–961. doi: 10.1890/07-0965.1.

Edlund, M. B. et al. (2009) 'Twentieth century eutrophication of the St. Croix River (Minnesota-Wisconsin, USA) reconstructed from the sediments of its natural impoundment', Journal of Paleolimnology, 41(4), pp. 641–657. doi: 10.1007/s10933-008-9296-1.

Ewing, H. A. (2000) Ecosystem development and response to climatic change: a comparative study of forest-lake ecosystems on different substrates. University of Minnesota.

Fritz, S. C., Juggins, S. and Battarbee, R. W. (1993) 'Diatom Assemblages and Ionic Characterization of Lakes of the Northern Great Plains, North America: A Tool for Reconstructing Past Salinity and Climate Fluctuations', Canadian Journal of Fisheries and Aquatic Sciences, 50(9), pp. 1844–1856. doi: 10.1139/f93-207.

Fritz, S. C. et al. (2010) 'Diatoms as indicators of hydrologic and climatic change in saline lakes', in The Diatoms: Applications for the Environmental and Earth Sciences, Second Edition, pp. 186–208. doi: 10.1017/CBO9780511763175.011.

Fritz, S. C. et al. (2000) 'Hydrologic variation in the northern Great Plains during the last two millennia', Quaternary Research, 53(2), pp. 175–184. doi: 10.1006/qres.1999.2115.Gajewski, K. (1988) 'Late holocene climate changes in eastern North America estimated from pollen data', Quaternary Research, 29(3), pp. 255–262. doi: 10.1016/0033-5894(88)90034-8.

Gajewski, K. (1988) 'Late Holocene climate changes in eastern North America estimated from pollen data', Quaternary Research, 29(3), pp. 255–262. doi: 10.1016/0033-5894(88)90034-8.

Gajewski, K., Winkler, M. G. and Swain, A. M. (1985) 'Vegetation and fire history from three lakes with varved sediments in northwestern Wisconsin (U.S.A.)', Review of Palaeobotany and Palynology, 44(3–4), pp. 277–292. doi: 10.1016/0034-6667(85)90021-1.

Gavin, D. G. et al. (2011) 'Abrupt Holocene climate change and potential response to solar forcing in western Canada', Quaternary Science Reviews, 30(9–10), pp. 1243–1255. doi: 10.1016/j.quascirev.2011.03.003.

Grimm, E. C. (1984) 'Fire and Other Factors Controlling the Big Woods Vegetation of Minnesota in the Mid-Nineteenth Century', Ecological Monographs, 54(3), pp. 291–311. doi: 10.2307/1942499.

Grimm, E. C. (1983) ‘Chronology And Dynamics Of Vegetation Change In The Prairie‐Woodland Region Of Southern Minnesota, U.S.A.’, New Phytologist, 93(2), pp. 311–350. doi: 10.1111/j.1469-8137.1983.tb03434.x.

Grimm, E. C. (1987) ‘Constrained Cluster Analysis By the Method of Incremental Sum of Squares’, Computers and Geosciences, 13(1), pp. 13–35. doi: 10.1016/0098-3004(87)90022-7.

Grimm, E. C., Donovan, J. J. and Brown, K. J. (2011) ‘A high-resolution record of climate variability and landscape response from Kettle Lake, northern Great Plains, North America’, Quaternary Science Reviews, 30(19–20), pp. 2626–2650. doi: 10.1016/j.quascirev.2011.05.015.

Gushulak, C. A. C. et al. (2017) ‘Water depth is a strong driver of intra-lake diatom distributions in a small boreal lake’, Journal of Paleolimnology, 58(2), pp. 231–241. doi: 10.1007/s10933-017-9974-y.

He, H. S., Mladenoff, D. J. and Crow, T. R. (1999) ‘Linking an ecosystem model and a landscape model to study forest species response to climate warming’, Ecological Modeling, 114(2–3), pp. 213–233. doi: 10.1016/S0304-3800(98)00147-1.

Hobbs, W. O. et al. (2011) ‘Environmental history of a closed-basin lake in the US Great Plains: Diatom response to variations in groundwater flow regimes over the last 8500 cal. yr BP’, Holocene, 21(8), pp. 1203–1216. doi: 10.1177/0959683611405242.

Hobbs, W. O. et al. (2011) ‘Biogeochemical responses of two alpine lakes to climate change and atmospheric deposition, Jasper and Banff National parks, Canadian Rocky Mountains’, Canadian Journal of Fisheries and Aquatic Sciences, 68(8), pp. 1480–1494. doi: 10.1139/f2011-058.

Hoffmann, G., Lange-Bertalot, H. and Werum, M. (2006) Diatomeen im Süßwasser-Benthos von Mitteleuropa: Bestimmungsflora Kieselalgen für die ökologische Praxis; über 700 der häufigsten Arten und ihrer Ökologie. 1st edn. Edited by H. Lange-Bertalot. Konigstein: Koeltz Scientific Books.

Hotchkiss, S. C., Calcote, R. and Lynch, E. A. (2007) ‘Response of vegetation and fire to Little Ice Age climate change: Regional continuity and landscape heterogeneity’, Landscape Ecology, 22(SUPPL. 1), pp. 25–41. doi: 10.1007/s10980-007-9133-3.

Ireland, A. W. et al. (2013) ‘A comparative study of within-basin and regional peatland development: Implications for peatland carbon dynamics’, Quaternary Science Reviews, 61, pp. 85–95. doi: 10.1016/j.quascirev.2012.10.035.

Jackson, S. T. and Hobbs, R. J. (2009) ‘Ecological restoration in the light of ecological history’, Science, pp. 567–569. doi: 10.1126/science.1172977.

Jensen, K. et al. (2007) 'Interpretation of charcoal morphotypes in sediments from Ferry Lake, Wisconsin, USA: Do different plant fuel sources produce distinctive charcoal morphotypes?', Holocene, 17(7), pp. 907–915. doi: 10.1177/0959683607082405.

Juggins, S. (2013) 'Quantitative reconstructions in palaeolimnology: New paradigm or sick science?', Quaternary Science Reviews, pp. 20–32. doi: 10.1016/j.quascirev.2012.12.014.

Juggins, S. (2017) 'rioja: Analysis of Quaternary Science Data, R package version (0.9-15.1)'.

Juggins, S. and Birks, H. J. B. (2012) 'Quantitative environmental reconstructions from biological data', in Tracking Environmental Change Using Lake Sediments, Data Handling and Numerical Tehcnqiues, pp. 431–494. doi: 10.1007/0-306-47669-X.

Juggins, S. et al. (2013) 'Reconstructing epilimnetic total phosphorus using diatoms: Statistical and ecological constraints', Journal of Paleolimnology, 49(3), pp. 373–390. doi: 10.1007/s10933-013-9678-x.

Kingsbury, M. V., Laird, K. R. and Cumming, B. F. (2012) 'Consistent patterns in diatom assemblages and diversity measures across water-depth gradients from eight Boreal lakes from north-western Ontario (Canada)', Freshwater Biology, 57(6), pp. 1151–1165. doi: 10.1111/j.1365-2427.2012.02781.x.

Knox, J. C. (1993) 'Large increases in flood magnitude in response to modest changes in climate', Nature, 361(6411), pp. 430–432. doi: 10.1038/361430a0.

Krammer, K. (2003) Cymbopleura, Delicata, Navicymbula, Gomphocymbellopsis, Afrocymbella. In: Diatoms of Europe, Diatoms of the European Inland waters and comparable habitats. 4th edn. Edited by H. Lange-Bertalot. Rugell: A.R.G. Gantner Verlag K.G.

Krammer, K. and Lange-Bertalot, H. (1986) Bacillariophyceae. 1. Teil: Naviculaceae, Süßwasserflora von Mitteleuropa. Available at: http://www.springer.com/br/book/9783827426154.

Krammer, K. and Lange-Bertalot, H. (1988) Bacillariophyceae. 2. Teil: Bacillariaceae, Epithemiaceae, Surirellaceae, SüBwasserflora von Mitteleuropa. doi: 10.1016/0304-3770(90)90067-U.

Krammer, K. and Lange-Bertalot, H. (1991) Bacillariophyceae Teil 4: Achnanthaceae, Kritische Ergänzungen zu Achnanthes s.l., Navicula s.str., Gomphonema, Süssewasserflora von Mitteleurope. 2nd edn. Edited by E. D. Ettl, H; Gerloff, J; Heynig, H; Mollenhauer. Stuttgart: Gustav Fischer Verlag.

Krammer, K. and Lange-Bertalot, H. (1991) Bacillariophyceae 3. Teil: Centrales, Fragilariaceae, Eunotiaceae, Süßwasserflora von Mitteleuropa. Available at: http://www.springer.com/br/book/9783827419125.

Laird, K. R. et al. (2003) 'Lake sediments record large-scale shifts in moisture regimes across the northern prairies of North America during the past two millennia', Proceedings of the National Academy of Sciences, 100(5), pp. 2483–2488. doi: 10.1073/pnas.0530193100.

Laird, K. R. and Cumming, B. F. (2009) 'Diatom-inferred lake level from near-shore cores in a drainage lake from the Experimental Lakes Area, northwestern Ontario, Canada', Journal of Paleolimnology, 42(1), pp. 65–80. doi: 10.1007/s10933-008-9248-9.

Laird, K. R. and Cumming, B. F. (2008) 'Reconstruction of Holocene lake level from diatoms, chrysophytes and organic matter in a drainage lake from the Experimental Lakes Area (northwestern Ontario, Canada)', Quaternary Research, 69(2), pp. 292–305. doi: 10.1016/j.yqres.2007.11.003.

Laird, K. R., Fritz, S. C. and Cumming, B. F. (1998) 'A diatom-based reconstruction of drought intensity, duration, and frequency from Moon Lake, North Dakota: A sub-decadal record of the last 2300 years', Journal of Paleolimnology, 19(2), pp. 161–179. doi: 10.1023/A:1007929006001.

Laird, K. R. et al. (1996)a 'Century scale paleoclimatic reconstruction from Moon Lake, a closed-basin lake in the northern Great Plains', Limnology and Oceanography, 41(5), pp. 890–902. doi: 10.4319/lo.1996.41.5.0890.

Laird, K. R. et al. (1998) 'Early-Holocene limnological and climatic variability in the Northern Great Plains', The Holocene, 8(3), pp. 275–285. doi: 10.1191/095968398673895438.

Laird, K. R. et al. (1996)b 'Greater drought intensity and frequency before ad 1200 in the Northern Great Plains, USA', Nature, 384(6609), pp. 552–554. doi: 10.1038/384552a0.

Laird, K. R. et al. (2011) 'Diatom-inferred depth models in 8 Canadian boreal lakes: Inferred changes in the benthic:planktonic depth boundary and implications for assessment of past droughts', Quaternary Science Reviews, 30(9–10), pp. 1201–1217. doi: 10.1016/j.quascirev.2011.02.009.

Lavoie, I., Hamilton, P., Campeau, S., Grenier, M., Dillon, P. (2008) Guide d'identification des diatomées des rivières de l'Est du Canada. Laurier, Quebec: Presses De L'Universite` Du Que`bec.

LeBlanc, M., Gajewski, K. and Hamilton, P. B. (2004) 'A diatom-based Holocene palaeoenvironmental record from a mid-arctic lake on Boothia Peninsula, Nunavut, Canada', Holocene, 14(3), pp. 417–425. doi: 10.1191/0959683604hl717rp.

Legendre, P. and Gallagher, E. D. (2001) 'Ecologically meaningful transformations for ordination of species data', Oecologia, 129(2), pp. 271–280. doi: 10.1007/s004420100716.

Lynch, E. A., Calcote, R. and Hotchkiss, S. (2006) 'Late-Holocene vegetation and fire history from Ferry Lake, northwestern Wisconsin, USA', Holocene, 16(4), pp. 495–504. doi: 10.1191/0959683606hl945rp.

Lynch, E. A. et al. (2014) 'Presence of lakes and wetlands decreases resilience of jack pine ecosystems to late-Holocene climatic changes', Canadian Journal of Forest Research, 44(11), pp. 1331–1343. doi: 10.1139/cjfr-2014-0107.

Ma, S. et al. (2013) 'Diatom-inferred changes in effective moisture during the late Holocene from nearshore cores in the southeastern region of the Winnipeg River Drainage Basin (Canada)', Holocene, 23(4), pp. 568–578. doi: 10.1177/0959683612463103.

Magnuson, J. J. et al. (1997) 'Potential effects of climate changes on aquatic systems: Laurentian Great Lakes and Precambrian Shield region', Hydrological Processes, 11(8), pp. 825–871. doi: 10.1002/(SICI)1099-1085(19970630)11:8<825::AID-HYP509>3.0.CO;2-G.

Matthews, J. A. and Briffa, K. R. (2005) 'The "Little Ice Age": Re-Evaluation of an Evolving Concept', Geografiska Annaler: Series A, Physical Geography, 87(1), pp. 17–36. doi: 10.1111/j.0435-3676.2005.00242.x.

McAndrews, J. H. (1967) Quaternary Paleoecology: Pollen analysis and vegetational history of the Itasca region, Minnesota. Edited by H. E. J. Cushing, E.J. and Wright. New Haven: Yale University Press.

McAndrews, J. H. (1968) 'Pollen evidence for the protohistoric development of the "big woods" in Minnesota (U.S.A.)', Review of Palaeobotany and Palynology, 7(3), pp. 201–211. doi: 10.1016/0034-6667(68)90023-7.

Milly, P. C. D. et al. (2002) 'Increasing risk of great floods in a changing climate', Nature, 415(6871), pp. 514–517. doi: 10.1038/415514a.

Minckley, T. A., Whitlock, C. and Bartlein, P. J. (2007) 'Vegetation, fire, and climate history of the northwestern Great Basin during the last 14,000 years', Quaternary Science Reviews, 26(17–18), pp. 2167–2184. doi: 10.1016/j.quascirev.2007.04.009.

Moos, M. T., Laird, K. R. and Cumming, B. F. (2005) 'Diatom assemblages and water depth in Lake 239 (Experimental Lakes Area, Ontario): Implications for paleoclimatic studies', Journal of Paleolimnology, 34(2), pp. 217–227. doi: 10.1007/s10933-005-2382-8.

Moos, M. T., Laird, K. R. and Cumming, B. F. (2009) 'Climate-related eutrophication of a small boreal lake in northwestern Ontario: A palaeolimnological perspective', Holocene, 19(3), pp. 359–367. doi: 10.1177/0959683608101387.

Myrbo, A. et al. (2013) LacCore LOI standard operating procedure. Available at: http://lrc.geo.umn.edu/laccore/assets/pdf/sops/loi.pdf.

Nevala-Plageman, C. (2011) A late-Holocene history of fire and drought at Cheney Lake: has local climate affected fire regimes in northwestern Wisconsin? Senior Thesis project under supervision of E.A. Lynch, Luther College.

Nelson, D. M. and Hu, F. S. (2008) 'Patterns and drivers of Holocene vegetational change near the prairie-forest ecotone in Minnesota: Revisiting McAndrews' transect', New Phytologist, 179(2), pp. 449–459. doi: 10.1111/j.1469-8137.2008.02482.x.

Nguetsop, V. F., Servant-Vildary, S. and Servant, M. (2004) 'Late Holocene climatic changes in west Africa, a high resolution diatom record from equatorial Cameroon', Quaternary Science Reviews, 23(5–6), pp. 591–609. doi: 10.1016/j.quascirev.2003.10.007.

Noren, A. (2008) Limnological Research Center Core Facility SOP Series: Image Acquisition. Available at: http://lrc.geo.umn.edu/laccore/assets/pdf/sops/imageacquisition.pdf.

O'Reilly, C. M. et al. (2015) 'Rapid and highly variable warming of lake surface waters around the globe', Geophysical Research Letters, pp. 1–9. doi: 10.1002/2015GL066235.Received.

Parshall, T. (2002) 'Late Holocene stand-scale invasion by hemlock (Tsuga canadensis) at its western range limit', Ecology, 83(5), pp. 1386–1398. doi: 10.1890/0012-9658(2002)083[1386:LHSSIB]2.0.CO;2.

Patrick, R. and Reimer, C. W. (1966) The Diatoms of the United States, Exclusive of Alaska and Hawaii: Fragilariaceae, Eunotiaceae, Achnanthaceae, Naviculacae. Academy of Natural Sciences.

Patrick, R. and Reimer, C. W. (1975) 'The Diatoms of the United States', in Monographs of the Academy of Natural Sciences of Philadelphia, p. 213.

Paul, C. A., Rühland, K. M. and Smol, J. P. (2010) 'Diatom-inferred climatic and environmental changes over the last ~9000 years from a low Arctic (Nunavut, Canada) tundra lake', Palaeogeography, Palaeoclimatology, Palaeoecology, 291(3–4), pp. 205–216. doi: 10.1016/j.palaeo.2010.02.030.

Pinter, N. et al. (2008) 'Flood trends and river engineering on the Mississippi River system', Geophysical Research Letters, 35(23). doi: 10.1029/2008GL035987.

Pribyl, P. and Shuman, B. N. (2014) 'A computational approach to Quaternary lake-level reconstruction applied in the central Rocky Mountains, Wyoming, USA', Quaternary Research (United States), 82(1), pp. 249–259. doi: 10.1016/j.yqres.2014.01.012.

R Development Core Team (2016) 'R: A Language and Environment for Statistical Computing', R Foundation for Statistical Computing Vienna Austria, 0, p. {ISBN} 3-900051-07-0. doi: 10.1038/sj.hdy.6800737.

Radeloff, V. C. et al. (1999) 'Forest landscape change in the northwestern Wisconsin Pine Barrens from pre-European settlement to the present', Canadian Journal of Forest Research, 29(11), pp. 1649–1659. doi: 10.1139/x99-089.

Ramstack, J. et al. (2008) Diatom Monitoring Protocol, Version 1.0, National Parks Service Program.

Ramstack, J. M. et al. (2003) 'The application of a diatom-based transfer function to evaluate regional water-quality trends in Minnesota since 1970', Journal of Paleolimnology, 29(1), pp. 79–94. doi: 10.1023/A:1022869205291.

Ramstack, J. M., Fritz, S. C. and Engstrom, D. R. (2004) 'Twentieth century water quality trends in Minnesota lakes compared with presettlement variability', Canadian Journal of Fisheries and Aquatic Sciences, 61(4), pp. 561–576. doi: 10.1139/f04-015.

Renberg, I. and Hansson, H. (2008) 'The HTH sediment corer', Journal of Paleolimnology, 40(2), pp. 655–659. doi: 10.1007/s10933-007-9188-9.

Rühland, K. M., Paterson, A. M. and Smol, J. P. (2015) 'Lake diatom responses to warming: reviewing the evidence', Journal of Paleolimnology. doi: 10.1007/s10933-015-9837-3.

Saros, J. E. and Anderson, N. J. (2015) 'The ecology of the planktonic diatom Cyclotella and its implications for global environmental change studies', Biological Reviews, 90(2), pp. 522–541. doi: 10.1111/brv.12120.

Saros, J. E. et al. (2012) 'Climate-induced changes in lake ecosystem structure inferred from coupled neo- and paleoecological approaches', Ecology, 93(10), pp. 2155–2164. doi: 10.1890/11-2218.1.

Sauchyn, D. J. et al. (2003) 'A Paleoclimatic Context for the Drought of 1999-2001 in the Northern Great Plains of North America', Source: The Geographical Journal The Geographical Journal, 169(2), pp. 158–167. doi: 10.1111/1475-4959.05003.

Sayer, C. D. (2001) 'Problems with the application of diatom-total phosphorus transfer functions: Examples from a shallow English lake', Freshwater Biology, 46(6), pp. 743–757. doi: 10.1046/j.1365-2427.2001.00714.x.

Schindler, D. W. (2009) 'Lakes as sentinels and integrators for the effects of climate change on watersheds, airsheds, and landscapes', Limnology and Oceanography, 54(6part2), pp. 2349–2358. doi: 10.4319/lo.2009.54.6_part_2.2349.

Shinneman, A. L. C. et al. (2010) 'Inferring lake depth using diatom assemblages in the shallow, seasonally variable lakes of the Nebraska sand hills (USA): Calibration, validation, and application of a 69-lake training set', Journal of Paleolimnology, 44(2), pp. 443–464. doi: 10.1007/s10933-010-9427-3.

Shuman, B. (2003) 'Controls on loss-on-ignition variation in cores from two shallow lakes in the northeastern United States', Journal of Paleolimnology, 30(4), pp. 371–385. doi: 10.1023/B:JOPL.0000007226.68831.e3.

Shuman, B. N. and Marsicek, J. (2016) 'The structure of Holocene climate change in mid-latitude North America', Quaternary Science Reviews, 141, pp. 38–51. doi: 10.1016/j.quascirev.2016.03.009.

Shuman, B. et al. (2009) 'Woodland-to-forest transition during prolonged drought in Minnesota after ca. AD 1300', Ecology, 90(10), pp. 2792–2807. doi: 10.1890/08-0985.1.

Shuman, B. et al. (2005) 'A record of late-quaternary moisture-balance change and vegetation response from the White Mountains, New Hampshire', Annals of the Association of American Geographers, 95(2), pp. 237–248. doi: 10.1111/j.1467-8306.2005.00458.x.

Smol, J. and Stoermer, E. (2010) The diatoms : Applications for the environmental and earth sciences. 2nd edn. New York: Cambridge University Press.

St. George, S. and Nielsen, E. (2002) 'Hydroclimatic change in southern Manitoba since A.D. 1409 inferred from tree rings', Quaternary Research, 58(2), pp. 103–111. doi: 10.1006/qres.2002.2343.

St. Jacques, J. M., Cumming, B. F. and Smol, J. P. (2008) 'A 900-year pollen-inferred temperature and effective moisture record from varved Lake Mina, west-central Minnesota, USA', Quaternary Science Reviews, 27(7–8), pp. 781–796. doi: 10.1016/j.quascirev.2008.01.005.

Stancheva, R. and Sheath, R. G. (2012) 'THE DIATOMS: APPLICATIONS FOR THE ENVIRONMENTAL AND EARTH SCIENCES', Journal of Phycology. doi: 10.1111/j.1529-8817.2011.01095.x.

Steig, E. J. (1999) 'Mid-Holocene climate change', Science, pp. 1485–1487. doi: 10.1126/science.286.5444.1485.

Swain, A. M. (1978) 'Environmental changes during the past 2000 years in north-central Wisconsin: Analysis of pollen, charcoal, and seeds from varved lake sediments', Quaternary Research, 10(1), pp. 55–68. doi: 10.1016/0033-5894(78)90013-3.

ter Braak, C. J. F. and Barendregt, L. G. (1986) 'Weighted averaging of species indicator values: Its efficiency in environmental calibration', Mathematical Biosciences, 78(1), pp. 57–72. doi: 10.1016/0025-5564(86)90031-3.

ter Braak, C. J. F. and Looman, C. W. N. (1986) 'Weighted averaging, logistic regression and the Gaussian response model', Vegetatio, 65(1), pp. 3–11. doi: 10.1007/BF00032121.

Tian, J., Nelson, D. M. and Hu, F. S. (2006) 'Possible linkages of late-Holocene drought in the North American midcontinent to Pacific Decadal Oscillation and solar activity', Geophysical Research Letters, 33(23). doi: 10.1029/2006GL028169.

Tomkins, J. D. et al. (2008) 'A simple and effective method for preserving the sediment-water interface of sediment cores during transport', Journal of Paleolimnology, 40(1), pp. 577–582. doi: 10.1007/s10933-007-9175-1.

Tranvik, L. J. et al. (2009) 'Lakes and reservoirs as regulators of carbon cycling and climate', Limnology and Oceanography, 54(6part2), pp. 2298–2314. doi: 10.4319/lo.2009.54.6_part_2.2298.

Tweiten, M. A. et al. (2009) 'The response of a jack pine forest to late-Holocene climate variability in northwestern Wisconsin', Holocene, 19(7), pp. 1049–1061. doi: 10.1177/0959683609340993.

U.S. Geological Survey (2017) 1/3rd arc-second Digital Elevation Models (DEMs) USGS National Map 3DEP Downloadable Data Collection.

Umbanhowar, C. E. (2004) 'Interaction of fire, climate and vegetation change at a large landscape scale in the Big Woods of Minnesota, USA', Holocene, 14(5), pp. 661–676. doi: 10.1191/0959683604hl745rp.

Umbanhowar, C. E. et al. (2006) 'Asymmetric vegetation responses to mid-Holocene aridity at the prairie-forest ecotone in south-central Minnesota', Quaternary Research, 66(1), pp. 53–66. doi: 10.1016/j.yqres.2006.03.005.

Valero-Garcés, B. L. et al. (1997) 'Holocene Climate in the Northern Great Plains Inferred from Sediment Stratigraphy, Stable Isotopes, Carbonate Geochemistry, Diatoms, and Pollen at Moon Lake, North Dakota', Quaternary Research, 48(3), pp. 359–369. doi: 10.1006/qres.1997.1930.

WDNR, W. C. V. (2016) 'Cheney Lake, Bois Brule River Watershed (LS04)'.

WDNR: Ecological Landscapes of Wisconsin Handbook 1805. (2011) Bedrock Geologic Map of Wisconsin.

Webster, K. E. et al. (1996) 'The influence of landscape position on lake chemical responses to drought in northern Wisconsin', Limnology and Oceanography, 41(5), pp. 977–984. doi: 10.4319/lo.1996.41.5.0977.

WICCI (2011) 'Wisconsin Initiative on Climate Change Impacts Forestry Working Group Report. Wisconsin Initiative on Climate Change Impacts first report, Wisconsin's Changing Climate: Impacts and Adaptation'. Available at: https://www.wicci.wisc.edu/climate-change.php.

Williamson, C. E. et al. (2008) 'Lakes and streams as sentinels of environmental change in terrestrial and atmospheric processes', Frontiers in Ecology and the Environment, pp. 247–254. doi: 10.1890/070140.

Williamson, C. E., Saros, J. E. and Schindler, D. W. (2009) 'Climate change: Sentinels of change', Science, pp. 887–888. doi: 10.1126/science.1169443.

Williamson, C. E. et al. (2009) 'Lakes and reservoirs as sentinels, integrators, and regulators of climate change', Limnology and Oceanography, 54(6part2), pp. 2273–2282. doi: 10.4319/lo.2009.54.6_part_2.2273.

Wilson, J. B. and Agnew, A. D. Q. (1992) 'Positive feedback switches in plant communities', Advances in Ecological Research, 23, pp. 263–336. doi: 10.1016/S0065-2504(08)60149-X.

Woodhouse, C. A. and Overpeck, J. T. (1998) '2000 Years of Drought Variability in the Central United States', Bulletin of the American Meteorological Society, 79(12), pp. 2693–2714. doi: 10.1175/1520-0477(1998)079<2693:YODVIT>2.0.CO;2.

Yang, J. R. and Duthie, H. C. (1995) 'Regression and Weighted Averaging Models Relating Surficial Sedimentary Diatom Assemblages to Water Depth in Lake Ontario', Journal of Great Lakes Research, 21(1), pp. 84–94. doi: 10.1016/S0380-1330(95)71023-1.

Appendix A: Community Ecology

Figure A1: Unconstrained cluster diagram using hierarchical clustering of all Cheney lake diatom samples, Ward.D2 method with *squared* Euclidean distances. Purple line through dendrogram indicates where the clusters were divided into significant clusters according to *squared* Euclidean distance measure. Sample number is according to depth for samples 1-71, 72-89 is the surface sediment samples.

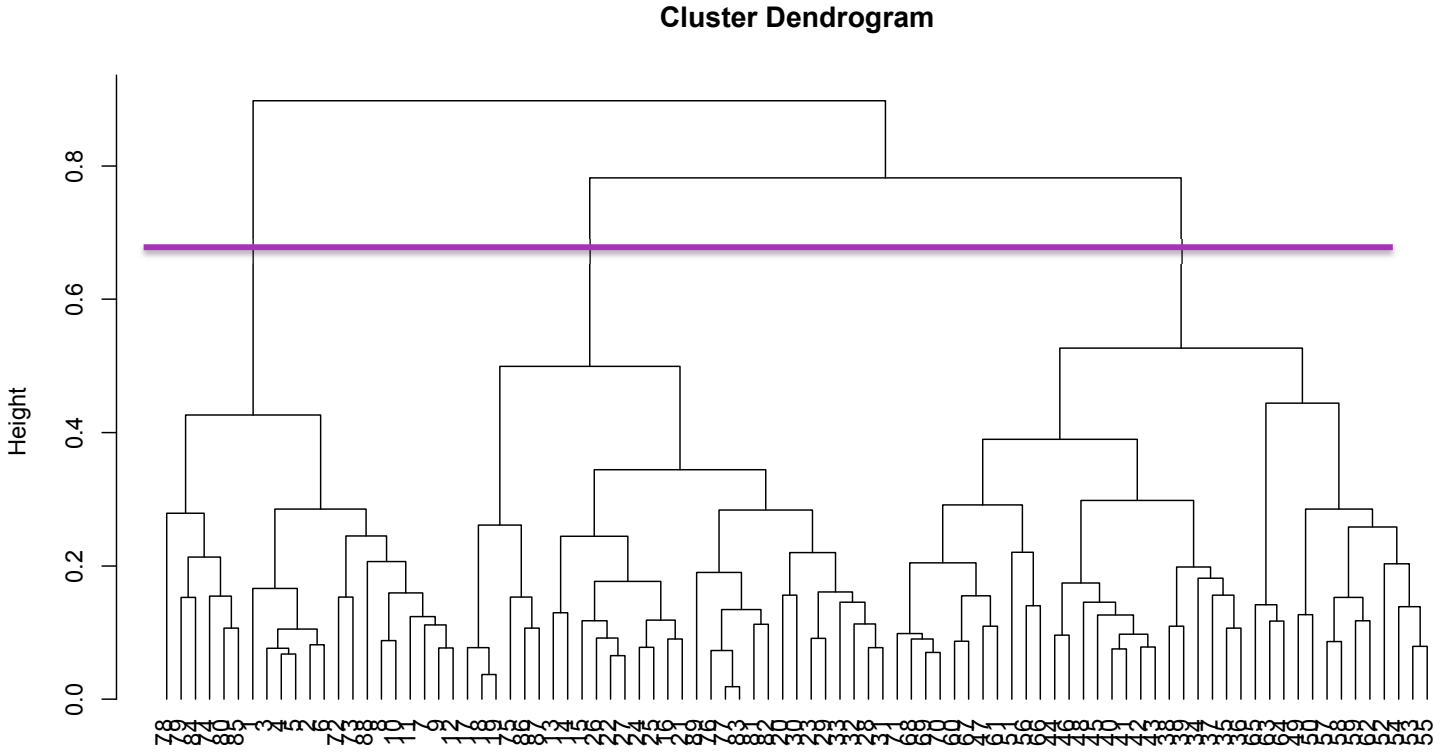

Figure A2: Bar plot of the most abundant taxa in all diatom samples arranged according to the zones determined by cluster analysis. Zone 1 is dominated by *Achnanthidium minutissimum* (ACHMINUT), Zone 2 is dominated by *Staurosira construens* var. *venter* (SRACONVE) and Zone 3 is dominated by *Staurosirella pinnata* (SLLPINNA) and *Lindavia radiosa* (CYCCOMRA).

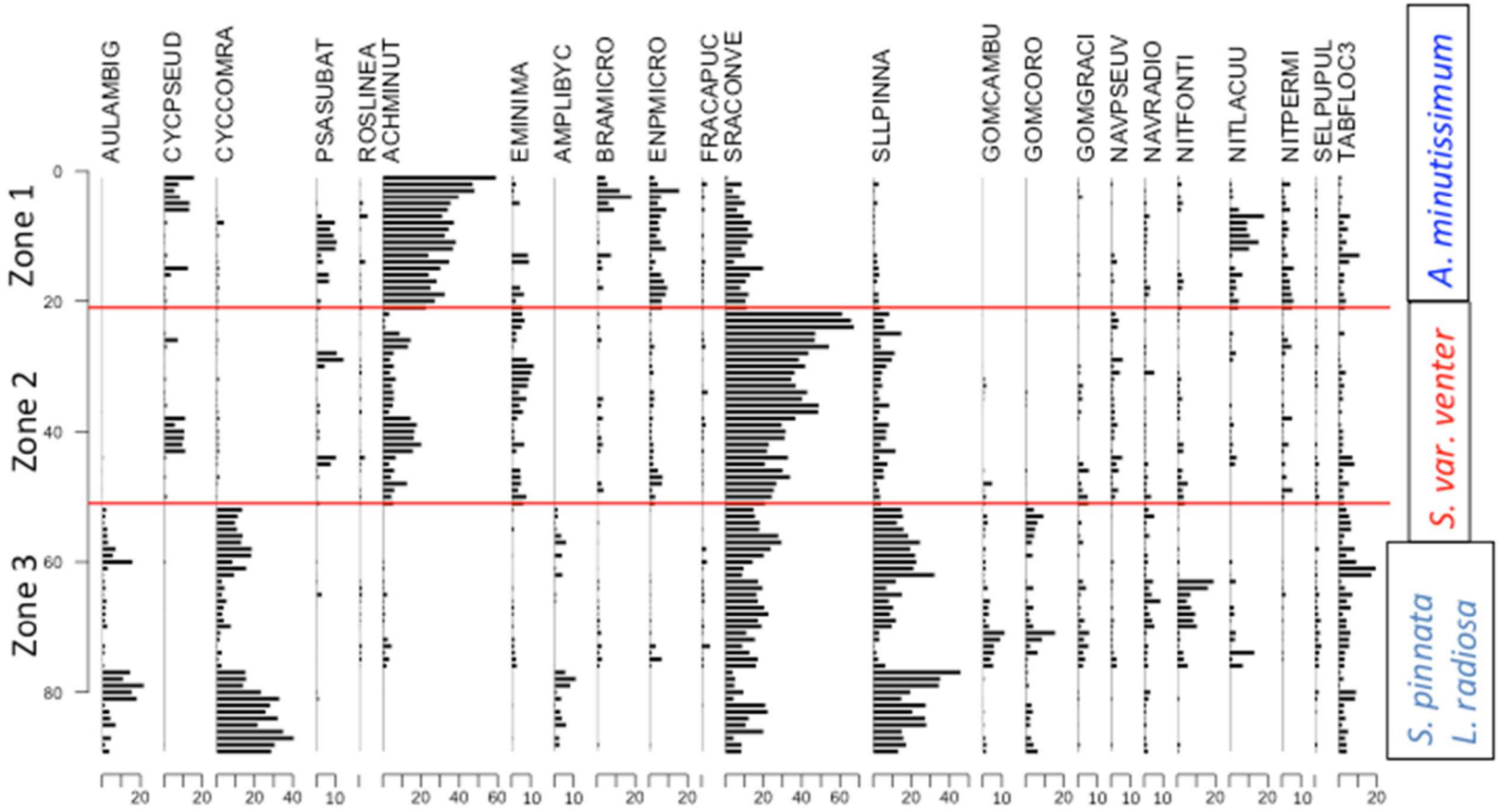

Figure A3: Unconstrained RDA (redundancy analysis) of fossil and surface samples combined, three significant zones. Zone 1 (blue) includes all the samples defined by the cluster analysis between the ages of 0 cal. yr BP and present, Zone 2 (red) includes all the samples between 0 and 700 cal. yr BP, Zone 3 (purple) includes all the samples between 700 and ~3500 cal. yr BP.

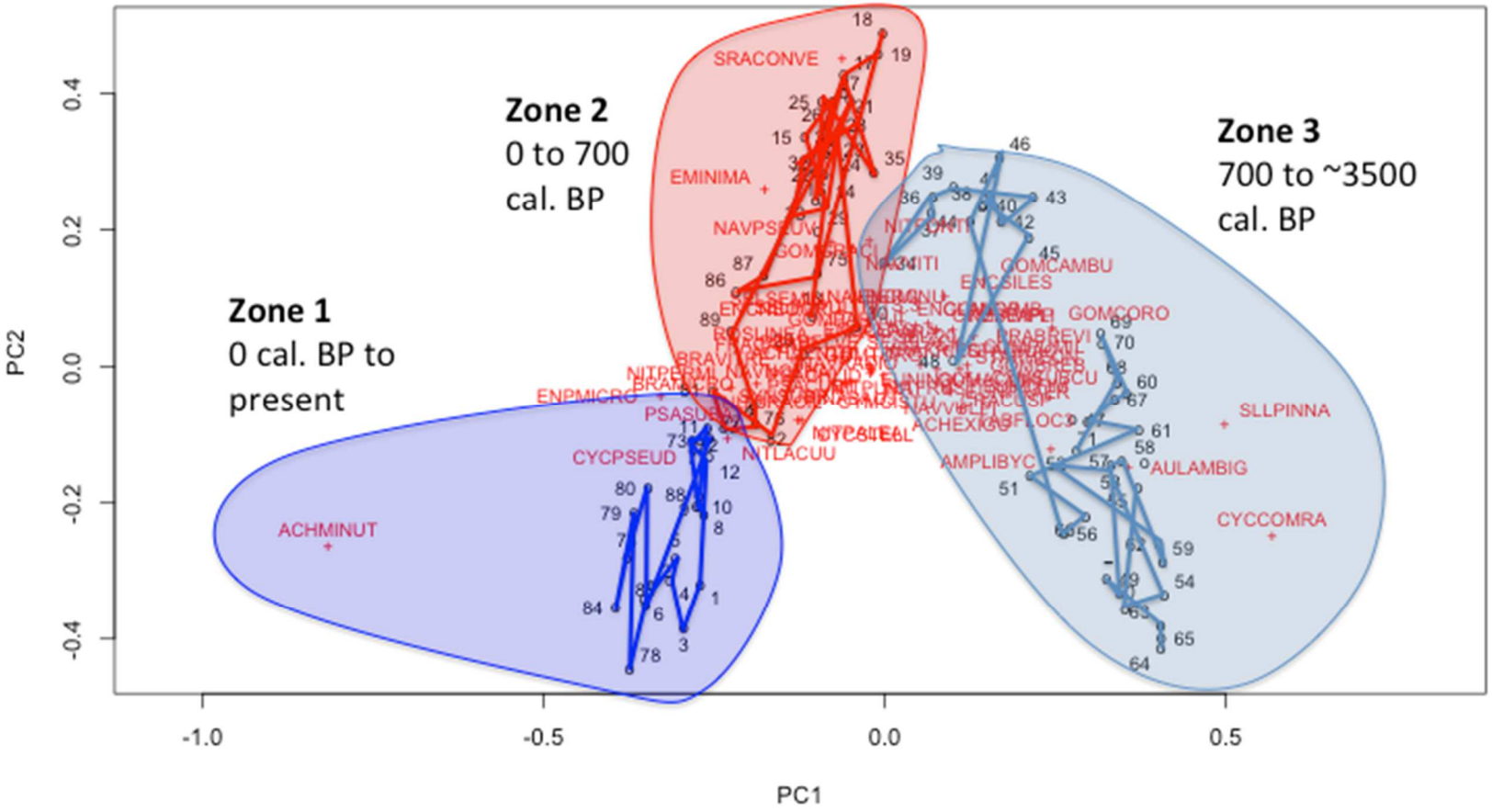

Figure A4: Constrained Cluster analysis (CONISS), cluster analysis for all 72 fossil diatom samples from core 5. The cluster analysis yielded 4 distinct groups by Euclidian distance measure, marked by red horizontal line. Samples are numbered according to depth (cm) in sediment.

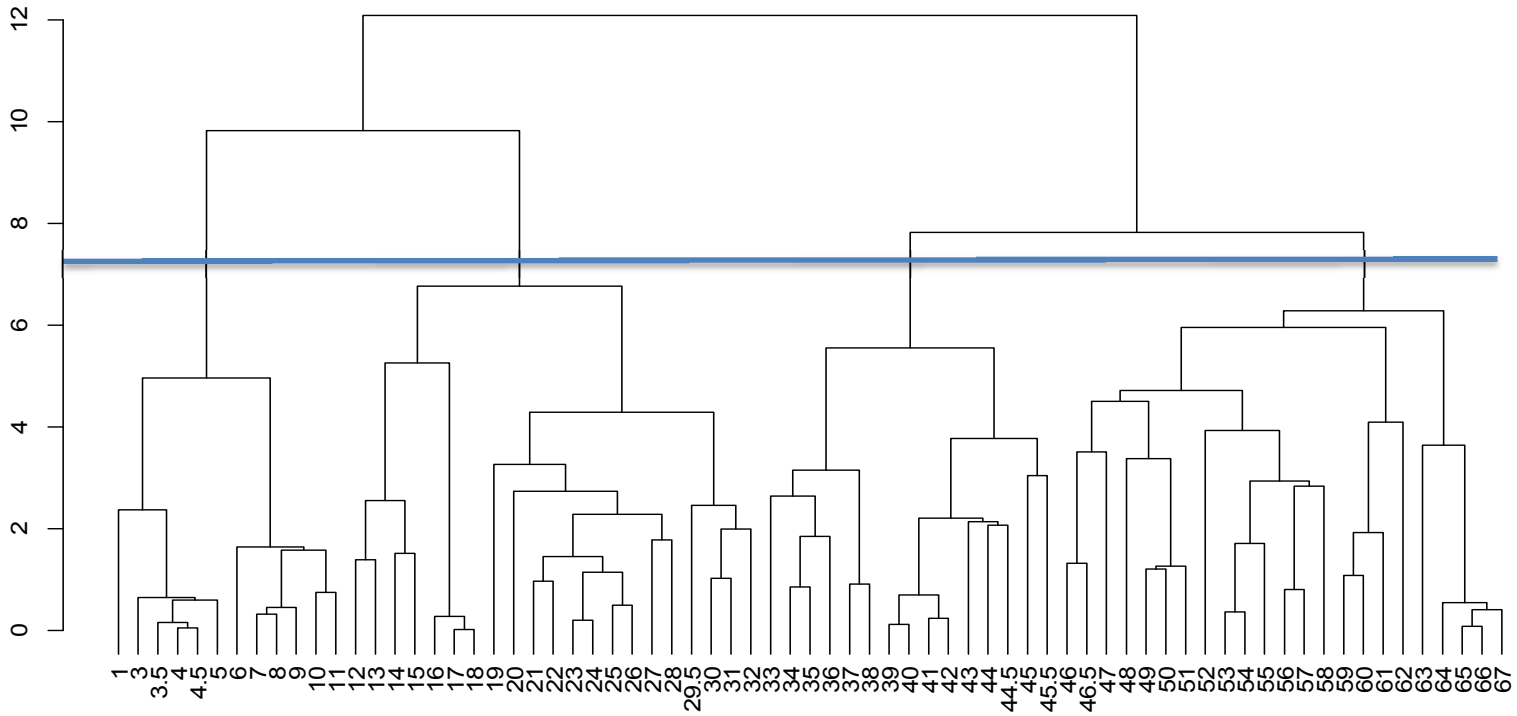

Figure A5: Unconstrained RDA, variation in the diatom community over time. Includes all 72 fossil diatom samples from core 5. Samples are spread throughout RDA space. Indicates that there is clear variation in the fossil assemblage.

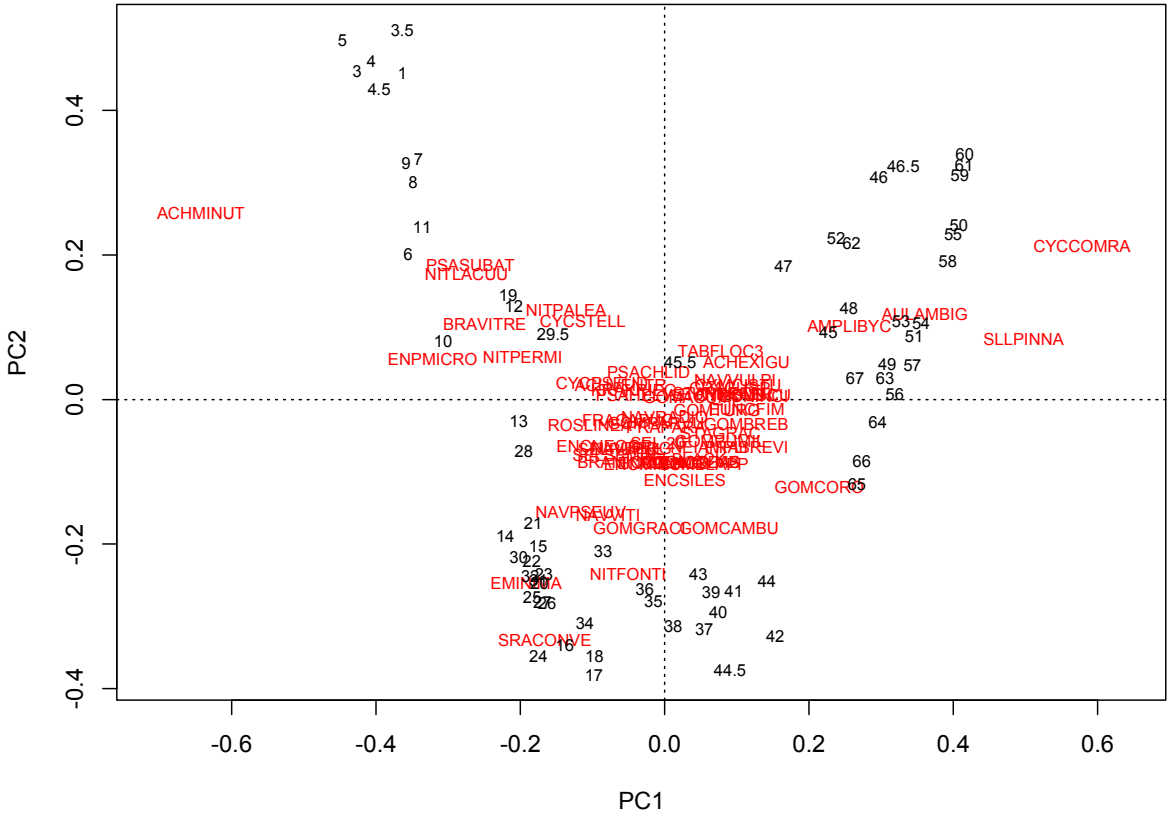

Figure A6: RDA (redundancy analysis) of surface sediment samples unconstrained by depth. Similar to PCA (principle components analysis) or NMDS (non-metric multidimensional scaling), the output data is not constrained by the tested variables. The figure shows dissimilarity among sites and diatom taxa in the calibration dataset.

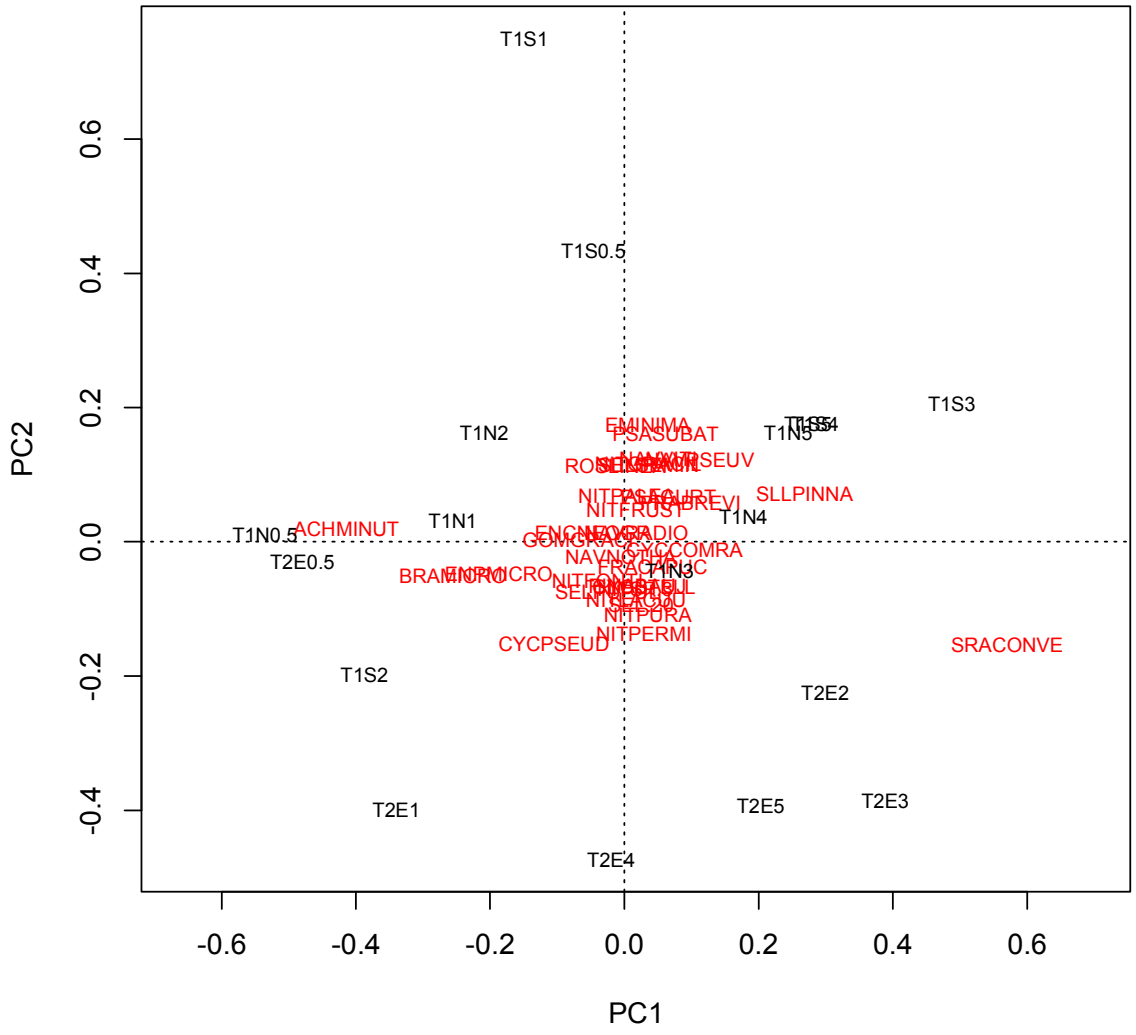

Figure A7: RDA of diatom surface sample training set constrained by depth; RDA axis 1 is arranged by depth on the first axis and the unknown variance PC1 on the second axis. ~27% of the variance is explained by depth in this model, consistent with other diatom-depth models done in the Canadian boreal lakes.

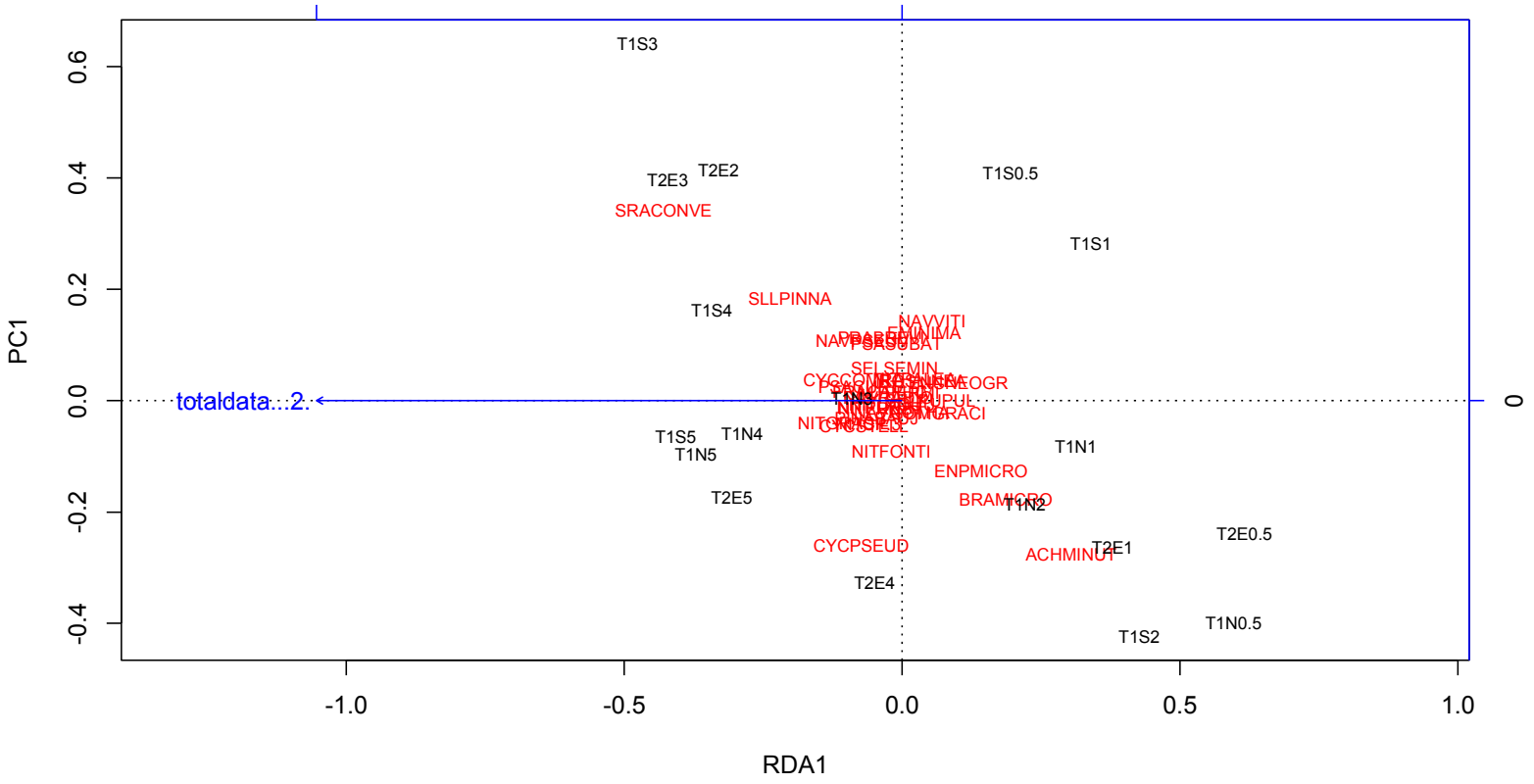

Figure A8: Surface sediment sample species abundance distributions for species above 1% relative abundance in at least two samples by depth.

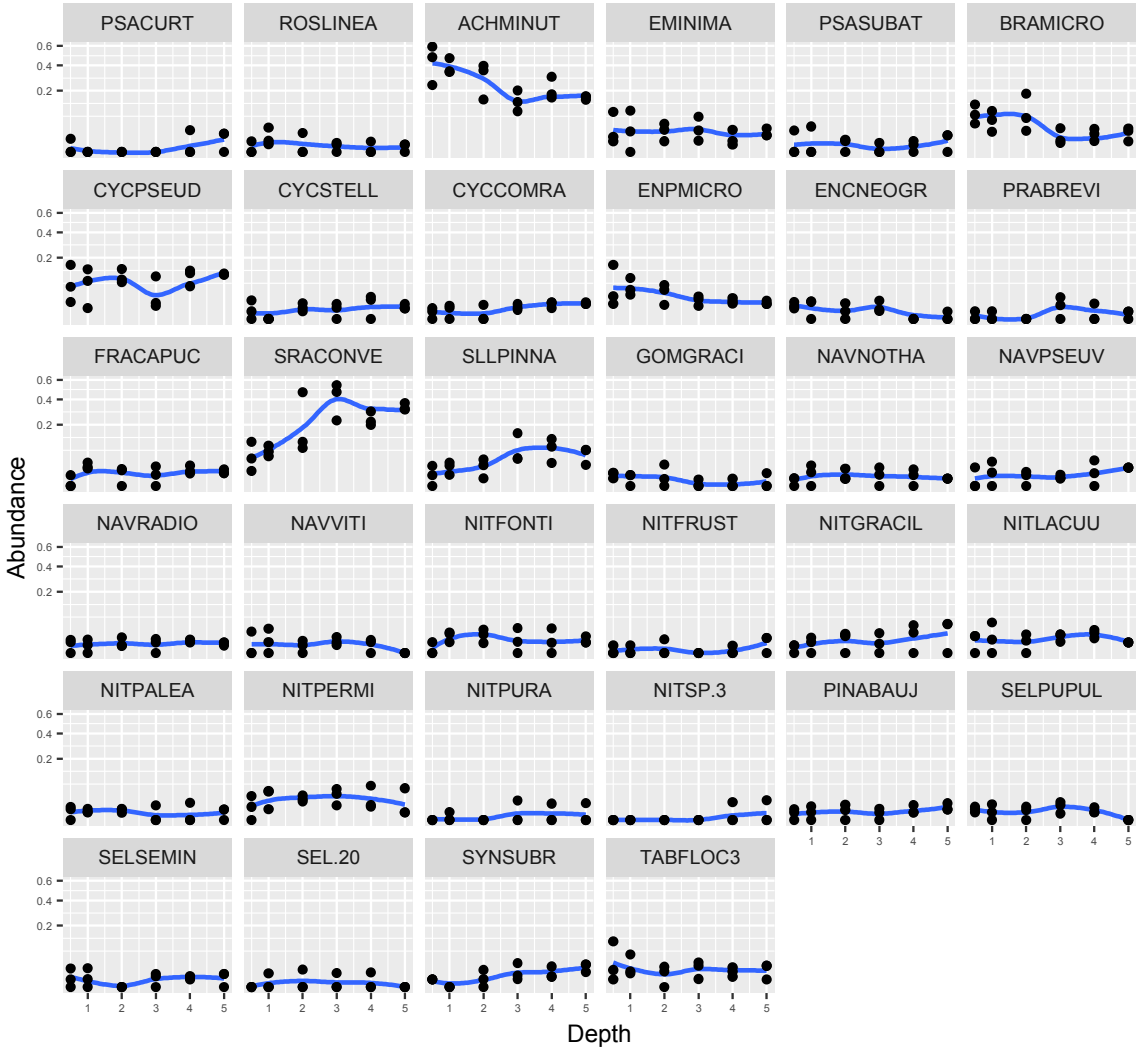

Figure A9: Diatom-depth model tested using modern analogue technique (MAT). Observed (X1) versus predicted (X2) depths for MAT model, r^2 of 0.503.

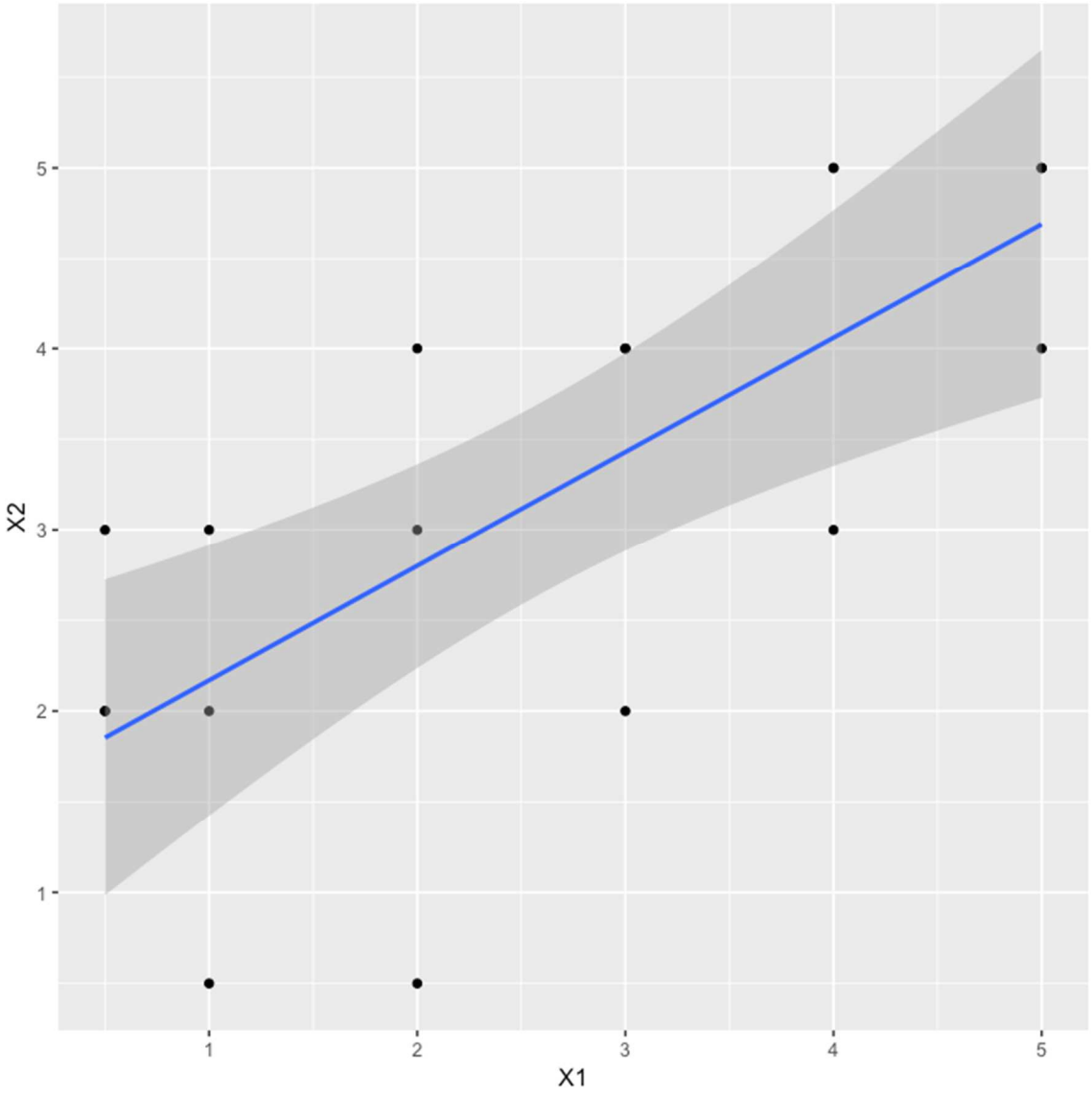

Figure A10: Diatom-depth reconstruction using both MAT and WA techniques. MAT in red and WA in black. Similar trajectories with respect to timing of lake level change, but the magnitude of lake level increases are different. MAT was excluded from the main body of text because r^2 of 0.503 was low compared to WA $r^2$of 0.89.

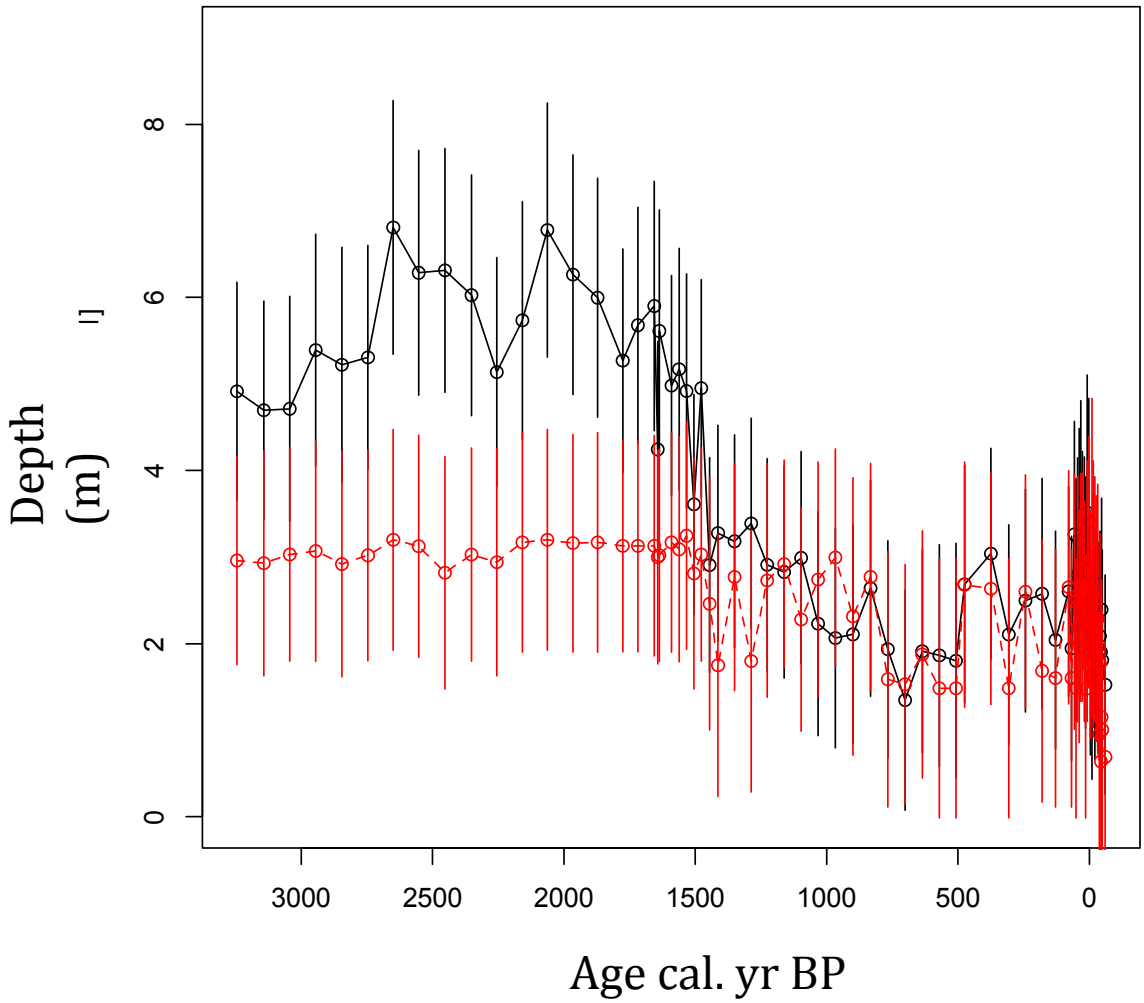

Table A1: Lake fluctuation reconstruction using Google Earth images. Distances to shoreline were measured from a fixed point on a structure using satellite images going back to the early 1990s. Data suggest that not only does the lake fluctuate on a regular basis; the fluctuations are upwards of a meter in depth. Table lists change in distance as well as annual precipitation for the given year.

Date	**Dist. (m)**	**Precip. annual sum (inches)**	**Temp. annual mean (° F)**
5/4/92	7.707317073	28.67	41
4/25/98	6.893292683	31.52	45
12/31/04	9.356707317	29.83	40
5/31/05	9.368902439	32.39	41
6/3/06	10.41768293	24.55	43
6/22/08	10.63719512	31	39
12/30/09	11.10060976	29.1	40
8/28/10	11.06097561	35.6	42
4/14/15	7.850609756	32.29	42
6/5/17	7.756097561	37.57	35

Appendix B: Dating Models

Figure B1: Age-depth curve for core 5 using mixed AMS radiocarbon dates with an *Ambrosia* rise and a surface age. One date falls outside the curve and was removed from the final age-depth model to preserve chronology continuity. The date at ~915 cal. yr BP with a depth in sediment of 25 cm, the dated material is thought to have been repositioned when lake levels fluctuated. This phenomenon has also been recorded in core 6 when woody material was found and dated older above younger sediments. Because the lake fluctuates significantly on an annual basis it is probable that the lake would redistribute large amounts of woody material.

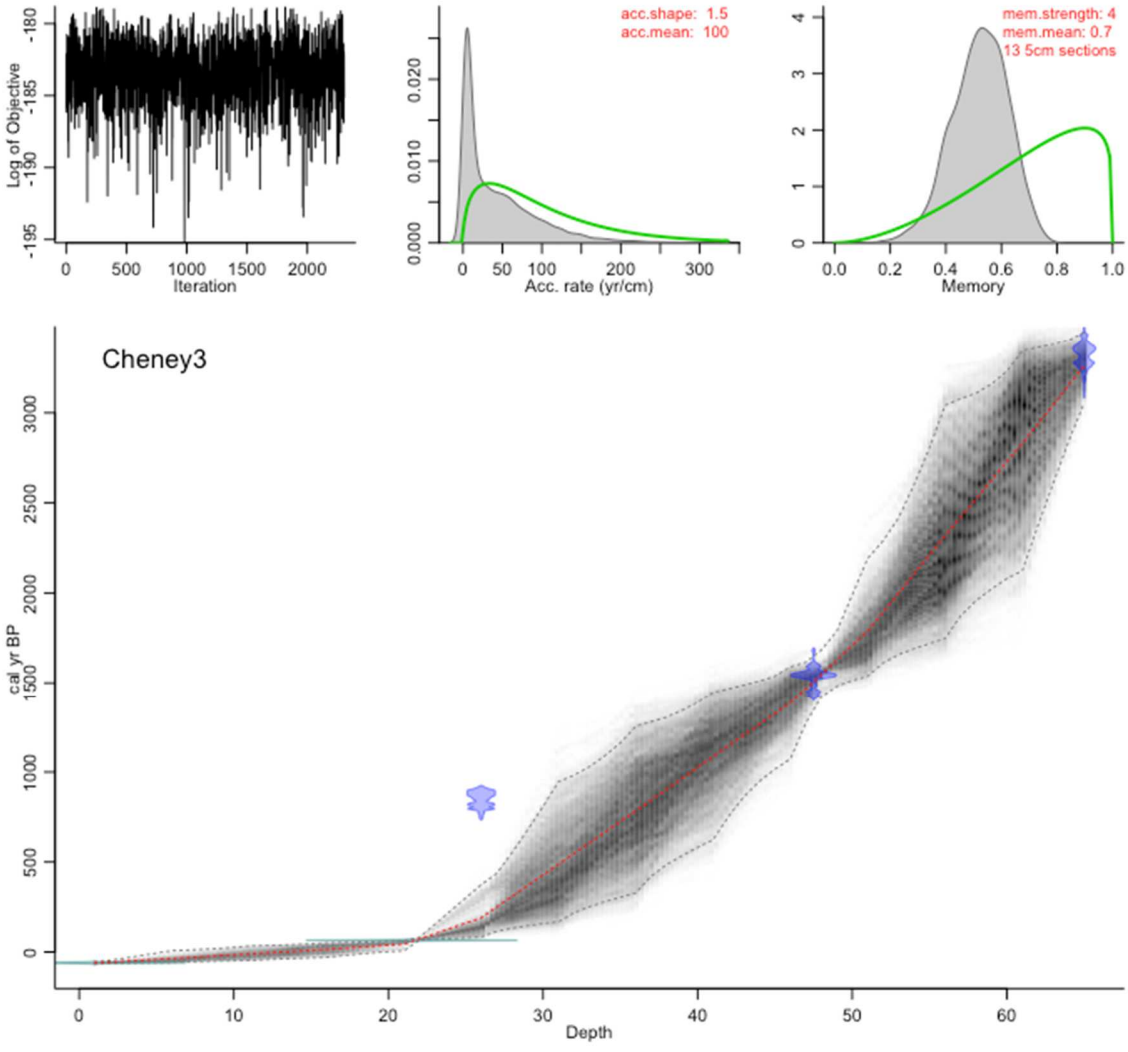

Appendix C: Dominant Diatom Taxa

Sixty-eight diatom taxa are included in this appendix, each of which had a species abundance maximum of over 1% relative abundance in a least two samples in either the surface sample training set or the fossil assemblage. These criteria for removing minor taxa follow Laird et al. (2011). Taxa are presented alphabetically in the text description; diatom images and species names follow in table C1, and plates C1 and C2. Depth was reconstructed using the training set assemblage from Cheney Lake that is included in the species descriptions. Species data from the training set were analyzed with RDA (a form of constrained ordination analysis) to determine the main drivers of variation in the dataset. RDA resulted in ~27% of the variance being explained by depth. Since we were only testing for depth, this is the only available explanatory variable in the dataset.

The Diatom Flora of Cheney Lake, WI

***Achnanthidium exiguum* (Grunow) Czarn. 1994**

REFERENCE: Krammer and Lange-Bertalot 1991
METRICS: Length Range: 5-17 µm, Width Range: 4.5-6.2 µm, Striae in 10 µm: 24-34 in center of raphe valve, 20-25 in center of rapheless valve, up to 45 at apices
NOTES: Found in the bottom half of core 5A, maximum relative abundance = 0.033% at 59 cm. Not found in training set assemblage in high abundance.

***Achnanthidium minutissimum* (Kützing) Czarn. 1994**

REFERENCE: Krammer and Lange-Bertalot 1991
METRICS: Length Range: 6-21 µm, Width Range: 1.5-3.3 µm, Striae in 10 µm: 25-35
NOTES: Found throughout core 5A, maximum relative abundance = 0.38% at 3 cm.
DEPTH OPTIMUM: 2.290925 m
DEPTH TOLERANCE: 1.6330202 m

***Achnanthes ventralis* Krasske 1923**

REFERENCE: Krammer and Lange-Bertalot 2004
METRICS: Length Range: 6-21 µm, Width Range: 1.5-3.3 µm, Striae in 10 µm: 25-35
NOTES: Found scattered throughout core 5A, maximum relative abundance = 0.025% at 1 cm. Not found in training set assemblage in high abundance.

***Amphora libyca* Ehrenberg 1840**

REFERENCE: Fallu, Allaire and Pienitz 2000
METRICS: Length range: 27.7-30.7 µm, Width range: 8-8.3 µm, Striae in 10 µm: 14-15
NOTES: Found in the deeper sections of core 5A, maximum relative abundance = 0.33% at 59 cm. Not found in training set assemblage in high abundance.

***Aulacoseira ambigua* (Grunow) Simonsen 1979**

REFERENCE: Krammer and Lange-Bertalot 1991
METRICS: Diameter 3-12 µm, Mantle height 5-15 µm, Rows of areolae in 10 µm: 17-22.
NOTES: Found in the deeper sections of core 5A, maximum relative abundance = 0.21% at 60 cm. Not found in training set assemblage in high abundance.

***Brachysira microcephala* (Grunow) Compère 1986**

REFERENCE: Lavoie, I., Hamilton, P., Campeau, S., Grenier, M., Dillon 2008
METRICS: Length Range: 17-30 µm, Width Range: 3.5-7 µm, Striae in 10 µm: 30-36.
NOTES: Found throughout core 5A, maximum relative abundance = 0.035% at 31 cm.
DEPTH OPTIMUM: 2.110333 m
DEPTH TOLERANCE: 1.5779999 m

***Brachysira vitrea* (Grunow) R.Ross in B.Hartley 1986**

REFERENCE: Patrick and Reimer 1966
METRICS: Length Range: 12-25 µm, Width Range: 4.3-5.9 µm, Striae in 10 µm: 32-36
NOTES: Found throughout core 5A, maximum relative abundance = 0.057% at 4.5 cm. Not found in training set assemblage in high abundance.

***Craticula cuspidata (*Kütz.) D.G.Mann 1990**

REFERENCE: Patrick and Reimer 1975
METRICS: Length Range: 95-157 µm, Width Range: 24-36 µm, Striae in 10 µm: 12-14 transverse, 24-26 longitudinally.
NOTES: Found throughout the bottom half of core 5A, maximum relative abundance = 0.0124% at 57 cm. Not found in training set assemblage in high abundance.

***Cymbella cistula* (Ehrenberg) O.Kirchner 1878**

REFERENCE: Patrick and Reimer 1966
METRICS: Length Range: 32-85 µm, Width Range: 11-22 µm, Striae in 10 µm: 7-10 at valve center, 10-13 near the apices.
NOTES: Found throughout the bottom half of core 5A, maximum relative abundance = 0.022% at 57 cm. Not found in training set assemblage in high abundance.

***Cymbopleura subcuspidata* (Krammer) Krammer 2003**

REFERENCE: Krammer and Lange-Bertalot 1991
METRICS: Length Range: 67-111 µm, Width Range: 19-25 µm, Striae in 10 µm: 9-12 at valve center, 12-16 near the apices.
NOTES: Found throughout the bottom half of core 5A, maximum relative abundance = 0.029% at 59 cm. Not found in training set assemblage in high abundance.

***Cymbopleura sublanceolata* (Krammer) Krammer 2003**

REFERENCE: Krammer 2003
METRICS: Length Range: 29-50 µm, Width Range: 10.1-12.4 µm, Striae in 10 µm: 12-16 at the valve center, 16-19 near the apices
NOTES: Not found throughout core 5A in high abundance. Not found in training set assemblage in high abundance.

***Cymbopleura lapponica* (Krammer) Krammer 2003**

REFERENCE: Krammer and Lange-Bertalot 1991
METRICS: Length Range: 27-47 µm, Width Range: 7.2-9.6 µm, Striae in 10 µm: 16-19 at valve center, 20-22 near the apices.
NOTES: Found throughout the bottom half of core 5A, maximum relative abundance = 0.040% at 38 cm. Not found in training set assemblage in high abundance.

***Discostella pseudostelligera* (Hust.) Houk & Klee 2004**

REFERENCE: Krammer and Lange-Bertalot 1991
METRICS: Diameter 3.7-6.5 µm, Rows of areolae in 10 µm: 22-24.
NOTES: Found throughout core 5A, maximum relative abundance = 0.035% at 7 cm.
DEPTH OPTIMUM: 2.717123 m
DEPTH TOLERANCE: 1.69414 m

***Discostella pseudostelligera* (Hust.) Houk & Klee 2004**

REFERENCE: Krammer and Lange-Bertalot 1991
METRICS: Diameter 3.7-13.8 µm, Rows of areolae in 10 µm: 14-17.
NOTES: Found throughout core 5A, maximum relative abundance = 0.054% at 7 cm.
DEPTH OPTIMUM: 3.085051 m
DEPTH TOLERANCE: 1.6006012 m

***Encyonema cespitosum* Kützing 1849**

REFERENCE: Lavoie, I., Hamilton, P., Campeau, S., Grenier, M., Dillon 2008
METRICS: Length 21-31 µm, Width 9-11 µm, Striae 10-13 in 10 µm.
NOTES: Found throughout the middle of core 5A, maximum relative abundance = 0.036% at 33 cm. Not found in training set assemblage in high abundance.

***Encyonema lange-bertaloti* Krammer 1997**

REFERENCE: Lavoie, I., Hamilton, P., Campeau, S., Grenier, M., Dillon 2008
METRICS: Length 14-29 µm, Width 5-6 µm, Striae 15-21 in 10 µm.
NOTES: Found throughout the middle of core 5A, maximum relative abundance = 0.023% at 39 cm. Not found in training set assemblage in high abundance.

***Encyonopsis microcephala* (Grunow) Krammer 1997**

REFERENCE: Krammer and Lange-Bertalot 1991
METRICS: Length 10-16 µm, Width 3-4 µm, Striae 22-24 in 10 µm.
NOTES: Found throughout core 5A, maximum relative abundance = 0.094% at 10 cm.
DEPTH OPTIMUM: 2.181192 m
DEPTH TOLERANCE: 1.5895726 m

***Encyonema minutum* (Hilse) D.G.Mann in Round, R.M.Crawford & D.G.Mann 1990**

REFERENCE: Lavoie, I., Hamilton, P., Campeau, S., Grenier, M., Dillon 2008
METRICS: Length 9-16 µm, Width 3-4 µm, Striae 15-21 in 10 µm.
NOTES: Found throughout core 5A, maximum relative abundance = 0.089% at 33 cm. Not found in training set assemblage in high abundance.

***Encyonema neogracile* (Krammer) 1997**

REFERENCE: Lavoie, I., Hamilton, P., Campeau, S., Grenier, M., Dillon, 2008
METRICS: Length 33-49 µm, Width 5-7 µm, Striae 13-15 in 10 µm.
NOTES: Found throughout core 5A, maximum relative abundance = 0.026% at 20 cm.
DEPTH OPTIMUM: 1.733304 m
DEPTH TOLERANCE: 1.3091356 m

***Encyonema silesiacum* (Bleisch) D.G.Mann in Round, R.M.Crawford & D.G.Mann 1990**

REFERENCE: Lavoie, I., Hamilton, P., Campeau, S., Grenier, M., Dillon, 2008
METRICS: Length 10-39 µm, Width 5-9 µm, Striae 14 in 10 µm.
NOTES: Found throughout core 5A, maximum relative abundance = 0.044% at 44 cm. Not found in training set assemblage in high abundance.

***Eolimna minima* (Grunow) Lange-Bertalot in Moser *et al.* 1998**

REFERENCE: Lavoie, I., Hamilton, P., Campeau, S., Grenier, M., Dillon, 2008
METRICS: Length 7-12 µm, Width 3 µm, Striae 23-24 in 10 µm.
NOTES: Found throughout core 5A, maximum relative abundance = 0.116% at 14 cm.
DEPTH OPTIMUM: 2.449384 m
DEPTH TOLERANCE: 1.6375167 m

***Eunotia implicata* (Nörpel, Lange-Bertalot & Alles) in Alles, Nörpel-Schempp & Lange-Bertalot 1991**

REFERENCE: Lavoie, I., Hamilton, P., Campeau, S., Grenier, M., Dillon, 2008
METRICS: Length 24-41 µm, Width 3-6 µm, Striae 12-16 in 10 µm.
NOTES: Found throughout core 5A, maximum relative abundance = 0.030% at 56 cm. Not found in training set assemblage in high abundance.

***Eunotia incisa* W.Sm. ex W.Greg. 1854**

REFERENCE: Patrick and Reimer 1966
METRICS: Length 12-50 µm, Width 2.8-5 µm, Striae 16-21 in 10 µm.
NOTES: Found throughout core 5A in low abundance, maximum relative abundance = 0.048% at 67 cm. Not found in training set assemblage in high abundance.

***Eunotia praerupta* Ehrenberg 1843**

REFERENCE: Lavoie, I., Hamilton, P., Campeau, S., Grenier, M., Dillon, 2008
METRICS: Length 19-45 µm, Width 5-13 µm, Striae 7-15 in 10 µm.
NOTES: Found throughout core 5A in low abundance, maximum relative abundance = 0.055% at 52 cm. Not found in training set assemblage in high abundance.

***Fragilaria capucina* Desmazières 1830**

REFERENCE: Lavoie, I., Hamilton, P., Campeau, S., Grenier, M., Dillon, 2008
METRICS: Length 33-57 µm, Width 2-3 µm, Striae 18-25 in 10 µm.
NOTES: Found throughout core 5A in low abundance, maximum relative abundance = 0.044% at 33 cm.
DEPTH OPTIMUM: 2.795667 m
DEPTH TOLERANCE: 1.6237319 m

***Gomphonema acumniatum* Ehrenberg 1832**

REFERENCE: Patrick and Reimer 1975
METRICS: Length 19-77 µm, Width 7-12 µm, Striae 9-14 in 10 µm.
NOTES: Found throughout core 5A in low abundance, maximum relative abundance = 0.046% at 62 cm. Not found in training set assemblage in high abundance.

***Gomphonema brebissonii* Kützing 1849**

REFERENCE: Patrick and Reimer 1975
METRICS: Length 17-48 µm, Width 6-9 µm, Striae 9-12 in 10 µm.
NOTES: Found in lower sections of core 5A in low abundance, maximum relative abundance = 0.024% at 67 cm. Not found in training set assemblage in high abundance.

***Gomphonema camburnii* Metzeltin & Lange-Bertalot 1998**

REFERENCE: Camburn and Charles 2000
METRICS: Length 14-38 µm, Width 3.8-5.5 µm, Striae in 10 µm: 12-13 at the valve center, 15 at the apices.
NOTES: Found throughout core 5A, maximum relative abundance = 0.114% at 37 cm. Not found in training set assemblage in high abundance.

***Gomphonema coronatum* Ehrenberg 1840**

REFERENCE: Lavoie, I., Hamilton, P., Campeau, S., Grenier, M., Dillon, 2008
METRICS: Length 49-58 µm, Width 8-9 µm, Striae in 10 µm: 9-11.
NOTES: Found throughout core 5A, maximum relative abundance = 0.155% at 37 cm. Not found in training set assemblage in high abundance.

***Gomphonema cf. cymbelliclinum* Reichardt et Lange-Bertalot 1999**

REFERENCE: Lavoie, I., Hamilton, P., Campeau, S., Grenier, M., Dillon, 2008
METRICS: Length 19-25 µm, Width 4-5 µm, Striae in 10 µm: 14-16.
NOTES: Found throughout core 5A, maximum relative abundance = 0.063% at 44 cm. Not found in training set assemblage in high abundance.

***Gomphonema gracile* Ehrenberg 1838**

REFERENCE: Krammer and Lange-Bertalot 1991
METRICS: Length 33-55 µm, Width 5-7 µm, Striae in 10 µm: 13-16.
NOTES: Found throughout core 5A, maximum relative abundance = 0.058% at 22 cm.
DEPTH OPTIMUM: 1.885849 m
DEPTH TOLERANCE: +/-1.5912744 m

***Gomphonema parvulum* (Kützing) Kützing 1849**

REFERENCE: Lavoie, I., Hamilton, P., Campeau, S., Grenier, M., Dillon, 2008
METRICS: Length 11-21 µm, Width 4-7 µm, Striae in 10 µm: 14-20.
NOTES: Found throughout core 5A, maximum relative abundance = 0.029% at 52 cm. Not found in training set assemblage in high abundance.

***Gomphonema pumilum* (Grunow) E.Reichardt & Lange-Bertalot 1991**

REFERENCE: Lavoie, I., Hamilton, P., Campeau, S., Grenier, M., Dillon, 2008
METRICS: Length 16-25 µm, Width 2-4 µm, Striae in 10 µm: 12-18.
NOTES: Found throughout core 5A, maximum relative abundance = 0.044% at 38 cm. Not found in training set assemblage in high abundance.

***Gomphonema turgidum* Ehrenberg 1854**

REFERENCE: Lavoie, I., Hamilton, P., Campeau, S., Grenier, M., Dillon, 2008
METRICS: Length 42 µm, Width 15 µm, Striae in 10 µm: 11.
NOTES: Found in the bottom half of core 5A, maximum relative abundance = 0.016% at 65 cm. Not found in training set assemblage in high abundance.

***Lindavia radiosa* (Grunow) De Toni and Forti 1900**

REFERENCE: Krammer and Lange-Bertalot 1991
METRICS: Diameter: 10.9-23.8 µm, Rows of areolae in 10 µm: 14-18
NOTES: Found throughout core 5A, most abundant in lower sections of the core, maximum relative abundance = 0.404% at 50 cm.
DEPTH OPTIMUM: 3.155085 m
DEPTH TOLERANCE: 1.6348854 m

***Navicula bergeri* Krasske 1932**

REFERENCE: Fallu, Allaire and Pienitz 2000
METRICS: Length 9.3-11 µm, Width 2.7-3 µm, Striae in 10 µm: 19-21
NOTES: Most abundant in top sections of core 5A, maximum relative abundance = 0.020% at 20 cm. Not found in training set assemblage in high abundance.

***Navicula pseudoventralis* Hustedt 1953**

REFERENCE: Camburn and Charles 2000
METRICS: Length 9-10 µm, Width 4 µm, Striae in 10 µm: 20
NOTES: Found throughout core 5A, maximum relative abundance = 0.059% at 19 cm.
DEPTH OPTIMUM: 3.006535 m
DEPTH TOLERANCE: 1.7283802 m

***Navicula radiosa* Kützing 1844**

REFERENCE: Patrick and Reimer 1975
METRICS: Length 52-105 µm, Width 8.8-11.2 µm, Striae in 10 µm: 9-11
NOTES: Found throughout core 5A, maximum relative abundance = 0.085% at 44 cm.
DEPTH OPTIMUM: 2.766544 m
DEPTH TOLERANCE: 1.6276952 m

***Nupela vitiosa* (Schim.) Siver & Hamilton 2005**

REFERENCE: Lavoie, I., Hamilton, P., Campeau, S., Grenier, M., Dillon, 2008
METRICS: Length 7-15 µm, Width 2.7-3.6 µm, Striae in 10 µm: 35-40
NOTES: Found throughout core 5A, maximum relative abundance = 0.042% at 30 cm.
DEPTH OPTIMUM: 2.108582 m
DEPTH TOLERANCE: 1.3299045 m

***Navicula vulpina* Kützing 1844**

REFERENCE: Lavoie, I., Hamilton, P., Campeau, S., Grenier, M., Dillon, 2008METRICS: Length 85-110 µm, Width 17-19 µm, Striae in 10 µm: 5-6 in the central area, 6-8 at the apices.
NOTES: Found in the bottom sections of core 5A, maximum relative abundance = 0.018% at 56 cm.
DEPTH OPTIMUM: 2.108582 m
DEPTH TOLERANCE: 1.3299045 m

***Neidium ampliatum* (Ehrenberg) Krammer in Krammer & Lange-Bertalot 1985**

REFERENCE: Lavoie, I., Hamilton, P., Campeau, S., Grenier, M., Dillon, 2008
METRICS: Length 45-73 µm, Width 11-15 µm, Striae in 10 µm: 25-27.
NOTES: Found in the bottom sections of core 5A, maximum relative abundance = 0.019% at 66 cm. Not found in training set assemblage in high abundance.

***Nitzschia fonticola* (Grunow) Grunow in Van Heurck 1881**

REFERENCE: Lavoie, I., Hamilton, P., Campeau, S., Grenier, M., Dillon, 2008
METRICS: Length 10-55 µm, Width 2.4-5.5 µm, Striae in 10 µm: 24-47, Fibule in 10 µm: 10-13.
NOTES: Found throughout core 5A, maximum relative abundance = 0.055% at 32 cm.
DEPTH OPTIMUM: 2.687279 m

DEPTH TOLERANCE: 1.5423976 m

Nitzschia frustulum (Kützing) Grunow in Cleve & Grunow 1880

REFERENCE: Lavoie, I., Hamilton, P., Campeau, S., Grenier, M., Dillon, 2008
METRICS: Length 10-13 µm, Width 2-3 µm, Striae in 10 µm: 27, Fibule in 10 µm: 13.
NOTES: Not found throughout core 5A in high abundance, mainly found in the training set. Maximum relative abundance = 0.012% in sample T1S5.
DEPTH OPTIMUM: 3.291281 m
DEPTH TOLERANCE: 1.9869642 m

Nitzschia gracilis Hantzsch 1860

REFERENCE: Lavoie, I., Hamilton, P., Campeau, S., Grenier, M., Dillon, 2008
METRICS: Length 39-59 µm, Width 3-4 µm, Striae in 10 µm: n.v., Fibule in 10 µm: 14-18.
NOTES: Not found throughout core 5A in high abundance, mainly found in the training set. Maximum relative abundance = 0.044% in sample T1N5.
DEPTH OPTIMUM: 3.1757 m
DEPTH TOLERANCE: 1.6302186 m

Nitzschia lacuum Lange-Bertalot 1980

REFERENCE: Lavoie, I., Hamilton, P., Campeau, S., Grenier, M., Dillon, 2008
METRICS: Length 15-17 µm, Width 3 µm, Striae in 10 µm: n.v., Fibule in 10 µm: 16-17.
NOTES: Found throughout core 5A in relatively high abundance. Maximum relative abundance = 0.181% at 1 cm.
DEPTH OPTIMUM: 2.669052 m
DEPTH TOLERANCE: 1.5881179 m

Nitzschia palea (Kützing) W.Smith 1856

REFERENCE: Lavoie, I., Hamilton, P., Campeau, S., Grenier, M., Dillon 2008
METRICS: Length 26-50 µm, Width 4-5 µm, Striae in 10 µm: n.v., Fibule in 10 µm: 11-14.
NOTES: Found throughout core 5A in low abundance. Maximum relative abundance = 0.045% at 8 cm.
DEPTH OPTIMUM: 2.380409 m
DEPTH TOLERANCE: 1.6677641 m

***Nitzschia perminuta* (Grunow) M.Peragallo 1903**

REFERENCE: Lavoie, I., Hamilton, P., Campeau, S., Grenier, M., Dillon 2008
METRICS: Length 14-22 µm, Width 2-3 µm, Striae in 10 µm: 27-30, Fibule in 10 µm: 15.
NOTES: Found throughout core 5A in low abundance. Maximum relative abundance = 0.061% at 8 cm.
DEPTH OPTIMUM: 2.607275 m
DEPTH TOLERANCE: 1.5316408 m

***Nitzschia pura* Hustedt 1954**

REFERENCE: Lavoie, I., Hamilton, P., Campeau, S., Grenier, M., Dillon 2008
METRICS: Length 52-57 µm, Width 3 µm, Striae in 10 µm: n.v., Fibule in 10 µm: 14-17.
NOTES: Not found throughout core 5A in high abundance, mainly found in surface sample training set. Maximum relative abundance = 0.020% in sample T1N5.
DEPTH OPTIMUM: 3.562074 m
DEPTH TOLERANCE: 1.4721139 m

Nitzschia* sp. *#3

REFERENCE: N/A
METRICS: Length 14-35 µm, Width 3 µm, Striae in 10 µm: n.v., Fibule in 10 µm: 13-18.
NOTES: Found throughout core 5A. Maximum relative abundance = 0.034% at 10 cm.
DEPTH OPTIMUM: 4.525434 m
DEPTH TOLERANCE: 0.7071068 m

***Pinnularia abaujensis* (Pantocsek) R.Ross 1947**

REFERENCE: Krammer and Lange-Bertalot 1991
METRICS: Length 50-90 µm, Width 8-12 µm, Striae in 10 µm: 9-12.
NOTES: Not found throughout core 5A in high abundance, mainly found in surface sample training set. Maximum relative abundance = 0.012% in sample T1S2.
DEPTH OPTIMUM: 2.946451 m
DEPTH TOLERANCE: 1.7048275 m

***Psammothidium chlidanos* (M.H.Hohn & Hellerman) Lange-Bertalot 1999**

REFERENCE: Antoniades *et al.* 2008
METRICS: Length 12-18 µm, Width 4.8-6.2 µm, Striae in 10 µm: 27-33.
NOTES: Found throughout core 5A in low abundance. Maximum relative abundance = 0.018% at 19 cm. Not found in training set assemblage in high abundance.

***Psammothidium curtissimum* (J.R.Carter) Aboal 2003**

REFERENCE: Krammer and Lange-Bertalot 1991
METRICS: Length 5-9 µm, Width 3.5-4.0 µm, Striae in 10 µm: 27-31.
NOTES: Not found throughout core 5A in high abundance, mainly found in surface sample training set. Maximum relative abundance = 0.025% in sample T1S4.
DEPTH OPTIMUM: 3.870736 m
DEPTH TOLERANCE: 1.9208858 m

***Psammothidium helveticum* (Hustedt) Bukhtiyarova & Round 1996**

REFERENCE: Krammer and Lange-Bertalot 1991
METRICS: Length 12-26 µm, Width 5.1-7.8 µm, Striae in 10 µm: 24-30.
NOTES: Found throughout core 5A in low abundance. Maximum relative abundance = 0.033% at 13 cm. Not found in training set assemblage in high abundance.

***Psammothidium subatomoides* (Hust.) Bukht. & Round 1996**

REFERENCE: Krammer and Lange-Bertalot 1991
METRICS: Length 6-11 µm, Width 3.2-6.0 µm, Striae in 10 µm: 30-40.
NOTES: Found throughout core 5A in low abundance. Maximum relative abundance = 0.141% at 13 cm.
DEPTH OPTIMUM: 2.675831 m
DEPTH TOLERANCE: 1.8637465 m

***Pseudostaurosira brevistriata* (Grunow) D.M.Williams & Round 1987**

REFERENCE: Patrick and Reimer 1966
METRICS: Length 10-26 µm, Width 3.5-4.0 µm, Striae in 10 µm: 12-15.
NOTES: Found throughout core 5A in low abundance. Maximum relative abundance = 0.049% at 44.5 cm.
DEPTH OPTIMUM: 3.136432 m
DEPTH TOLERANCE: 1.5026025 m

***Pseudostaurosira parasitica* (W.Smith) E.Morales in E.Morales & Edlund 2003**

REFERENCE: Lavoie, I., Hamilton, P., Campeau, S., Grenier, M., Dillon 2008
METRICS: Length 9-18 µm, Width 4.5-5 µm, Striae in 10 µm: 19-21.
NOTES: Found throughout the bottom half core 5A in low abundance. Maximum relative abundance = 0.009% at 35 cm. Not found in training set assemblage in high abundance.

***Rossithidium lineare* (W.Smith) Round & Bukhtiyarova 1996**

REFERENCE: Patrick and Reimer 1975
METRICS: Length 12-26 µm, Width 3.7-4.5 µm, Striae in 10 µm: 24-29.
NOTES: Found throughout core 5A. Maximum relative abundance = 0.044% at 1 cm.
DEPTH OPTIMUM: 2.202522 m
DEPTH TOLERANCE: 1.5905455 m

***Sellaphora blackfordensis* D.G.Mann & S.Droop 2004**

REFERENCE: Hoffmann, Lange-Bertalot and Werum 2006
METRICS: Length 19-57 µm, Width 8.1-9.3 µm, Striae in 10 µm: 18-22.
NOTES: Found throughout the bottom half of core 5A in low abundance. Maximum relative abundance = 0.016% at 43 cm. Not found in training set assemblage in high abundance.

***Sellaphora pupula* (Kützing) Mereschkovsky 1902**

REFERENCE: Patrick and Reimer 1975
METRICS: Length 16-28 µm, Width 6.3-7 µm, Striae in 10 µm: 21-24.
NOTES: Found throughout core 5A. Maximum relative abundance = 0.033% at 33 cm.
DEPTH OPTIMUM: 2.167045 m
DEPTH TOLERANCE: 1.3453405 m

***Sellaphora seminulum* (Grunow) D.G.Mann 1989**

REFERENCE: Lavoie, I., Hamilton, P., Campeau, S., Grenier, M., Dillon 2008
METRICS: Length 7-9 µm, Width 3 µm, Striae in 10 µm: 20-30.
NOTES: Found throughout core 5A. Maximum relative abundance = 0.049% at 14 cm.
DEPTH OPTIMUM: 2.709704 m
DEPTH TOLERANCE: 1.8214296 m

***Sellaphora* sp. #20**

REFERENCE: N/A
METRICS: Length 8-11 µm, Width 3-4 µm, Striae in 10 µm: 20-25.
NOTES: Found throughout core 5A in low abundance. Maximum relative abundance = 0.022% at 15 cm.
DEPTH OPTIMUM: 2.494806 m
DEPTH TOLERANCE: 1.2673059 m

***Stauroneis gracilis* Ehrenberg 1843**

REFERENCE: Patrick and Reimer 1975
METRICS: Length 71-80 µm, Width 11-14 µm, Striae in 10 µm: 19-22.
NOTES: Found throughout core 5A in low abundance. Maximum relative abundance = 0.029% at 37 cm. Not found in training set assemblage in high abundance.

***Stauroneis phoenicenteron* (Nitzsch) Ehrenberg 1843**

REFERENCE: Patrick and Reimer 1975
METRICS: Length 70-380 µm, Width 16-53 µm, Striae in 10 µm: 12-17.
NOTES: Found throughout core 5A in low abundance. Maximum relative abundance = 0.027% at 49 cm. Not found in training set assemblage in high abundance.

***Staurosira construens* var. *venter* (Ehrenberg) P.B.Hamilton in Hamilton, Poulin, Charles & Angell 1992**

REFERENCE: Lavoie, I., Hamilton, P., Campeau, S., Grenier, M., Dillon 2008
METRICS: Length 5-9 µm, Width 3-4 µm, Striae in 10 µm: 15-18.
NOTES: Found throughout core 5A. Maximum relative abundance = 0.672% at 18 cm.
DEPTH OPTIMUM: 3.066572 m
DEPTH TOLERANCE: 1.5135259 m

***Staurosirella pinnata* (Ehrenberg) D.M.Williams & Round 1988**

REFERENCE: Lavoie, I., Hamilton, P., Campeau, S., Grenier, M., Dillon 2008
METRICS: Length 4-17 µm, Width 3-6 µm, Striae in 10 µm: 8-15.
NOTES: Found throughout core 5A. Maximum relative abundance = 0.457% at 61 cm.
DEPTH OPTIMUM: 3.120028 m
DEPTH TOLERANCE: 1.5002606 m

***Tabellaria flocculosa* (Roth) Kützing 1844**

REFERENCE: Patrick and Reimer 1975
METRICS: Length 7-39 µm, Width 4-8 µm, Striae in 10 µm: 16-21.
NOTES: Found throughout core 5A. Maximum relative abundance = 0.194% at 52 cm. Not found in training set assemblage in high abundance.

Table C1: Species name and corresponding number to plates C1 and C2.

Number	Species Name	Number	Species Name
1	*Lindavia radiosa*	35	*Gomphonema gracile*
2	*Discostella stelligera*	36	*Gomphonema acuminatum*
3	*Discostella pseudostelligera*	37	*Gomphonema pumilum*
4	*Aulacoseira ambigua*	38	*Gomphonema brebissonii*
5 a and b	*Staurosira construens* var. *venter*	39	*Nitzschia gracilis*
6 a and b	*Pseudostaurosira brevistriata*	40	*Nitzschia pura*
7	*Fragilaria capucina*	41	*Nitzschia palea*
8	*Pseudostaurosira parasitica*	42	*Nitzschia frustulum*
9	*Tabellaria flocculosa* strain #3	43	*Nitzschia fonticula*
10 a,b,and c	*Staurosirella pinnata*	44	*Nitzschia lacuum*
11	*Cymbopleura subcuspidata*	45	*Nitzschia sp. #3*
12	*Encyonopsis microcephala*	46	*Nitzschia perminuta*
13	*Cymbopleura sublanceolata*	47	*Craticula cuspidata*
14	*Amphora libyca*	48	*Stauroneis phoenicenteron*
15	*Cymbopleura lapponica*	49	*Stauroneis gracilis*
16	*Cymbella cistula*	50	*Navicula vulpina*
17	*Encyonopsis neogracile*	51	*Kraskella kriegeriana*
18	*Encyonopsis silesacium*	52	*Brachysira vitrea*
19	*Encyonopsis lange-bertalotii*	53	*Brachysira microcephala*
20	*Encyonema caespitosum*	54	*Eolimna minima*
21	*Encyonopsis minuta*	55	*Navicula (Nupela) vitiosa*
22 a and b	*Achnanthidium minutissimum*	56	*Navicula pseudoventralis*
23	*Rossithidium linearis*	57	*Sellaphora* sp.#20
24	*Achnanthes exigua*	58	*Sellaphora seminulum*
25	*Achnanthidium ventralis*	59	*Navicula bergerii*
26	*Psammothidium subatomoides*	60	*Navicula notha*
27	*Psammothidium chlidanos*	61	*Sellaphora pupula*
28	*Psammothidium curtissimum*	62	*Sellaphora blackfordensis*
29	*Psammothidium helvetica*	63	*Pinnularia abaujensis*
30	*Gomphonema coronatum*	64	*Navicula radiosa*
31	*Gomphonema parvulum*	65	*Neidium ampliatum*
32 a and b	*Gomphonema cymbelliclinum*	66	*Eunotia incisa*
33 a and b	*Gomphonema camburnii*	67	*Eunotia c.f. implicata*

34	*Gomphonema turgidum*	68	*Eunotia praerupta*

Plate C1: Centric, araphid, monoraphid, asymmetrical biraphid and nitzschioid taxa.

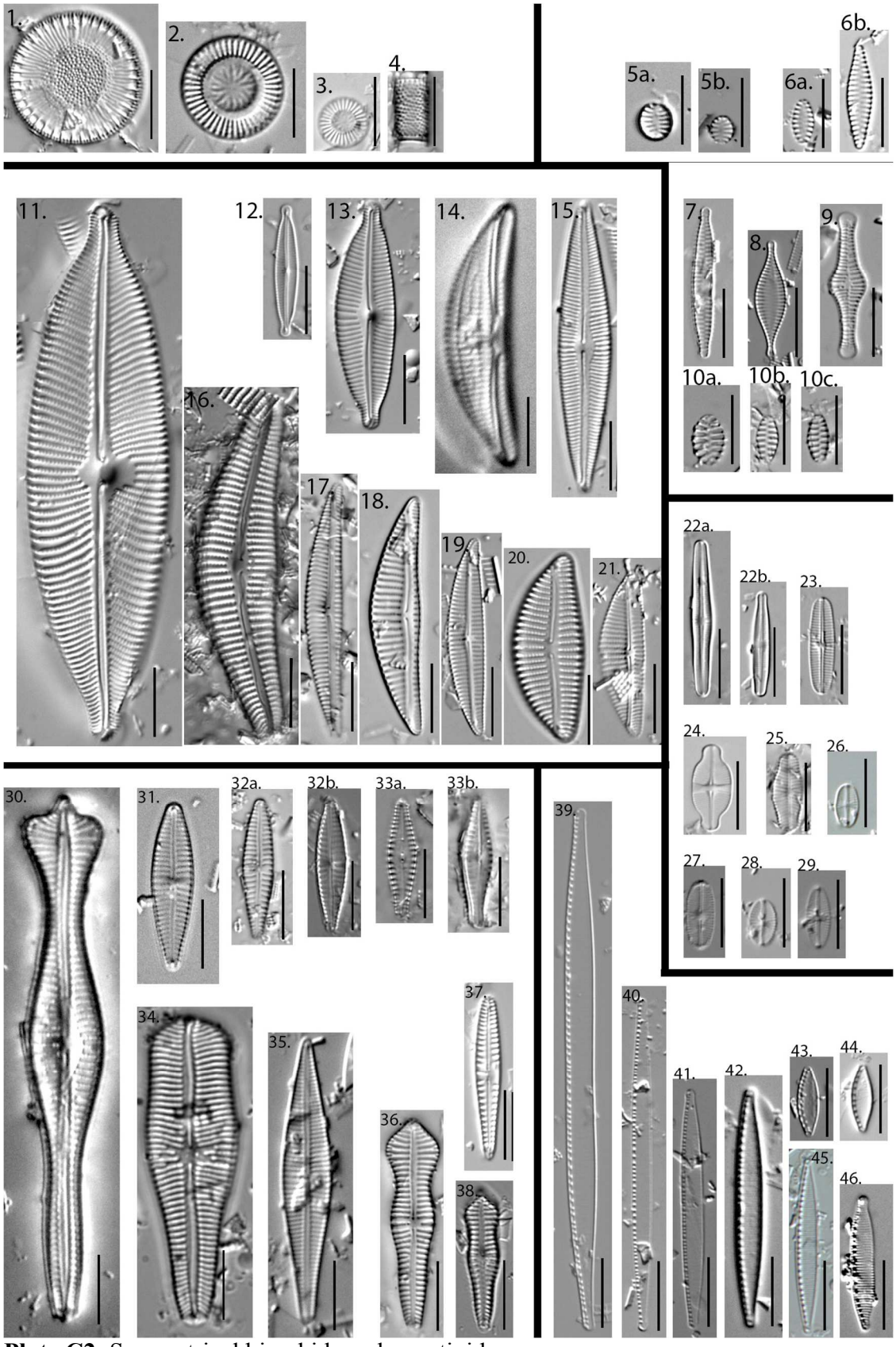

Plate C2: Symmetrical biraphids and eunotioids.

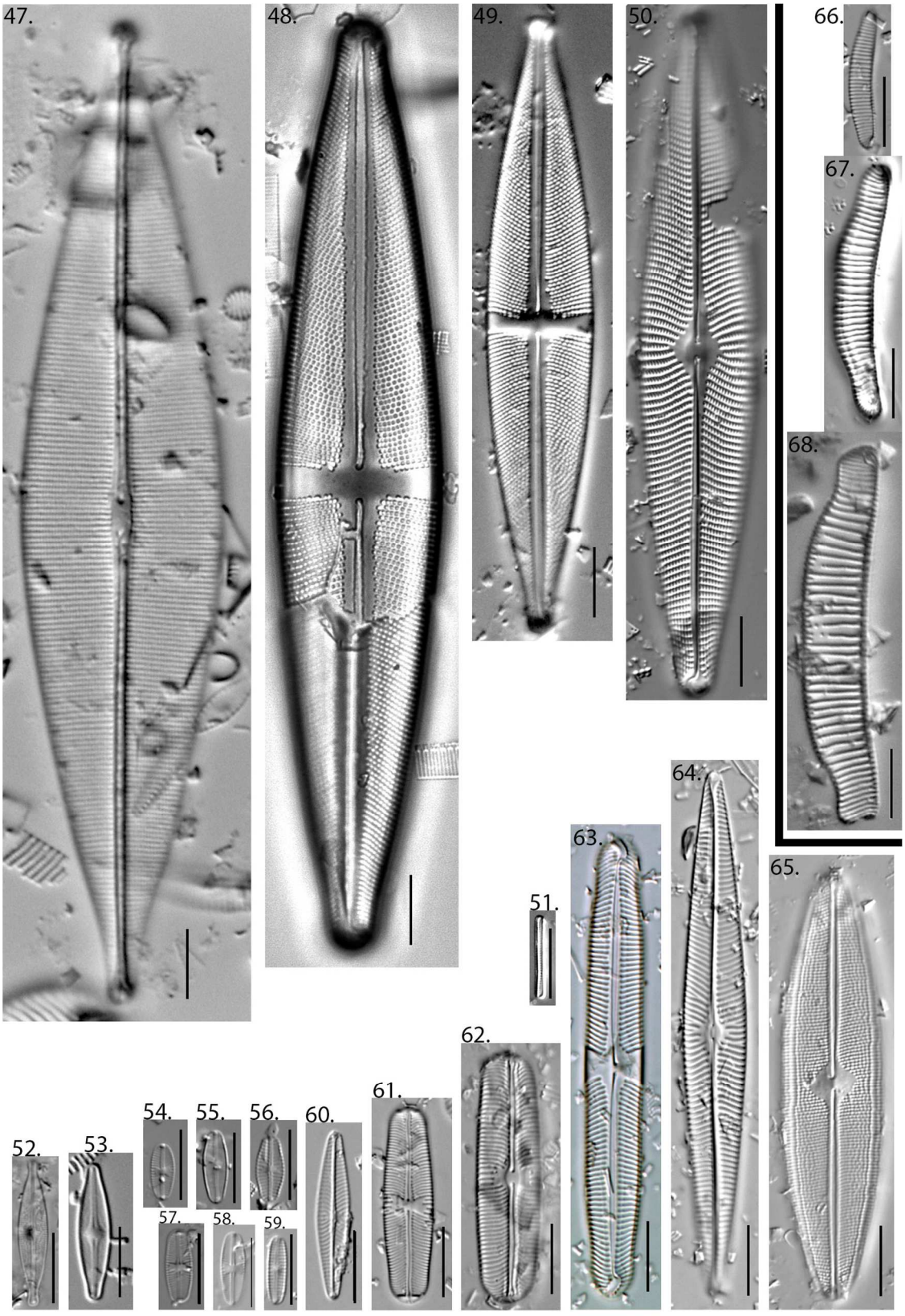

Appendix D: Diatom Counts

Slides were prepared for diatom analysis following techniques from the Diatom Monitoring Protocol (National Park Service, Ramstack et al., 2008). 71 samples were analyzed down core to compare diatom species assemblages to surface sediment samples (n=18) taken in 2012. At least 300 valves were counted in most samples except for a few samples that had poor preservation. Included in the tables are all the raw counts for all 92 taxa for core 5A and all 136 taxa for the surface sediment sample training set. Table D1 is a list of species numbers and corresponding species names. Table D2 lists the raw counts by species number and core depth. Surface sediment counts follow in Tables D3 and D4, also with a table of species number and corresponding species names.

Table D1: 92 Species names and numbers for data table D2.

Name	**Species Number**	***Name***	**Species Number**
Aulacoseira ambigua	1	*Gomphonema camburnii*	47
Aulacoseira valida	2	*Gomphonema coronatum*	48
Psammothidium chlidanos	3	*Gomphonema cymbelliclinum*	49
Psammothidium helvetica	4	*Gomphonema dichotomum*	50
Achnanthes exigua	5	*Gomphonema gracile*	51
Rossithidium linearis	6	*Gomphonema parvulum*	52
Achnanthidium minutissimum	7	*Gomphonema pumilum*	53
Eolimna minima	8	*Gomphonema truncatum*	54
Psammothidium subatomoides	9	*Gomphonema turgidum*	55
Achnanthidium ventralis	10	*Hantzschia elongata*	56
Amphora libyca	11	*Kraskella kriegeriana*	57

Brachysira microcephala	12	*Navicula bergeri*	58
Brachysira vitrea	13	*Navicula cryptocephala*	59
Craticula cuspidata	14	*Navicula notha*	60
Cyclotella meneghiniana	15	*Navicula pseudoventralis*	61
Discostella pseudostelligera	16	*Navicula radiosa*	62
Discostella stelligera	17	*Navicula vitiosa*	63
Lindavia radiosa	18	*Navicula vulpina*	64
Cymbella cistula	19	*Neidium ampliatum*	65
Encyonopsis cesatii	20	*Nitzschia fonticula*	66
Cymbopleura lapponica	21	*Nitzschia lacuum*	67
Encyonema lunatum	22	*Nitzschia linearis*	68
Cymbella neocistula	23	*Nitzschia palea*	69
Encyonopsis neogracile	24	*Nitzschia pura*	70
Encyonopsis microcephala	25	*Nitzschia perminuta*	71
Encyonema caespitosum	26	*Nitzschia sp. #3*	72
Encyonopsis minuta	27	*Placoneis explanata*	73
Encyonopsis lange-bertalotii	28	*Pinnularia abaujensis*	74
Encyonema silesiacum	29	*Pinnularia biceps*	75
Cymbella subcuspidata	30	*Pinnularia major*	76
Diploneis finnica	31	*Pinnularia microstauron*	77
Eunotia bilunaris	32	*Pinnularia rupestris*	78
Eunotia cf. implicata	33	*Reimeria uniseriata*	79
Eunotia minor	34	*Sellaphora blackfordensis*	80
Eunotia incisa	35	*Sellaphora pupula*	81
Eunotia monodon	36	*Sellaphora seminulum*	82
Eunotia paludosa	37	*Sellaphora rectangularis*	83
Eunotia praerupta	38	*Sellaphora* sp.#20	84
Pseudostaurosira brevistriata	39	*Sellaphora* sp.#22	85
Pseudostaurosira parasitica	40	*Sellaphora stroemii*	86

Fragilaria capucina	41	*Stauroneis gracilis*	87
Staurosira construens	42	*Stauroneis phoenicenteron*	88
Staurosira construens var. *venter*	43	*Stauroneis siberica*	89
Staurosirella pinnata	44	*Synedra subrhombica*	90
Gomphonema acuminatum	45	*Synedra ulna*	91
Gomphonema brebissonii	46	*Tabellaria flocculosa* strain #3	92

Table D2. Raw diatom counts by species number (see Table D1) by core depth (cm) for all samples from core 5A. Includes all taxa as well as chrysophyte counts.

Sample Codes➔	**1**	**2**	**3**	**4**	**5**	**6**	**7**
Depth (cm)							
1	0	0	0	0	4	19	121
3	0	0	0	0	0	0	170
3.5	0	0	0	0	0	0	175
4	0	0	0	0	0	2	125
4.5	0	0	0	0	0	0	118
5	0	0	0	0	0	1	154
6	0	0	0	1	0	1	147
7	0	0	6	0	0	2	107
8	0	0	0	1	0	3	117
9	0	0	3	0	0	2	175
10	0	0	0	0	0	3	156
11	0	0	1	1	0	7	141
12	0	0	3	2	0	0	38
13	0	0	1	11	0	2	26
14	0	0	0	0	0	3	42
15	0	0	1	0	0	0	41
16	0	0	0	0	0	1	28
17	0	0	0	0	0	0	10
18	0	0	0	0	0	0	12
19	2	0	7	9	0	11	64
20	1	0	0	3	0	4	30
21	0	0	0	2	0	1	62
22	1	0	0	0	0	2	59
23	0	0	0	0	0	0	57
24	0	0	0	0	0	3	65
25	0	0	0	0	0	4	42
26	0	0	0	0	0	2	56
27	0	0	0	0	0	3	58
28	0	0	0	0	0	0	56
29.5	0	0	6	0	0	2	42
30	0	0	0	0	0	2	76
31	1	0	1	0	0	2	83
32	0	0	0	0	0	0	46
33	0	0	0	0	0	0	46
34	5	0	0	0	0	5	67
35	1	0	0	0	0	4	50

36	3	0	0	0	0	1	30
37	4	0	0	0	0	3	20
38	0	0	0	0	0	0	3
39	6	0	0	0	1	1	11
40	6	0	0	0	1	2	20
41	6	0	0	0	2	2	16
42	10	0	0	0	0	1	5
43	4	0	0	0	1	2	13
44	7	0	0	0	0	2	10
44.5	6	0	0	0	2	5	11
45	33	0	1	0	1	0	3
45.5	3	0	10	7	2	6	46
46	47	0	5	0	3	0	3
46.5	60	0	1	0	4	0	1
47	56	0	3	0	3	0	12
48	0	0	0	0	0	0	0
49	4	0	0	0	1	0	3
50	14	0	0	0	0	0	0
51	11	0	0	0	0	0	1
52	10	0	0	0	0	0	3
53	4	0	0	0	0	0	1
54	13	0	0	0	4	0	0
55	14	0	0	0	3	0	0
56	9	0	0	0	1	0	0
57	18	0	0	0	1	0	0
58	23	0	0	0	5	0	1
59	33	0	0	0	10	0	0
60	76	0	0	0	10	0	1
61	48	0	0	0	4	0	1
62	2	2	0	0	4	0	0
63	10	0	0	0	1	0	0
64	5	0	0	0	1	0	0
65	3	0	0	0	1	0	0
66	7	0	0	0	0	0	0
67	6	0	0	0	3	0	3
Sample codes➔	**8**	**9**	**10**	**11**	**12**	**13**	**14**
Depth (cm)							
1	0	12	11	0	1	17	0
3	0	50	5	0	6	11	0
3.5	0	46	6	0	3	19	0

4	0	25	3	0	2	19	0
4.5	0	30	4	0	2	19	0
5	0	37	4	0	0	12	0
6	25	1	0	0	0	18	0
7	0	22	0	0	0	9	0
8	7	7	0	0	0	8	0
9	0	28	0	0	3	21	0
10	18	0	0	0	13	0	0
11	23	8	0	0	0	17	0
12	0	38	6	0	0	6	0
13	26	46	3	0	0	4	0
14	40	15	0	0	0	7	0
15	15	6	0	0	8	0	0
16	20	0	0	0	3	0	0
17	24	2	0	1	1	0	0
18	21	2	0	0	6	0	0
19	0	38	0	1	1	12	0
20	18	5	0	0	0	7	0
21	27	2	2	0	0	14	0
22	15	2	0	0	0	18	0
23	11	0	0	0	0	5	0
24	29	2	0	0	12	0	0
25	33	0	2	0	0	7	0
26	28	0	0	0	0	18	0
27	27	0	0	0	0	10	0
28	15	4	0	0	0	19	0
29.5	0	18	0	0	0	8	0
30	22	5	0	0	0	16	0
31	11	0	0	0	11	0	0
32	18	0	0	0	9	0	1
33	18	0	0	0	9	0	1
34	5	1	0	1	9	0	0
35	8	1	0	0	9	0	0
36	9	0	0	1	4	0	1
37	6	0	0	0	4	0	0
38	0	0	0	0	8	0	0
39	4	1	0	1	3	1	2
40	3	0	0	1	2	0	3
41	1	1	0	1	6	0	2
42	3	0	0	0	3	0	0
43	0	2	0	1	3	0	1

44	2	1	0	3	2	0	1
44.5	2	0	0	0	3	0	0
45	0	0	0	1	0	1	0
45.5	0	11	0	4	0	5	0
46	0	2	0	4	0	0	0
46.5	0	4	0	12	0	1	0
47	0	2	0	0	0	4	0
48	0	0	0	0	0	0	0
49	0	0	0	7	2	0	1
50	1	0	0	8	0	0	3
51	0	0	0	0	0	0	0
52	0	0	0	3	1	0	3
53	1	0	0	2	0	0	1
54	0	0	0	11	0	0	2
55	0	0	0	13	0	0	2
56	0	0	0	12	0	0	3
57	1	0	0	13	0	0	4
58	0	0	0	20	0	0	2
59	0	0	0	34	0	0	3
60	0	0	0	29	0	0	4
61	0	0	0	19	0	0	4
62	0	1	0	13	0	0	2
63	0	0	0	20	1	0	0
64	0	0	0	6	0	0	1
65	0	0	0	2	2	0	0
66	3	0	0	3	0	0	0
67	2	0	0	5	0	0	0

Sample codes➔	**15**	**16**	**17**	**18**	**19**	**20**	**21**
Depth (cm)							
1	0	0	8	4	0	4	0
3	0	2	8	0	0	7	0
3.5	0	7	2	19	0	3	0
4	0	0	12	2	0	4	0
4.5	0	2	9	4	0	0	0
5	0	0	20	1	0	0	0
6	0	3	1	3	0	2	0

7	0	12	2	4	0	0	0
8	1	4	1	3	0	4	0
9	0	0	8	3	0	1	0
10	0	4	3	6	0	0	5
11	0	5	3	4	0	0	0
12	0	1	1	2	0	0	0
13	0	0	0	1	0	0	0
14	0	1	0	1	0	1	0
15	0	5	1	2	0	0	0
16	0	1	0	1	0	0	0
17	0	0	0	3	0	0	0
18	0	0	0	1	0	0	0
19	0	4	0	3	0	1	0
20	0	0	0	3	0	0	0
21	0	3	1	4	0	0	0
22	0	1	0	1	0	0	0
23	0	2	0	2	0	2	0
24	0	2	0	2	0	0	2
25	0	0	0	1	0	1	0
26	0	0	1	0	0	6	0
27	0	5	0	2	0	8	0
28	0	3	1	5	0	0	0
29.5	0	0	0	2	0	1	0
30	0	0	2	1	0	9	0
31	0	0	0	1	0	0	0
32	0	0	3	3	0	0	1
33	0	0	3	3	0	0	1
34	0	0	0	2	0	1	1
35	0	0	0	4	0	1	7
36	0	0	0	9	0	0	7
37	0	0	0	10	0	2	11
38	0	0	0	8	0	1	11
39	0	1	0	13	0	0	1
40	0	0	0	11	0	3	4
41	0	0	0	16	0	2	4
42	0	1	0	28	5	0	3
43	0	0	0	10	0	0	0
44	0	0	0	17	2	3	8
44.5	0	0	0	15	0	0	2
45	0	0	2	87	1	1	0
45.5	0	0	0	12	1	4	0

46	0	0	1	71	0	1	0
46.5	0	0	1	109	0	0	0
47	0	3	3	30	0	0	0
48	0	0	0	7	1	0	0
49	0	1	0	78	0	0	0
50	4	0	0	125	7	0	2
51	0	0	0	85	3	0	1
52	0	0	0	53	0	2	0
53	0	0	0	87	2	0	0
54	3	0	0	88	2	0	1
55	0	0	0	104	2	0	1
56	2	0	0	45	3	0	2
57	1	0	0	59	5	0	2
58	5	0	0	70	0	0	0
59	5	0	0	47	1	0	0
60	1	0	0	49	2	0	0
61	2	0	0	50	0	0	0
62	0	0	0	28	0	0	0
63	0	0	0	42	3	0	3
64	1	0	0	36	4	2	4
65	0	0	0	30	0	1	7
66	1	0	0	28	1	1	2
67	1	0	0	39	1	1	0
Sample codes➔	**22**	**23**	**24**	**25**	**26**	**27**	**28**
1	0	0	5	26	0	2	0
3	0	0	2	29	0	4	0
3.5	0	0	0	23	0	1	0
4	0	0	3	19	0	0	0
9	0	0	0	33	0	4	0
10	0	0	1	38	5	0	4
11	0	0	3	26	0	0	0
12	0	0	0	5	0	0	0
13	0	0	0	2	0	0	0
14	0	0	3	5	0	0	0
15	0	0	2	8	1	0	0
16	0	0	2	3	0	1	0
17	0	0	2	2	1	1	0
18	0	0	1	0	2	0	0
19	0	0	3	7	0	0	0
20	0	0	8	2	0	0	0

21	0	0	1	1	0	0	0
22	0	0	8	15	0	0	0
23	0	0	5	7	0	0	0
24	0	0	4	10	1	0	0
25	0	0	1	7	0	0	0
26	0	0	3	0	0	3	1
27	0	0	4	11	0	2	6
28	0	0	0	22	0	0	0
29.5	0	0	3	5	0	4	0
30	0	0	7	10	0	1	1
31	0	0	7	5	1	0	0
32	0	0	3	24	3	6	3
33	0	0	3	24	3	6	3
34	0	0	2	12	13	32	5
35	0	0	1	22	1	9	7
36	0	0	1	3	2	10	1
37	0	0	5	4	6	8	1
38	0	0	5	3	8	6	7
39	0	0	3	1	4	8	8
40	0	0	2	1	4	14	6
41	0	0	3	3	6	11	0
42	0	0	2	1	2	7	3
43	0	0	2	2	4	3	2
44	0	0	4	1	2	8	1
44.5	0	0	2	1	1	6	2
45	0	0	2	0	0	3	0
45.5	0	0	0	2	0	3	0
46	0	0	0	0	0	0	0
46.5	0	0	0	0	0	0	0
47	0	0	0	0	0	0	0
48	0	0	0	0	0	0	0
49	0	0	2	1	0	3	0
50	0	0	2	0	0	0	0
51	0	0	0	0	3	1	0
52	0	1	0	0	0	0	0
53	0	0	0	0	0	0	0
54	0	0	0	0	0	1	0
55	0	0	0	0	3	0	0
56	0	0	0	0	1	0	0
57	0	0	2	0	3	0	0
58	0	0	0	0	1	0	0

59	0	0	1	0	0	0	0
60	0	0	1	0	0	0	0
61	0	0	0	0	2	0	0
62	1	5	0	1	0	0	0
63	0	0	0	0	3	0	0
64	0	0	1	0	1	0	1
65	0	0	0	0	2	0	5
66	0	0	2	0	1	0	0
67	0	0	1	1	5	0	0
Sample codes➔	**29**	**30**	**31**	**32**	**33**	**34**	**35**
Depth (cm)							
1	0	0	0	0	0	0	0
3	0	0	0	0	0	0	0
3.5	0	0	0	0	0	0	1
4	2	0	0	0	0	0	0
4.5	1	0	0	0	0	0	0
5	0	0	0	0	0	0	0
6	0	0	0	0	3	0	1
7	3	0	0	0	0	0	0
8	1	0	0	0	2	0	0
9	2	0	0	0	0	0	1
10	0	0	0	0	0	0	0
11	0	0	0	0	0	0	1
12	0	0	0	0	0	0	0
13	0	0	0	0	0	0	1
14	2	0	0	0	0	0	0
15	0	0	0	0	1	0	1
16	0	0	0	0	1	0	0
17	1	0	0	0	0	0	0
18	0	1	0	0	2	0	2
19	0	0	0	0	0	0	0
20	2	0	0	0	0	0	2
21	3	2	0	0	0	0	2
22	1	0	0	0	0	0	0
23	5	1	0	0	1	0	0
24	3	0	0	0	0	0	0
25	6	0	0	0	0	0	0
26	2	1	0	0	0	0	0
27	7	1	0	0	0	0	1
28	0	0	0	0	0	0	0

29.5	6	5	0	0	0	0	0
30	3	3	0	0	0	0	0
31	5	0	0	0	0	0	0
32	3	0	0	0	4	0	1
33	3	0	0	0	4	0	1
34	2	1	0	0	0	0	0
35	2	2	0	0	2	0	0
36	1	3	0	0	0	0	0
37	1	3	0	0	1	0	1
38	3	1	0	0	0	0	1
39	7	1	0	0	0	0	0
40	13	2	0	0	0	0	3
41	5	1	0	0	3	0	3
42	9	2	0	0	1	0	1
43	8	0	0	0	3	0	0
44	14	2	0	0	3	0	1
44.5	9	0	0	0	3	0	2
45	1	0	0	0	0	0	0
45.5	8	2	0	0	0	0	1
46	4	0	0	0	0	0	3
46.5	1	0	0	0	0	0	2
47	9	0	0	0	0	0	0
48	0	1	0	0	0	0	1
49	1	2	0	0	4	0	0
50	0	2	0	0	3	0	6
51	0	1	0	0	7	0	8
52	0	3	0	1	0	10	0
53	0	1	0	0	1	0	2
54	3	1	0	0	4	0	2
55	0	2	0	0	3	0	1
56	1	5	0	0	10	0	2
57	3	4	0	0	4	0	4
58	1	5	0	0	9	0	0
59	0	9	0	0	3	0	3
60	0	9	0	0	4	0	1
61	0	5	0	0	0	0	2
62	1	3	1	0	0	9	0
63	3	4	0	0	1	0	3
64	3	0	0	0	6	0	11
65	12	0	0	0	5	0	13
66	6	0	0	0	6	0	12

67	4	0	0	0	5	0	14
Sample codes➔	**36**	**37**	**38**	**39**	**40**	**41**	**42**
Depth (cm)							
1	0	0	0	0	0	0	0
3	0	0	0	0	0	0	0
3.5	0	0	0	0	0	0	0
4	0	0	0	0	0	0	0
4.5	0	0	0	0	0	4	0
5	0	0	0	0	0	2	0
6	0	0	0	2	0	1	0
7	0	0	2	0	0	4	0
8	0	0	0	0	0	3	0
9	0	0	0	0	0	5	0
10	0	0	0	0	0	3	0
11	0	0	2	0	0	3	0
12	0	0	0	0	0	0	0
13	0	0	0	0	0	1	0
14	0	0	0	0	0	0	0
15	0	0	0	0	0	0	0
16	0	0	0	0	0	0	0
17	0	0	2	0	0	0	0
18	0	0	1	0	0	0	0
19	0	0	0	0	0	1	0
20	0	0	0	1	0	0	0
21	0	0	1	5	0	0	0
22	0	0	1	0	0	2	0
23	0	0	0	1	0	9	0
24	0	0	0	0	0	1	0
25	0	0	0	0	0	0	0
26	0	0	0	3	0	1	0
27	0	0	1	5	0	0	0
28	0	0	0	1	0	1	0
29.5	0	0	0	3	0	1	0
30	0	0	0	1	0	1	0
31	0	0	0	3	0	1	0
32	0	1	0	0	2	3	0
33	0	1	0	0	2	3	0
34	0	0	1	1	0	16	0
35	0	0	1	1	4	3	0
36	0	0	0	9	14	3	0

37	0	0	4	6	8	1	0
38	0	0	1	1	1	2	0
39	0	0	5	5	10	1	0
40	0	0	3	3	4	0	0
41	0	0	2	17	2	2	0
42	0	0	3	7	1	5	0
43	0	0	0	15	3	3	0
44	0	0	2	12	1	5	0
44.5	0	0	0	17	1	3	0
45	0	0	4	16	0	12	0
45.5	0	0	8	17	0	6	0
46	0	0	0	7	0	0	0
46.5	0	0	2	8	0	0	0
47	0	0	0	4	0	10	0
48	0	0	0	0	0	0	0
49	0	0	8	6	0	0	0
50	0	0	16	5	0	0	0
51	0	0	31	7	1	0	0
52	1	0	19	0	0	2	1
53	0	0	16	2	0	1	0
54	0	0	8	1	0	0	0
55	0	0	8	1	0	0	0
56	0	0	10	3	0	0	0
57	0	0	9	1	0	0	0
58	0	0	3	3	0	0	0
59	0	0	9	0	0	0	0
60	0	0	2	4	0	0	0
61	0	0	1	2	0	0	0
62	0	0	10	0	0	0	0
63	0	0	7	0	0	0	0
64	0	0	29	1	0	0	0
65	0	0	27	1	0	0	0
66	0	0	33	2	0	1	0
67	0	0	40	2	0	0	0
Sample codes➔	**43**	**44**	**45**	**46**	**47**	**48**	**49**
Depth (cm)							
1	42	4	0	0	0	0	0
3	54	5	0	0	0	0	0
3.5	65	4	0	0	0	0	0
4	42	2	0	0	0	0	0

4.5	48	2	0	0	0	0	0
5	32	0	0	0	0	0	0
6	47	11	1	0	0	0	0
7	44	11	0	0	0	0	0
8	33	9	1	0	0	0	0
9	46	9	0	0	0	0	0
10	32	1	1	0	0	0	0
11	44	14	0	0	0	0	0
12	154	40	0	0	0	0	0
13	125	32	0	0	0	0	0
14	144	24	2	0	1	0	0
15	175	30	0	0	1	2	0
16	218	30	0	0	1	0	0
17	231	20	0	0	0	1	2
18	265	24	0	1	0	0	0
19	122	12	0	0	0	0	0
20	145	10	1	0	0	0	1
21	102	12	0	0	3	0	0
22	98	18	3	0	2	3	1
23	119	7	4	0	2	3	0
24	150	13	0	0	2	2	0
25	116	15	0	0	0	0	1
26	122	16	4	0	6	0	0
27	85	13	1	0	6	0	0
28	107	18	0	0	0	1	2
29.5	50	18	0	0	0	0	0
30	74	15	0	0	4	5	0
31	80	10	0	0	2	0	3
32	97	7	0	2	18	1	0
33	97	7	0	2	18	1	0
34	32	2	0	1	21	9	0
35	58	9	0	5	14	4	0
36	53	21	0	2	18	3	0
37	44	6	0	3	21	22	0
38	41	12	3	0	42	57	0
39	70	36	0	2	10	14	1
40	79	31	4	3	11	6	7
41	69	48	0	6	6	10	9
42	70	36	0	3	12	15	11
43	58	40	2	7	3	2	8
44	54	26	0	2	12	4	20

44.5	67	24	1	4	9	14	7
45	112	91	8	0	7	0	0
45.5	66	60	1	0	0	0	0
46	29	59	6	0	0	0	0
46.5	15	49	4	0	1	0	0
47	51	80	3	0	5	0	0
48	4	3	0	0	0	0	0
49	22	44	0	3	5	11	2
50	14	49	0	2	4	9	0
51	25	39	0	3	5	19	0
52	33	72	17	0	5	0	0
53	65	85	0	4	1	10	0
54	76	70	1	4	2	13	0
55	40	88	0	4	1	8	0
56	91	60	0	2	3	15	0
57	65	71	0	0	2	12	0
58	35	90	0	4	2	8	0
59	16	106	0	2	2	2	0
60	17	120	0	2	0	6	0
61	13	150	0	5	0	4	0
62	27	97	14	0	2	0	0
63	95	79	2	1	0	11	0
64	50	50	0	2	7	30	0
65	55	38	0	2	8	19	11
66	46	41	1	2	3	13	5
67	43	43	0	7	1	13	14
Sample codes➔	**50**	**51**	**52**	**53**	**54**	**55**	**56**
Depth (cm)							
1	0	2	0	0	0	0	0
3	0	1	0	0	0	0	0
3.5	0	0	0	2	0	0	0
4	0	0	1	3	0	0	0
4.5	0	1	4	0	0	0	0
5	0	0	1	1	0	0	0
6	0	2	1	0	0	0	0
7	0	4	0	0	0	0	0
8	0	0	1	0	0	0	0
9	0	0	1	0	0	0	0
10	0	2	1	5	0	0	0
11	0	3	1	0	0	0	0

12	0	0	0	1	0	0	0
13	0	0	2	0	0	0	0
14	0	5	0	0	0	0	0
15	0	0	0	0	0	0	0
16	0	1	0	0	0	0	0
17	0	0	1	0	0	0	0
18	0	2	0	2	0	2	0
19	0	2	0	0	0	0	0
20	0	5	2	0	0	0	0
21	0	0	3	0	0	0	0
22	0	19	5	0	0	0	0
23	0	5	1	0	0	0	0
24	0	9	2	2	0	0	0
25	0	4	1	0	0	0	0
26	0	9	4	0	0	0	0
27	0	18	0	0	0	0	0
28	0	2	6	0	0	0	0
29.5	0	7	3	2	0	0	0
30	0	20	4	0	0	0	0
31	0	8	6	0	0	0	0
32	0	7	9	0	0	0	1
33	0	7	9	0	0	0	1
34	0	20	2	12	0	0	0
35	0	13	7	10	0	2	0
36	0	9	0	10	0	0	0
37	0	10	6	6	0	2	0
38	0	22	7	15	0	3	0
39	0	5	2	6	0	2	0
40	0	4	0	4	0	1	0
41	0	14	5	4	0	0	0
42	0	6	0	5	0	0	0
43	0	9	0	0	0	0	0
44	0	2	0	1	0	2	0
44.5	0	15	0	3	0	0	0
45	0	1	7	0	0	0	0
45.5	0	6	7	0	0	1	0
46	0	2	5	1	0	0	0
46.5	0	3	3	0	0	0	0
47	0	0	9	2	0	1	0
48	0	0	0	0	0	0	0
49	0	3	2	0	0	0	0

50	0	0	0	2	0	1	0
51	0	1	0	3	0	3	0
52	1	0	10	1	1	0	0
53	0	1	0	2	0	2	0
54	0	0	2	4	0	1	0
55	0	0	0	5	0	2	0
56	0	4	0	5	0	2	0
57	0	3	0	3	0	0	0
58	0	1	0	4	0	5	0
59	0	0	0	0	0	1	0
60	0	0	0	0	0	1	0
61	0	0	0	0	0	0	0
62	0	0	3	1	3	0	0
63	0	9	4	0	0	1	0
64	0	1	7	10	0	4	0
65	0	6	2	11	0	5	0
66	0	1	1	3	0	0	0
67	0	0	0	2	0	0	0
Sample codes➔	**57**	**58**	**59**	**60**	**61**	**62**	**63**
Depth (cm)							
1	0	0	0	0	0	12	0
3	0	0	0	0	0	7	0
3.5	0	0	4	0	0	6	0
4	0	0	0	0	0	6	0
4.5	0	0	0	0	0	5	0
5	0	0	0	0	0	4	0
6	3	0	2	2	3	10	2
7	6	0	0	1	4	1	0
8	4	0	0	0	2	2	2
9	0	0	0	0	7	6	0
10	4	4	0	6	0	13	0
11	3	0	0	1	0	5	1
12	0	0	0	1	3	3	9
13	2	0	0	0	20	1	6
14	0	0	0	0	5	2	8
15	1	4	2	0	6	1	8
16	0	3	1	1	9	0	14
17	0	2	0	2	14	2	10
18	0	4	0	1	14	0	6
19	0	0	0	0	22	1	0

20	1	6	1	3	6	2	6
21	0	4	0	4	5	1	4
22	0	4	0	2	13	2	4
23	0	1	0	6	3	0	2
24	1	4	0	3	6	2	6
25	0	1	0	8	15	17	6
26	0	5	0	4	4	0	2
27	0	1	0	1	8	13	3
28	2	2	1	1	3	6	2
29.5	0	0	0	2	7	5	0
30	1	1	0	2	4	3	15
31	0	1	0	1	12	4	4
32	0	0	2	3	4	5	1
33	0	0	2	3	4	5	1
34	0	0	8	6	3	8	0
35	0	0	2	3	10	5	3
36	0	0	3	0	10	7	7
37	0	0	1	0	5	6	6
38	0	0	0	0	3	5	0
39	0	0	3	2	4	6	4
40	0	0	3	0	0	10	6
41	0	0	2	1	6	17	2
42	0	0	0	0	4	20	3
43	1	0	2	0	4	16	2
44	0	0	1	0	0	27	2
44.5	0	0	3	0	2	9	2
45	10	0	0	0	0	2	0
45.5	0	0	1	2	1	16	0
46	0	0	0	0	0	10	0
46.5	0	0	0	1	2	8	0
47	0	0	0	1	5	7	0
48	0	0	0	0	0	0	1
49	0	1	0	0	2	4	0
50	0	0	0	0	0	3	0
51	0	0	0	0	0	6	0
52	0	0	0	0	2	3	0
53	0	0	0	0	0	3	0
54	0	0	0	0	0	3	0
55	0	0	0	0	0	1	0
56	0	0	0	0	0	9	0
57	0	0	0	0	0	6	0

58	0	0	0	0	0	4	0
59	0	0	0	0	0	0	0
60	0	0	0	0	0	0	0
61	0	0	0	0	0	0	0
62	0	0	0	0	0	3	0
63	0	0	0	0	0	1	0
64	0	0	0	1	1	17	0
65	0	0	0	0	0	4	0
66	0	0	0	0	0	2	0
67	0	0	0	1	0	7	0
Sample codes➔	**64**	**65**	**66**	**67**	**68**	**69**	**70**
Depth (cm)							
1	0	1	0	78	0	14	0
3	0	2	0	71	0	4	0
3.5	0	0	0	44	0	16	0
4	0	0	0	32	0	13	0
4.5	0	0	0	35	0	4	0
5	0	0	0	38	0	8	0
6	0	0	3	9	0	7	0
7	0	0	8	23	0	16	0
8	1	0	1	15	0	14	0
9	0	0	14	14	0	5	0
10	0	0	11	15	0	0	0
11	0	0	9	18	0	9	0
12	0	1	0	12	0	7	0
13	0	0	0	6	0	0	0
14	0	2	1	0	0	1	0
15	0	1	4	4	0	0	0
16	0	0	3	0	0	0	0
17	0	2	3	0	0	0	0
18	0	1	2	0	0	1	0
19	0	1	0	14	0	0	0
20	0	0	4	0	0	0	0
21	0	0	6	0	0	0	0
22	0	1	9	0	0	0	0
23	0	0	4	0	0	0	0
24	0	1	10	0	0	0	0
25	0	1	3	0	0	0	0
26	0	3	4	0	0	1	0
27	0	5	12	0	0	1	0

28	0	1	7	0	0	4	0
29.5	0	2	0	7	0	2	0
30	0	2	14	1	0	0	0
31	0	2	9	0	0	7	0
32	2	2	20	0	1	1	1
33	2	2	20	0	1	1	1
34	1	3	3	1	0	0	0
35	0	5	12	5	0	0	0
36	0	2	18	23	0	0	0
37	0	2	11	45	0	0	0
38	0	6	5	12	0	0	0
39	0	1	25	8	0	0	0
40	1	2	33	9	0	0	0
41	0	2	34	2	0	0	0
42	1	7	38	0	0	0	0
43	0	1	64	11	0	0	0
44	0	1	16	0	0	0	0
44.5	0	5	55	0	0	0	0
45	1	4	4	0	0	1	0
45.5	1	1	28	0	0	1	0
46	0	0	0	0	0	3	0
46.5	1	2	3	0	0	0	0
47	1	2	4	5	0	1	0
48	0	0	0	0	0	0	0
49	1	1	4	0	0	0	0
50	3	1	0	0	0	0	0
51	2	2	2	0	0	0	0
52	0	2	0	0	0	0	0
53	2	2	0	0	0	0	0
54	3	2	0	0	0	0	0
55	1	1	0	0	0	0	0
56	6	3	0	0	0	0	0
57	3	2	1	0	0	0	0
58	1	2	0	0	0	0	0
59	1	2	0	0	0	0	0
60	4	0	0	0	0	0	0
61	0	2	0	0	0	0	0
62	1	2	2	1	0	0	0
63	6	1	0	0	0	0	0
64	0	1	1	0	0	0	0
65	1	4	0	0	0	0	0

66	2	5	2	0	0	0	0
67	6	0	1	0	0	0	0
Sample codes➔	**71**	**72**	**73**	**74**	**75**	**76**	**77**
Depth (cm)							
1	0	0	0	2	0	0	0
3	4	0	0	1	0	0	0
3.5	13	0	0	0	0	0	0
4	13	0	0	0	0	0	0
4.5	9	0	0	0	0	0	0
5	7	0	0	0	0	0	0
6	20	0	0	0	0	0	0
7	10	0	0	0	0	0	0
8	19	0	0	0	0	0	0
9	18	0	0	0	0	0	0
10	18	14	0	2	0	0	0
11	21	0	0	0	0	0	0
12	7	0	0	0	0	0	0
13	0	0	0	0	0	0	0
14	4	0	0	2	0	0	0
15	4	9	0	0	0	0	0
16	1	2	0	0	0	0	0
17	0	2	0	2	0	0	0
18	2	0	0	2	0	0	0
19	0	0	0	0	0	0	0
20	2	0	0	0	0	0	0
21	3	0	0	1	0	0	0
22	0	0	0	3	0	0	0
23	2	0	0	1	0	0	0
24	0	7	0	0	0	0	0
25	2	0	0	0	0	0	0
26	0	0	0	0	0	0	0
27	5	0	0	0	0	0	0
28	8	0	0	1	0	0	0
29.5	4	0	0	0	0	0	0
30	3	0	0	1	0	0	0
31	18	0	0	1	0	0	0
32	0	0	1	2	1	0	0
33	0	0	1	2	1	0	0
34	0	0	0	3	0	0	0
35	2	3	0	1	0	0	0

36	0	7	0	0	0	0	0
37	2	7	0	2	0	0	0
38	1	6	0	5	0	0	0
39	2	7	0	0	0	0	0
40	0	1	0	1	0	0	0
41	2	5	0	1	0	0	0
42	0	0	0	3	0	0	0
43	1	5	0	1	0	0	0
44	0	3	0	0	0	0	0
44.5	2	1	0	2	0	0	0
45	0	0	0	1	0	0	0
45.5	8	0	0	2	0	0	0
46	0	0	0	0	0	0	0
46.5	0	0	0	0	0	0	0
47	1	0	0	1	0	0	0
48	0	0	0	0	0	0	0
49	0	3	0	1	0	0	0
50	0	0	0	0	0	0	0
51	0	0	0	1	0	0	0
52	1	0	1	1	0	1	1
53	0	0	0	0	0	0	0
54	0	0	0	2	0	0	0
55	0	0	0	1	0	0	0
56	0	0	0	1	0	0	0
57	0	0	0	1	0	0	0
58	0	0	0	3	0	0	0
59	0	1	0	0	0	0	0
60	0	0	0	1	0	0	0
61	0	0	0	0	0	0	0
62	0	0	0	0	0	1	0
63	0	0	0	0	0	0	0
64	0	0	0	2	0	0	0
65	0	0	0	1	0	0	0
66	0	0	0	0	0	0	0
67	1	0	0	3	0	0	0
Sample codes➔	**78**	**79**	**80**	**81**	**82**	**83**	**84**
Depth (cm)							
1	0	0	0	6	0	0	0
3	0	0	0	2	0	0	0
3.5	0	0	0	2	0	0	0

4	0	0	0	2	0	0	0
4.5	0	0	0	1	0	0	0
5	0	0	0	1	0	0	0
6	0	0	0	1	4	0	0
7	0	0	0	3	0	0	0
8	0	0	0	3	1	0	0
9	0	0	0	2	0	0	0
10	0	0	0	2	0	0	2
11	0	0	0	2	0	0	0
12	0	0	0	3	6	0	0
13	0	0	0	1	0	0	0
14	0	0	0	1	17	0	0
15	0	0	0	1	2	0	8
16	0	0	0	0	2	0	7
17	0	0	2	2	0	0	0
18	0	0	1	3	0	0	4
19	0	0	0	4	0	0	0
20	0	0	0	2	9	0	0
21	0	0	0	3	6	0	0
22	0	0	0	2	1	0	0
23	0	0	0	1	2	0	0
24	0	0	3	1	2	0	0
25	0	0	0	4	7	0	0
26	0	0	0	5	0	0	0
27	0	0	0	8	2	0	0
28	0	0	0	2	2	0	0
29.5	0	0	0	5	0	0	0
30	0	0	0	6	6	0	0
31	0	0	0	4	2	0	0
32	2	1	0	6	0	4	0
33	2	1	0	6	0	4	0
34	0	0	2	12	0	0	4
35	0	0	3	6	3	0	2
36	0	0	2	7	0	0	3
37	0	0	5	8	1	0	0
38	0	0	5	10	1	0	1
39	0	0	1	5	0	0	3
40	0	0	3	6	0	0	3
41	0	0	5	12	0	0	0
42	0	0	6	5	1	0	0
43	0	0	2	2	1	0	2

44	0	0	5	3	0	0	0
44.5	0	0	4	4	0	0	1
45	0	0	0	10	0	0	0
45.5	0	0	0	9	0	0	0
46	0	0	0	6	0	0	0
46.5	0	0	0	4	0	0	0
47	0	0	0	3	0	0	0
48	0	0	1	0	0	0	0
49	0	0	1	3	0	0	0
50	0	0	0	0	0	0	0
51	0	0	1	1	0	0	0
52	0	0	0	2	0	0	0
53	0	0	0	0	0	0	0
54	0	0	0	2	0	0	0
55	0	0	0	0	0	0	0
56	0	0	0	0	0	0	0
57	0	0	0	0	0	0	0
58	0	0	0	0	0	0	1
59	0	0	0	0	0	0	0
60	0	0	0	0	0	0	0
61	0	0	0	0	0	0	0
62	0	0	0	4	0	0	0
63	0	0	0	0	0	0	0
64	0	0	0	0	0	0	0
65	0	0	0	1	0	0	0
66	0	0	0	1	0	0	0
67	0	0	0	1	0	0	0
Sample codes➔	**85**	**86**	**87**	**88**	**89**	**90**	**91**
Depth (cm)							
1	0	0	0	9	0	0	0
3	0	0	0	2	0	0	0
3.5	0	0	0	0	0	0	0
4	0	0	0	0	0	0	0
4.5	0	0	0	3	0	0	0
5	0	0	0	0	0	0	0
6	0	0	0	0	0	0	0
7	0	0	0	0	0	0	0
8	0	0	0	1	0	0	0
9	0	0	0	0	0	0	0
10	0	0	1	3	0	0	0

11	0	0	0	0	0	0	0
12	0	0	0	2	0	0	0
13	0	0	0	2	0	0	0
14	0	0	0	0	0	0	0
15	0	0	0	0	0	0	0
16	0	0	0	1	0	0	0
17	0	0	3	0	0	0	0
18	0	0	4	1	0	0	0
19	0	0	0	2	0	0	0
20	0	0	0	1	0	0	0
21	0	0	0	0	0	0	0
22	0	0	0	2	0	0	0
23	0	0	0	1	0	0	0
24	0	0	1	0	0	0	0
25	0	0	0	2	0	0	0
26	0	0	0	6	0	0	0
27	0	0	0	5	0	0	0
28	0	0	0	3	0	0	0
29.5	0	0	0	0	0	0	0
30	0	0	0	2	0	0	0
31	0	0	0	0	0	0	0
32	1	1	0	1	1	3	0
33	1	1	0	1	1	3	0
34	0	0	0	1	0	0	0
35	0	0	1	0	0	0	0
36	0	0	0	1	0	0	0
37	0	0	3	1	0	0	0
38	0	0	11	1	0	0	0
39	0	0	2	1	0	0	0
40	0	0	1	1	0	0	0
41	0	0	2	2	0	0	0
42	0	0	1	2	0	0	0
43	0	0	3	1	0	0	0
44	0	0	2	4	0	0	0
44.5	0	0	2	1	0	0	0
45	0	0	0	1	0	0	0
45.5	0	0	0	1	0	0	0
46	0	0	0	4	0	0	0
46.5	0	0	0	0	0	0	0
47	0	0	0	0	0	0	0
48	0	0	0	0	0	0	0

49	0	0	0	7	0	0	0
50	0	0	8	4	0	0	0
51	0	0	5	5	0	0	0
52	0	0	0	4	0	0	3
53	0	0	1	1	0	0	0
54	0	0	2	2	0	0	0
55	0	0	0	3	0	0	0
56	0	0	1	6	0	0	0
57	0	0	2	4	0	0	0
58	0	0	3	6	0	0	0
59	0	0	0	3	0	0	0
60	0	0	0	2	0	0	0
61	0	0	4	6	0	0	0
62	0	0	0	4	0	0	2
63	0	0	1	3	0	0	0
64	0	0	1	4	0	0	0
65	0	0	1	4	0	0	0
66	0	0	3	0	0	0	0
67	0	0	1	0	0	0	0

Sample codes➔	**92**	**Chryso phyte**
Depth (cm)		
1	26	12
3	20	7
3.5	13	26
4	17	15
4.5	6	2
5	8	12
6	11	10
7	10	11
8	12	8
9	12	7
10	5	16
11	13	13
12	2	21
13	3	10
14	5	7
15	2	9
16	1	12
17	0	30
18	1	40

19	27	28
20	5	35
21	5	29
22	8	37
23	5	36
24	9	27
25	12	23
26	10	46
27	10	67
28	7	17
29.5	20	27
30	11	55
31	8	27
32	20	49
33	20	44
34	20	48
35	11	41
36	10	104
37	12	145
38	23	164
39	22	188
40	8	173
41	17	189
42	15	183
43	5	95
44	14	210
44.5	12	147
45	40	261
45.5	29	108
46	28	229
46.5	29	504
47	33	249
48	1	200
49	11	538
50	11	725
51	13	222
52	66	165
53	9	471
54	9	528
55	12	489
56	10	337

57	13	435
58	6	689
59	8	745
60	3	535
61	4	555
62	52	253
63	7	405
64	18	237
65	20	185
66	17	244
67	12	304

Table D3: One hundred and thirty-six names and corresponding numbers for the surface sediment training set raw counts.

Aulacoseira ambigua	*1*	*Encyonema ceaspitosum*	*31*
Psammothidium curtissima	*2*	*Encyonema minutum*	*32*
Psammothidium chlidanos	*3*	*Encyonopsis neogracile*	*33*
Achnanthidium didymum	*4*	*Encyonema silesiacum*	*34*
Achnanthes exigua	*5*	*Cymbopleura naviculiformis*	*35*
Psammothidium grischunum	*6*	*Diploneis finnica*	*36*
Psammothidium helvetica	*7*	*Eunotia bilunaris*	*37*
Planothidium lanceolatum	*8*	*Eunoitia curvata*	*38*
Rossithidium linearis	*9*	*Eunotia* cf. *implicata*	*39*
Achnanthidium minutissimum	*10*	*Eunotia incisa*	*40*
Eolimna minima	*11*	*Eunotia monodon major*	*41*
Rossithidium nodosum	*12*	*Eunotia pectinalis*	*42*
Achnanthidium reimeri	*13*	*Eunotia praerupta*	*43*
Psammothidium subatomoides	*14*	*Eunotia serra*	*44*
Brachysira brebissoni	*15*	*Pseudostaurosira brevistriata*	*45*
Brachysira microcephala	*16*	*Fagilaria capucina*	*46*
Asterionella formosa	*17*	*Fagilaria capucina* var. *gracilis*	*47*
Eucocconeis flexella	*18*	*Fagilaria capucina var. mesolepta*	*48*
Eucocconeis laevis	*19*	*Fagilaria capucina var. vaucheriae*	*49*
Cocconeis placentula	*20*	*Staurosira construens* var. *venter*	*50*
Discostella pseudostelligera	*21*	*Pseudostaurosira parasitica*	*51*
Discostella stelligera	*22*	*Staurosirella pinnata*	*52*
Lindavia radiosa	*23*	*Fragilaria tenera*	*53*
Encyonopsis cesatii	*24*	*Fragilaria crassirhombica*	*54*
Cymbopleura lapponica	*25*	*Frustulia crassinervia*	*55*
Encyonopsis lange-bertalotii	*26*	*Gomphonema acuminatum*	*56*
Cymbella subcuspidata	*27*	*Gomphonema camburnii*	*57*

Cymbella hybrida	*28*	*Gomphonema gracile*	*58*
Encyonema hebridicum	*29*	*Gomphonema hebridicum*	*59*
Encyonopsis microcephala	*30*	*Gomphonema minutum*	*60*
Gomphonema parvulum	*61*	*Nitzschia amphioxys*	*91*
Gomphonema pumilum	*62*	*Nitzschia angustatum*	*92*
Gomphopnema spp. #1	*63*	*Nitzschia archibaldii*	*93*
Gomphonema truncatum	*64*	*Nitzschia austriaca*	*94*
Gomphonema varistriatum	*65*	*Nitzschia fonticula*	*95*
Kraskella kriegeriana	*66*	*Nitzschia frustulum*	*96*
Navicula bergeri	*67*	*Nitzschia gracilis*	*97*
Navicula cyrptocephala	*68*	*Nitzschia intermedia*	*98*
Navicula difficillima	*69*	*Nitzschia lacuum*	*99*
Navicula germanii	*70*	*Nitzschia linearis*	*100*
Navicula kuelbsii	*71*	*Nitzschia palea*	*101*
Navicula lenzii	*72*	*Nitzschia perminuta*	*102*
Navicula leptostriata	*73*	*Nitzschia pura*	*103*
Navicula medioconvexa	*74*	*Nitzschia radicula*	*104*
Nacicula minuscula	*75*	*Nitzschia recta*	*105*
Navicula notha	*76*	*Nitzschia suchlandtii*	*106*
Navicula pseudoventralis	*77*	*Nitzschia* sp. #3	*107*
Navicula radiosa	*78*	*Pinnularia abaujensis*	*108*
Navicula seminulum	*79*	*Pinnularia biceps*	*109*
Navicula soehrensis	*80*	*Pinnularia interrupta*	*110*
Navicula sp. #2	*81*	*Pinnularia legumen*	*111*
Navicula sp. #22	*82*	*Pinnularia major*	*112*
Naviicula submolesta	*83*	*Pinnularia mesolepta*	*113*
Navicula submuralis	*84*	*Pinnularia microstauron*	*114*
Navicula subtilisima	*85*	*Pinnularia* sp. #4	*115*
Naviula tridentula	*86*	*Pinnularia viridis*	*116*
Navicula vitiosa	*87*	*Sellaphora americana*	*117*
Navicula vulpina	*88*	*Sellaphora blackfordensis*	*118*
Neidium ampliatum	*89*	*Sellaphora laevissima*	*119*
Neidium iridis	*90*	*Sellaphora pupula*	*120*
Sellaphora seminulum	*121*		
Sellaphora stroemeii	*122*		

Sellaphora sp. # 20	*123*			
Sellaphora sp. #22	*124*			
Stenopterobia anceps	*125*			
Stenopterobia delicatissima	*126*			
Stenopterobia curvula	*127*			
Stauroneis anceps	*128*			
Stauroneis neohyalina	*129*			
Stauroneis phoenicenteron	*130*			
Stauroneis gracilis	*131*			
Stauroneis siberica	*132*			
Surirella linearis	*133*			
Synedra subrhombica	*134*			

Table D4: Diatom raw counts for surface sediment training set. Includes all 136 taxa found in the surface sediment samples. Taxa are numbered according to Table D3 with sediment depths 0.5 to 5 meters.

Depth (m)	1	2	3	4	5	6	7	8	9	10	11	12	13	14	15	16	17	18	19	20	21	22	23	24	25
0.5	0	3	3	0	0	2	3	0	2	78	28	0	0	8	0	24	0	0	0	0	5	1	2	2	0
1	0	0	1	0	0	2	4	2	10	110	29	0	0	11	0	7	0	1	0	0	2	0	3	0	0
2	0	0	0	0	0	0	0	0	0	129	2	0	1	0	0	59	0	0	0	0	27	1	0	0	0
3	1	0	1	0	0	2	0	0	2	39	11	0	0	2	0	2	1	0	0	0	4	0	2	1	0
4	0	8	1	0	0	0	3	0	0	56	2	2	0	2	0	2	3	0	0	0	18	0	2	0	0
5	0	6	0	1	0	0	1	0	1	55	5	0	0	5	0	2	0	0	0	0	35	2	4	1	0
0.5	0	0	0	0	0	0	0	0	0	193	2	0	0	0	0	14	0	0	15	0	51	6	1	1	0
1	0	0	0	0	0	0	0	0	1	146	7	0	0	0	0	17	0	0	1	0	24	0	0	0	0
2	0	0	0	0	0	0	0	0	6	109	13	0	0	2	1	19	0	0	1	0	41	2	0	2	0
3	0	0	0	0	1	0	0	0	1	67	22	0	0	0	0	10	0	0	0	0	32	4	4	0	0
4	1	0	0	0	0	0	3	0	2	54	9	0	0	1	0	6	0	0	0	0	38	9	5	3	0
5	0	6	0	1	0	0	1	0	1	55	5	0	0	5	0	8	0	0	0	0	35	2	4	1	0
0.5	0	0	0	0	0	0	0	0	0	156	4	0	0	0	0	39	0	3	0	0	18	0	0	0	0
1	0	0	0	0	0	0	0	0	2	103	0	0	0	0	0	27	0	0	0	0	40	0	2	0	0
2	0	0	0	0	0	0	0	0	0	55	10	0	0	3	0	9	0	0	0	0	27	5	4	0	0
3	0	0	0	0	0	0	0	0	0	39	2	0	0	0	0	2	0	0	0	0	4	2	2	2	0
4	0	0	0	0	0	0	0	0	0	106	1	0	0	0	0	10	0	0	0	0	44	7	5	0	2
5	0	0	0	0	0	0	0	0	0	49	10	0	0	0	0	10	0	0	0	0	37	4	5	0	1

Depth (m)	26	27	28	29	30	31	32	33	34	35	36	37	38	39	40	41	42	43	44	45	46	47	48	49	50
0.5	0	0	0	0	4	0	0	2	2	0	1	4	0	0	0	0	1	0	1	1	0	0	0	0	34
1	0	0	0	0	10	0	0	5	3	0	0	2	0	0	0	0	0	0	0	1	6	0	0	1	15
2	0	0	0	0	20	0	0	0	0	0	0	0	0	0	0	0	0	0	0	0	5	1	0	0	25
3	0	0	0	0	4	0	1	2	1	1	0	0	0	0	0	0	0	0	0	11	3	0	0	0	207
4	0	0	0	0	4	0	0	0	1	0	0	0	0	0	0	0	0	0	0	4	7	0	0	0	93
5	0	0	0	0	4	0	1	0	1	0	0	0	0	0	0	0	0	0	0	1	3	0	0	0	105
0.5	0	0	0	0	9	0	1	5	1	0	0	0	6	0	0	0	0	0	0	0	0	0	0	0	4
1	0	0	0	0	14	0	0	0	0	0	0	0	0	0	0	0	0	0	0	0	9	0	0	0	27
2	0	0	0	1	14	0	0	1	0	0	0	0	0	1	0	0	0	0	0	0	0	0	0	0	32
3	0	0	0	0	7	2	0	6	4	0	0	0	0	0	0	0	0	1	0	0	0	0	0	0	76
4	0	1	0	0	8	0	0	0	0	3	0	0	0	0	0	0	0	0	0	0	4	0	0	0	75
5	0	0	0	0	4	0	1	0	1	0	0	0	0	0	0	0	0	0	0	1	3	0	0	0	105
0.5	0	0	1	0	51	0	0	3	0	0	0	0	0	2	0	0	0	2	0	0	2	0	0	0	13
1	0	0	0	0	27	0	0	5	0	0	0	0	0	1	0	0	0	0	0	0	5	0	0	0	19
2	0	0	0	0	4	0	0	5	0	0	0	0	0	0	0	0	0	0	0	0	5	0	1	0	176
3	0	0	0	0	8	0	0	1	1	0	0	0	0	0	0	0	0	0	0	3	6	0	0	0	159
4	6	0	0	0	6	0	0	0	0	0	0	0	0	0	0	0	0	0	0	0	3	0	0	0	70
5	0	2	0	0	6	0	0	1	0	0	0	0	0	0	1	2	0	0	0	0	5	0		0	123

Depth (m)	51	52	53	54	55	56	57	58	59	60	61	62	63	64	65	66	67	68	69	70	71	72
0.5	0	7	0	0	1	0	1	3	0	0	0	0	0	0	1	2	2	1	1	0	0	1
1	1	7	4	0	0	0	1	2	0	0	0	0	0	1	0	0	0	0	0	0	0	0
2	0	1	0	0	0	0	0	8	0	0	0	0	0	0	0	1	0	0	0	0	0	0
3	0	65	0	0	0	1	0	1	1	0	0	0	0	0	0	1	0	0	0	0	7	0
4	0	26	0	0	0	0	0	0	0	0	0	0	0	0	0	1	0	11	0	0	0	0
5	0	23	0	0	0	0	0	0	0	0	0	0	0	0	1	1	0	3	0	0	0	0
0.5	0	0	0	0	0	0	0	1	0	0	1	0	0	0	0	0	0	0	0	0	0	0
1	0	9	0	0	0	1	0	2	0	0	0	0	0	0	0	0	0	0	0	0	0	0
2	0	7	0	0	0	0	0	0	0	0	0	0	0	0	0	1	0	0	0	0	0	0
3	0	13	0	0	0	0	0	0	0	0	0	0	0	1	1	0	0	0	0	0	0	0
4	0	40	0	0	0	0	0	0	0	1	0	0	0	0	0	1	0	1	0	0	0	0
5	0	23	0	0	0	0	0	0	0	0	0	0	0	0	1	1	0	3	0	0	0	0
0.5	0	2	0	4	0	0	0	3	0	0	0	0	1	0	0	0	1	0	0	0	0	0
1	0	2	0	0	0	0	0	0	0	0	1	2	0	0	0	1	0	0	0	0	0	0
2	0	14	0	0	0	0	0	1	0	0	0	0	0	0	0	0	2	0	0	1	0	0
3	0	12	0	0	0	0	0	0	0	0	0	0	0	0	0	0	0	1	0	0	0	0
4	0	10	0	0	0	0	0	1	0	0	0	0	0	0	0	0	0	2	0	0	0	0
5	0	8	0	0	0	0	0	3	0	0	0	1	0	0	0	3	0	1	0	0	0	0

Depth (m)	73	74	75	76	77	78	79	80	81	82	83	84	85	86	87	88	89	90	91	92
0.5	1	2	1	1	6	3	0	0	0	0	0	0	0	0	8	0	0	2	1	0
1	0	0	0	0	10	3	0	1	0	0	0	1	0	2	10	1	2	0	0	0
2	0	0	0	1	0	1	0	0	0	0	0	0	0	0	0	0	0	0	0	0
3	3	1	0	0	3	0	0	0	0	0	0	0	0	0	6	0	0	0	0	1
4	0	0	0	2	11	3	0	2	0	0	0	0	0	0	2	0	0	0	0	0
5	2	1	0	1	6	2	0	1	0	0	0	0	0	0	0	0	0	0	0	0
0.5	3	0	0	0	0	0	0	0	0	0	0	0	0	0	0	0	0	0	0	0
1	1	2	0	7	3	0	0	0	0	0	0	0	0	0	2	0	0	0	0	0
2	0	1	0	5	2	4	0	0	0	1	1	2	0	1	1	0	0	0	0	0
3	1	0	0	6	1	2	0	0	0	0	0	0	0	0	2	0	0	0	0	0
4	0	0	0	5	3	2	1	0	0	0	0	0	0	0	3	0	1	0	0	0
5	2	1	0	1	6	2	0	1	0	0	0	0	0	0	0	0	0	0	0	0
0.5	0	0	0	1	0	2	0	0	1	0	0	0	2	0	0	0	0	0	0	0
1	0	0	0	3	0	1	0	1	1	0	0	0	0	0	0	0	0	0	0	0
2	0	0	0	1	4	1	0	0	0	0	0	0	0	0	3	0	0	0	0	0
3	0	0	0	2	1	3	0	0	0	2	0	0	0	1	1	0	0	0	0	0
4	0	0	0	0	0	3	0	0	0	0	0	0	0	1	0	0	2	0	0	0
5	0	0	0	1	6	1	0	0	0	0	0	0	0	0	0	0	0	0	0	0

Depth (m)	93	94	95	96	97	98	99	100	101	102	103	104	105	106	107	108	109	110	111	112	113
0.5	0	0	0	1	0	0	5	0	3	10	0	0	0	0	0	2	0	0	0	0	1
1	0	0	2	0	4	0	0	0	1	2	0	0	2	0	0	0	0	0	0	0	0
2	0	0	6	0	5	0	6	0	2	6	0	0	0	0	0	4	0	0	0	0	0
3	0	0	0	0	2	1	8	0	5	5	0	0	2	0	0	0	0	0	0	0	1
4	0	0	0	0	7	0	7	0	5	3	0	1	0	0	0	1	0	0	0	0	0
5	0	0	2	4	15	0	2	0	2	1	0	0	0	1	0	2	0	0	0	0	1
0.5	0	0	2	0	1	0	0	0	0	0	0	0	0	0	0	1	0	0	0	0	0
1	0	0	7	1	2	0	3	0	2	14	0	0	0	0	0	1	0	0	0	0	0
2	0	0	9	3	6	0	0	0	2	7	0	0	0	0	0	0	0	0	0	0	0
3	0	0	11	0	7	0	6	0	0	12	0	1	0	0	0	1	1	0	1	0	0
4	0	0	11	1	14	0	4	0	0	4	0	0	0	0	0	4	0	0	0	1	0
5	0	0	2	4	15	0	2	0	2	1	0	0	0	1	0	2	0	0	0	0	1
0.5	0	0	0	0	1	0	5	0	2	3	0	0	0	0	0	0	0	0	0	0	0
1	0	0	6	0	0	0	15	0	1	13	1	0	0	0	0	3	0	0	0	2	0
2	0	0	2	0	0	3	3	0	1	12	0	0	0	0	0	2	1	0	0	0	0
3	0	0	2	0	0	1	2	0	0	15	6	0	0	0	0	2	0	0	0	0	0
4	5	0	2	0	0	0	10	0	0	22	5	0	0	0	6	1	0	1	0	0	0
5	0	1	5	0	0	0	2	1	0	18	5	0	0	0	7	5	0	0	0	0	0

Depth (m)	114	115	116	117	118	119	120	121	122	123	124	125	126	127	128	129	130
0.5	0	0	0	0	0	0	2	6	0	0	0	0	0	0	0	0	0
1	0	0	1	1	0	0	2	6	1	0	0	1	0	0	0	0	0
2	0	0	0	0	0	0	0	0	0	0	0	0	0	0	0	0	0
3	0	0	0	0	0	0	3	4	0	0	0	0	0	0	0	0	0
4	1	0	0	0	0	0	1	2	0	0	0	0	2	0	1	0	1
5	1	0	0	0	0	0	1	3	0	0	0	0	0	1	1	0	0
0.5	0	0	0	0	0	0	0	1	0	0	0	0	0	0	1	0	0
1	0	0	0	0	0	0	1	1	0	0	0	0	0	0	0	0	0
2	0	0	0	0	0	0	1	0	0	0	0	1	0	0	0	1	1
3	0	0	1	0	0	0	0	2	0	0	0	0	0	0	1	0	5
4	4	0	0	0	0	1	4	1	0	0	0	0	0	0	1	1	0
5	1	0	0	0	0	0	1	3	0	0	0	0	0	1	1	0	0
0.5	0	0	0	0	0	0	0	0	0	0	0	0	0	0	0	0	1
1	0	0	0	0	0	0	3	0	0	3	9	0	0	0	0	0	0
2	0	0	0	0	1	0	4	0	0	6	3	0	1	1	0	0	1
3	0	0	0	0	0	1	2	0	0	3	2	0	0	0	0	0	1
4	1	2	0	0	0	0	5	2	0	4	1	0	0	2	0	0	0
5	0	0	0	0	0	0	3	0	0	0	1	0	0	0	1	1	0

Depth (m)	131	132	133	134	135	136
0.5	0	0	0	1	1	36
1	0	1	0	0	0	18
2	0	0	0	5	0	7
3	0	0	0	3	1	14
4	0	1	0	7	0	4
5	1	0	0	9	0	8
0.5	0	0	0	1	0	5
1	0	0	0	0	0	4
2	0	0	0	1	0	4
3	1	0	0	10	0	8
4	0	0	1	2	0	7
5	1	0	0	9	0	8
0.5	0	0	0	1	0	1
1	0	0	0	0	0	3
2	2	0	0	0	0	0
3	0	0	0	1	0	1
4	0	0	0	2	0	2
5	0	0	0	4	0	1

Appendix E: R Code and R Sources

Includes all code for the production of models and graphical representations of data. All data analysis was completed using R. Code followed by the citations for different packages utilized to build models and figures.

```
age##Script authored by Adam J. Heathcote on November 11, 2013 and adapted by Phil Woods, 2018

setwd("~/Documents/WISP2 Diatom Stuff") #working directory
library(ecodist) ; library(rioja); library(grid); library(ggplot2); library(mgcv);
 library(reshape)
#code of useful R functions written by Steve Juggins
source("/Users/aheathco/Documents/R Functions/RFunctions.r")
#code for multiplotting in ggplot2
source("/Users/aheathco/Documents/R Functions/multiplot.r")

#read in preformatted species and env data
totaldata <- read.csv("~/Documents/WISP2 Diatom Stuff/SS TS -1%3.csv",
 row.names=2)

totaldata
str(totaldata)
paleo <- read.csv("~/Documents/WISP2 Diatom Stuff/chen10spec12192017.csv",
 row.names=1)

paleonames <- read.csv("~/Documents/WISP2 Diatom Stuff/Names fossil.csv",
 header=F)
TSnames <- read.csv("~/Documents/WISP2 Diatom Stuff/TS names3.csv", header=F)
paleonames
str(paleo)

names(paleo[,-c(1:2)]) <- paleonames[,1]
names(totaldata[,-c(1:2)]) <- TSnames[,1]

#species abdunance
total.m <- data.frame(cbind(melt(totaldata[,-c(1:2)]), totaldata$Depth..m.))
names(total.m) <- c("Species", "Abundance", "Depth")
```

```
ggplot(data=total.m, aes(x=Depth, y=Abundance)) +geom_smooth(se=F) + geom_point()
 + facet_wrap(~Species) + scale_y_sqrt() + theme(axis.text=element_text(size=5))

#Clusterdiagram
diss1 <- dist(totaldata[,-c(1:2)])
clust <- chclust(diss1)
bstick(clust, 10)
plot(clust, hang=-1)

diss <- dist(paleo[,-c(1:3, 65:70)])
clust <- chclust(diss)
bstick(clust, 10)
plot(clust, hang=-1)

spec.plot <- c(11, 15, 17:34, 37:47, 51:58, 61:62)
spec.plot

#dev.off()

x <- strat.plot(paleo[,-c(1:3, spec.plot)]*100, yvar=paleo$Age.Model, y.rev=T,
 clust=clust, title="Cheney Lake", x.names=paleonames[-c(spec.plot-3),1],
 cex.xlabel=0.6, srt.xlabel=45, cex.title=0.95, cex.axis=0.6, x.pc.omit0=T,
 scale.percent=F, x.Space=0.01, xLeft=0.1, ylabel="Age Model")
addClustZone(x, clust, 4, col="red")

x <- strat.plot(paleo[,-c(1:3, spec.plot)]*100, yvar=paleo$depth, y.rev=T, clust=clust,
 title="Cheney Lake", x.names=paleonames[-c(spec.plot-2),1], cex.xlabel=0.6,
 srt.xlabel=45, cex.title=0.95, cex.axis=0.6, x.pc.omit0=T, scale.percent=T,
 xSpace=0.01)
addClustZone(x, clust, 4, col="red")

#data frame of just environmental data
env.comb <- data.frame(totaldata[,2])
names(env.comb) <- c("Depth")
#data frame of just diatom abundances
diat <- totaldata[,3:34]
#convert diatom to rel. abundance
#paleo.rel <- paleo[,-c(1:2)]/apply(paleo[,-c(1:2)], 1, sum)
#data frame of diatom abundances log10 transformed
diat.sqrt <- sqrt(diat)
paleo.sqrt <- sqrt(paleo[,-c(1:3, 65:70)])
paleo.sqrt
paleo
#Change log10(0) to 0
#diat.log[diat.log == -Inf] <- 0
```

```
#data frame of remaining variables
#other <- totaldata[,1:2]

#chech structure of env variables
str(env.comb)

#RDA of all variables in both datsets
model5 <- rda(paleo.sqrt)

model4 <- rda(diat.sqrt)

model1 <- rda(diat.sqrt ~ ., data=env.comb)
model3 <- cca(diat.sqrt ~ ., data=env.comb)
#model1.cca <- cca(diat.sqrt ~ ., data=env.comb)
plot(model1)
plot(model3)
plot(model5)
model1
scores(model1)
scores(model3)

#variance explained by RDA1
model1$CCA$eig/model1$tot.chi
model3$CCA$eig/model1$tot.chi

anova(model1, by="terms")
#anova(model1.cca, by="terms")

#species scaled PCA of training set
model2 <- rda(diat.sqrt, data=env.comb)
plot(model2)

# % variance explained for first 10 PC axes
((model1$CCA$eig/model1$tot.chi)*100)[1:10]

((model2$CA$eig/model2$tot.chi)*100)[1:10]

#save site and species scores from RDA to vector objects
sites <- scores(model1, choose=c(1,2), scaling=2, display="sites")
sites <- data.frame(sites)

species <- scores(model1, choose=c(1,2), scaling=2, display="species")
```

```
#variance explained by RDA axes
(model1$CCA$eig/model1$tot.chi)*100
#(model1.cca$CCA$eig/model1.cca$tot.chi)*100

#eigenvalues for first 2 RDA axes
lambda1 <- as.numeric(round(model1$CCA$eig[1]/model1$tot.chi*100, 1)); lambda1
lambda2 <- as.numeric(round(model1$CA$eig[2]/model1$tot.chi*100, 1)); lambda2

#plot RDA with all sig variables
p1 <- ggplot(aes(RDA1, PC1), data=sites, asp=1) + geom_point(); p1

plot(model1)

#create a WA transfer function from the training set
tfunc <- WA(diat.sqrt, env.comb, tolDW=T)
tfunc2 <- WAPLS(diat.sqrt, env.comb, tolDW=T)
tfunc.mat <- MAT(diat.sqrt, env.comb[,1], dist.method="sq.chord", k=5, lean=FALSE)
performance(tfunc)
performance(tfunc2)
performance(tfunc.mat)

pred.mat <- predict(tfunc.mat, newdata=paleo.sqrt, k=5)
fit <- MAT(diat.sqrt, env.comb[,1], k=5)
pred.mat <- predict(fit, paleo.sqrt, k=5)
names(pred.mat)
plot(x=tfunc.mat$x, y=tfunc.mat$fitted.values[,1])

names(tfunc)
plot(x=tfunc$x, y=tfunc$fitted.values[,1])

wa.perf <- data.frame(cbind(tfunc$x, tfunc$fitted.values[,1]))
wa.perf1 <- data.frame(cbind(tfunc.mat$x, tfunc.mat$fitted.values[,1]))

ggplot(wa.perf, aes(x=X1, y=X2)) + geom_point() + stat_smooth(method="lm")
ggplot(wa.perf1, aes(x=X1, y=X2)) + geom_point() + stat_smooth(method="lm")

#predict DI-depth for the fossil sections using transfer function
di.depth <- predict(tfunc, newdata=paleo.sqrt, sse=TRUE)
di.depth1 <- predict(tfunc.mat, newdata=paleo.sqrt, k=1, sse=TRUE)
str(paleo)
```

```
plot(paleo$Age.Model, di.depth$fit.boot[,1], type="p", xlim=c(max(paleo$Age.Model),
 min(paleo$Age.Model)), ylim=c(0, 9))
lines(paleo$Age.Model, di.depth$fit.boot[,1])
segments(x0=paleo$Age.Model, y0=di.depth$fit.boot[,1] + di.depth$SEP.boot[,1],
 y1=di.depth$fit.boot[,1] - di.depth$SEP.boot[,1])

plot(paleo$Age.Model, di.depth1$fit.boot[,1], type="p", xlim=c(max(paleo$Age.Model),
 min(paleo$Age.Model)), ylim=c(0, 9))
lines(paleo$Age.Model, di.depth1$fit.boot[,1])
segments(x0=paleo$Age.Model, y0=di.depth1$fit.boot[,1] + di.depth1$SEP.boot[,1],
 y1=di.depth1$fit.boot[,1] - di.depth1$SEP.boot[,1])

#combined plot
plot(paleo$Age.Model, di.depth$fit.boot[,1], type="p", xlim=c(max(paleo$Age.Model),
 min(paleo$Age.Model)), ylim=c(0, 9))
lines(paleo$Age.Model, di.depth$fit.boot[,1])
segments(x0=paleo$Age.Model, y0=di.depth$fit.boot[,1] + di.depth$SEP.boot[,1],
 y1=di.depth$fit.boot[,1] - di.depth$SEP.boot[,1])
points(paleo$Age.Model, di.depth1$fit.boot[,1], col=2)
lines(paleo$Age.Model, di.depth1$fit.boot[,1], col=2, lty=2)
segments(x0=paleo$Age.Model, y0=di.depth1$fit.boot[,1] + di.depth1$SEP.boot[,1],
 y1=di.depth1$fit.boot[,1] - di.depth1$SEP.boot[,1], col=2)

di.depth1
di.depth

#calculate optima and tolerance of diatoms in transfer function
tfunc$coefficients
error.bar <- function(x, y, upper, lower=upper, length=0.1,...){
if(length(x) != length(y) | length(y) !=length(lower) | length(lower) != length(upper))
stop("vectors must be same length")
arrows(x,y+upper, x, y-lower, angle=90, code=3, length=length, ...)
}

optima.sort <- order(tfunc$coefficients[,1], decreasing=T)
bar.names <- TSnames[optima.sort,]
par(mar=c(11,3,0,0))
barx <- barplot(tfunc$coefficients[optima.sort,1], horiz=F, las=2, cex.names=0.75,
 ylim=c(0, 5.5), names.arg=bar.names)
error.bar(barx, tfunc$coefficients[optima.sort,1], tfunc$coefficients[optima.sort,2],
 length=0.05)
```

R Package References

Bennett, K. (1996) Determination of the number of zones in a biostratigraphic sequence. *New Phytologist*, **132**, 155-170.

Birks, H.J.B. & Gordon, A.D. (1985) *Numerical Methods in Quaternary Pollen Analysis* Academic Press, London.

Birks, H.J.B., Line, J.M., Juggins, S., Stevenson, A.C., & ter Braak, C.J.F. (1990) Diatoms and pH reconstruction. *Philosophical Transactions of the Royal Society of London*, **B, 327**, 263-278.

Blaauw, M. and Christen, J.A. (2011). Flexible paleoclimate age-depth models using an autoregressive gamma process. Bayesian Anal. 6 no. 3, 457–474. https://projecteuclid.org/download/pdf_1/euclid.ba/1339616472

Gordon, A.D. & Birks, H.J.B. (1972) Numerical methods in Quaternary paleoecology I. Zonation of pollen diagrams. *New Phytologist*, **71**, 961-979.

Grimm, E.C. (1987) CONISS: A FORTRAN 77 program for stratigraphically constrained cluster analysis by the method of incremental sum of squares. *Computers & Geosciences*, **13**, 13-35.

Juggins, S. (2017). rioja: Analysis of Quaternary Science Data, R package version (0.9-15.1). (http://cran.r-project.org/package=rioja).

Legendre, P. & Gallagher, E. (2001) Ecologically meaningful transformations for ordination of species. *Oecologia*, **129**, 271-280.

Legendre, P. and Legendre, L. (2012) *Numerical Ecology*. 3rd English ed. Elsevier.

McCune, B. (1997) Influence of noisy environmental data on canonical correspondence analysis. *Ecology* **78**, 2617-2623.

Overpeck, J.T., Webb, T., III, & Prentice, I.C. (1985) Quantitative interpretation of fossil pollen spectra: dissimilarity coefficients and the method of modern analogs. *Quaternary Research*, **23**, 87-108.

Palmer, M. W. (1993) Putting things in even better order: The advantages of canonical correspondence analysis. *Ecology* **74**,2215-2230.

R Core Team (2013). R: A language and environment for statistical computing. R Foundation for Statistical Computing, Vienna, Austria. URL http://www.R-project.org/.

ter Braak, C. J. F. (1986) Canonical Correspondence Analysis: a new eigenvector technique for multivariate direct gradient analysis. *Ecology* **67**, 1167-1179.

ter Braak, C.J.F. & Barendregt, L.G. (1986) Weighted averaging of species indicator values: its efficiency in environmental calibration. Mathematical Biosciences, 78, 57-72.

ter Braak, C.J.F. & Looman, C.W.N. (1986) Weighted averaging, logistic regression and the Gaussian response model. *Vegetatio*, **65**, 3-11.

ter Braak, C.J.F. & van Dam, H. (1989) Inferring pH from diatoms: a comparison of old and new calibration methods. *Hydrobiologia*, **178**, 209-223.

van der Voet, H. (1994) Comparing the predictive accuracy of models using a simple randomization test. *Chemometrics and Intelligent Laboratory Systems*, **25**, 313-323.

Special thanks to Sara Beth Mueller for her completed masters thesis document in formatting this masters thesis. Thank You.